Identification and characterization of the rodent carboxylesterase isozymes and transcriptional regulation of the mouse *carboxylesterase 2* gene

Tomomi Furihata

Laboratory of Pharmacology and Toxicology
Graduate School of Pharmaceutical Sciences
Chiba University

CONTENTS

INTRODUCTION·····3

Chapter I

Identification and characterization of the rodent carboxylesterase isozymes

I-I

Identification of di-(2-ethylhexyl)phthalate-induced carboxylesterase 1 in C57BL/6 mouse liver microsomes: purification, cDNA cloning, and baculovirus-mediated expression

I-I-I:Introduction·····6
I-I-II: Materials and Methods·····6
I-I-III: Results·····9
I-I-IV: Discussion ·····13

I-II

Purification, molecular cloning, and functional expression of inducible liver acylcarnitine hydrolase in C57BL/6 mouse, belonging to the carboxylesterase multigene family

I-II-I:Introduction·····17
I-II-II: Materials and Methods·····17
I-II-III: Results·····20
I-II-IV: Discussion····· 24

I-III

Dexamethasone-induced methylprednisolone hemisuccinate hydrolase: Its identification as a member of the rat carboxylesterase 2 family and its unique existence in plasma

I-III-I:Introduction·····27
I-III-II: Materials and Methods·····27
I-III-III: Results·····29
I-III-IV: Discussion·····35

Chapter II

Molecular characterization of the mouse *carboxylesterase 2* gene promoter

II-I

Synergistic role of specificity proteins and upstream stimulatory factor 1 in transactivation of the mouse *carboxylesterase2/microsomal acylcarnitine hydrolase* gene promoter

II-I-I:Introduction·····38
II-I-II: Materials and Methods·····39
II-I-III: Results·····42
II-I-IV: Discussion·····49

II-II

Hepatocyte nuclear factor-4 alpha plays pivotal roles in transactivation and bile acid-mediated repression of the *mouse carboxylesterase 2 gene* promoter

II-II-I:Introduction·····52
II-II-II: Materials and Methods·····52
II-II-III: Results·····55
II-II-IV: Discussion·····60

Conclusion·····63

References·····64

List of papers on publication·····74

Acknowledgements·····75

Reviewers·····76

INTRODUCTION

Carboxylesterases (CESs, EC.3.1.1.1) are members of an α, β-hydrolase-fold superfamily [1, 2] and they show ubiquitous tissue expression profiles with the high levels of CES activity present in the liver, kidney and small intestine in various mammals [1]. CESs exhibit such broad substrate specificities towards endogenous and xenobiotic chemicals that they are thought to play important roles in both drug and lipid metabolism. Several CES isozymes have been identified in mammals, and it has been proposed that they can be classified into four families according to homologies of their amino acid sequences [1]. In the field of drug metabolism, CESs are categorized as phase-I drug-metabolizing enzymes. They can hydrolyze ester-drugs, such as cocaine, heroin and meperidine [3, 4] and ester-prodrugs, such as angiotensin-converting enzyme inhibitors (temocapril, cilazapril, quinapril, and imidapril) [5] [6] and anti-tumor drugs (CPT-11 and Capecitabin) [7, 8]. In this regard, it is thought that CESs are one of the major determinants for pharmacokinetics and pharmacodynamics of ester-drugs. Actually, it has been shown that dog CES1 isozyme was involved in a pulmonary first-pass effect in the disposition of a propranolol ester prodrug [9]. It has also been shown that the expression level of human CES isozyme was correlated with the conversion ratio of CPT-11 to SN-38, the active metabolite, which is thought to be a key step for the chemotherapeutic action of this anti-tumor drug [10, 11]. A majority of CES isozymes involved in drug metabolism belongs to either CES1 family or CES2 family, and there are great differences between their substrate specificities. For example, the preferential substrates for a human CES1 family isozyme [1, 12] are thought to be compounds esterified by small alcohol moiety, while those for a human CES2 family isozyme are thought to be compounds esterified by relatively large alcohol moiety [2-4, 6]. It has been also known that some species differences exist within the CES1 or CES2 family isozymes [13-17]. These findings suggest that it is important to characterize both human and animal CES isozymes to understand the function of CESs in drug metabolism.

On the other hand, recent studies have suggested that CESs are involved in lipid metabolism because it has been shown that acyl-CoA [18, 19], acylcarnitine [20, 21], acylglycerol [14], and phospholipid [22] can be substrates for CESs. It has reported that mouse triacylglycerol hydrolase (mTGH), identical to mCES1, contributed to the hormone sensitive lipase-independent lipolytic activity in the white addipose tissue [23]. It has been also claimed that mTGH/mCES1 acts as a major microsomal lipase that is involved in very low-density lipoprotein assembly pathway in hepatocyte [24, 25]. Human CES1 was also termed neutral cholesterolester hydrolase (CEH), and it has been shown that overexpression of human CES1/CEH in agmACAT1 cells resulted in the reduction in the amount of lipid droplets containing cholesteryl ester [26]. In this way experimental evidences suggesting the importance of CESs to lipid metabolism have been accumulated, but the number of the evidences are still limited. Thus, further studies are absolutely required to clarify true impacts of CESs on lipid metabolism.

The studies aimed at elucidation of the mechanism controlling the *CES* gene transcription would provide important information to the studies for drug and lipid metabolisms in which CESs are involved. Although critical roles of CESs in lipid metabolism remain unknown, expression profiles of the *CES* gene should reflect their physiological functions. In addition, it has been known that the induction of expression of drug-metabolizing enzymes by chemicals is one of the main reasons for drug-drug interaction causing adverse effects and for the reduction in

pharmacological potencies of drugs [27, 28], and CES has been reported to be induced by some chemicals. For example, rodent CES isozyme(s) was induced by phenobarbital [29], aminopyrine [30], peroxisome proliferators (clofibrate, di (2-ethylhexyl)phthalate, and perfluorinated fatty acids) [20, 31, 32]. However, there are limited reports showing molecular mechanisms by which the *CES* gene transcription is regulated. Therefore, it is important to clarify these mechanisms for fully understanding the functions of CESs in drug and lipid metabolisms.

The purpose of the present study was to elucidate the functions of CESs in drug and lipid metabolism and the mechanisms controlling the *CES* gene transcription. In the chapter I, we reported the results of identification and characterization of three rodents CESs that were induced by treatment of xenobiotics. In chapter II, focusing on the mouse CES2 isozyme, mCES2, we characterized its promoter region. We also showed some experimental data that *mCES2* gene transcription was affected by physiological processes.

Chapter I

Identification and characterization of the rodent carboxylesterase isozymes

I-I

Identification of di-(2-ethylhexyl)phthalate-induced carboxylesterase 1 in C57BL/6 mouse liver microsomes: purification, cDNA cloning, and baculovirus-mediated expression

I-I-I Introduction

The mouse is one of the most widely used experimental animals in the process of development of a drug. Since pharmacokinetic and pharmacological data of ester-prodrugs obtained from preclinical experiments using various animals are generally used as references for human studies, it is important to clarify the biochemical properties of CES isozymes of experimental animals such as substrate specificity, tissue distribution and transcriptional regulation. Several mouse CES isozymes have been identified [1, 20, 33-37]. However, information on the involvement of mouse CESs in drug metabolism is limited. We have reported that exposure of C57BL/6 mice to di (2-ethylhexyl) phthalate (DEHP), a peroxisome proliferator, in their diet resulted in a significant increase in the amount of CES protein concomitant with an increase in the level of hydrolytic activity toward xenobiotics in mouse liver microsomes [17]. Our immunochemical study suggested that several mouse CES1 isozymes were induced by DEHP treatment, but they remained to be identified.

The purpose of this study was to identify mouse CES1 isozymes induced by DEHP. Purification, cDNA cloning and functional expression revealed that one of them is mCES1. Our data also showed that mCES1 contributes significantly to hydrolysis of temocapril, an ester-prodrug of an angiotensin-converting enzyme inhibitor, in mouse liver microsomes. Thus, we provided useful information for study of the metabolism and dispositions of ester-prodrugs as well as ester-drugs.

I-I-II Methods

Animals and preparation of solubilized fraction of mouse liver microsomes

Adult male C57BL/6 mice (Japan SLC Inc., Shizuoka, Japan) of 8 weeks in age were used in this study. The mice were fed a laboratory animal chow (CE-2, Japan Clea, Tokyo, Japan) with or without 2% (w/w) DEHP as described previously [17]. Each group consisted of three mice. The mice were sacrificed, and the livers were removed, weighed and perfused with 1.15% KCl. Microsomes were isolated by differential centrifugation as described previously [29] and were solubilized with 0.5% cholic acid in 10 mM Tris-HCl buffer (pH 8.0). The mixture was centrifuged at 10,000 x g for 30 min, and the supernatant was removed and used for following experiments. Solubilized fractions of control and DEHP-treated mouse liver microsomes are referred to here as Control Ms and DEHP Ms, respectively. Protein concentrations were determined by using a Bio-Rad Dc Protein Assay kit (Bio-Rad Laboratories, Hercules, CA, U.S.A). All subsequent procedures were performed at 0 - 4°C.

Purification of mouse CES1 from DEHP-treated C57BL/6 mouse liver microsomes

Purification of the CES isozyme that can hydrolyze temocapril from DEHP-treated C57BL/6 mouse liver was carried out essentially according to the procedure reported in our previous paper [29]. All steps were carried out at 4 °C, and the peak fraction was detected by *p*-nitrophenylacetate (PNPA) hydrolase activity. Microsomes were solubilized in 100 mM Tris-HCl buffer, pH 8.0, containing 1% (w/v) saponin, at a final protein concentration of 2.7 mg/ml. The solution was stirred for 60 min at 4 °C and then centrifuged at 105,000 x g for 60 min. The supernatant was fractionated by

ammonium sulfate precipitation. The 30-70% (w/v) precipitation was resuspended in 10 mM Tris-HCl buffer (pH 8.0). The solution was gel-filtered on a Sephadex G-150 column (2.6 x 90 cm) (Amersham Bioscience, Piscataway, NJ, U.S.A.) equilibrated with 10 mM Tris-HCl buffer (pH 8.0). Two peak fractions (high molecular weight and low molecular weight) were obtained. The high molecular weight fraction was applied to a column (3.0 x 8.0 cm) of Whatman DE-52 (Maidstone, U.K.) that had been equilibrated with 10 mM Tris-HCl buffer (pH 8.0). The column was washed with the same buffer and then eluted with a stepwise NaCl gradient in 10 mM Tris-HCl buffer (pH 8.0). One peak fraction was collected by elution with 60 mM NaCl. The peak fraction was pooled and dialyzed for 24 hr against three changes of 2 liters of 25 mM bis-Tris-HCl buffer (pH 6.5). The dialyzed fraction was applied to a column (1.0 x 30 cm) of chromatofocusing gel PBE 96 (Amersham Bioscience), equilibrated with 25 mM bis-Tris-HCl buffer (pH 6.5). The active fraction was eluted with 270 ml of Polybuffer 74 (Amersham Bioscience) and diluted at a ratio of 1:8. The pH of the fraction was adjusted to 4.5 with HCl. The active fraction was pooled and dialyzed for 24 hr against two changes of 2 liters of 20 mM Tris- HCl buffer (pH 7.6) containing 0.1 M NaCl, 0.1 mM $MgCl_2$ and 0.5 mM $CaCl_2$. The dialyzed fraction was applied to a column (1.5 x 5.0 cm) of Con A-Sepharose (Amersham Bioscience) and equilibrated with 20 mM Tris-HCl buffer (pH 7.6) containing 0.1 M NaCl, 0.1 mM $MgCl_2$ and 0.5 mM $CaCl_2$. The column was washed with 20 mM Tris-HCl buffer (pH 7.6) containing 0.5 M NaCl, 0.1 mM $MgCl_2$ and 0.5 mM $CaCl_2$ and subsequently eluted with 20 mM Tris-HCl buffer (pH 7.6) containing 0.2 M α-methylmannoside, 0.1 M NaCl, 0.1 mM $MgCl_2$ and 0.5 mM $CaCl_2$. The fractions showing a single protein band in SDS-PAGE were combined. The purified isozyme, termed mouse CES1, could be stored at -80 °C for several months without loss of enzyme activity.

Preparation of antibodies

Antibodies against purified CES P1, a porcine CES isozyme [7], were raised in male Japanese white rabbits (2.5 – 3.0 kg in body weight) according to a previously described procedure [29]. Anti-CES RL1 antibodies and anti-CES D1 antibodies were prepared as previously described [14, 19]. The IgG fraction of antiserum was purified from whole antibodies by using a HiTrap Protein A HP (Amersham Bioscience) and a PD-10 column (Amersham Bioscience) according to manufacturer's protocol.

Determination of hydrolase activity

p-Nitrophenylesters (PNPesters) were from the following sources: PNPA, *p*-nitrophenylbutylate (PNPB), *p*-nitrophenylvalerate (PNPV), *p*-nitrophenyhexanoate (PNPH), *p*-nitrophenyloctanoate (PNPO), and *p*-nitrophenyllaurate (PNPL) were from Nacalai Tesque (Kyoto, Japan), *p*-nitrophenylpropionate (PNPP) was from Wako Pure Chemicals (Osaka, Japan), and *p*-nitrophenyldecanoate (PNPD) was from Sigma (St. Louis, MO, U.S.A). Hydrolysis of PNPesters was determined colorimetrically in 50 mM Tris-HCl buffer (pH 8.0) at 30 °C by measuring the amount of *p*-nitrophenol released according to the method of Krisch [38]. The substrate concentration of PNPA for kinetic study ranged from 10 to 600 μ M, and that of other *p*-nitrophenol esters for determination of hydrolytic activity was 50 μ M.

Butanilicaine was obtained from Hoechst AG (Frankfurt, FRG). Butanilicaine hydrolase activity was also determined by spectrophotometric analysis in 50 mM Tris-HCl buffer (pH 8.6), 0.225% cholic acid, and 9.0% glycerol as previously described [14]. The substrate concentration of butanilicaine for kinetic study ranged from 62.5 μ M to 1.5 mM.

Temocapril hydrolase activity was assayed in 50 mM HEPES buffer (pH 7.4), and temocaprilat, a metabolite of temocapril, was analyzed by using the following HPLC method [39] with slight modifications. The HPLC system consisted of a model L-6000 pump (Hitachi, Tokyo, Japan), a model L4000H UV detector (Hitachi), a model AS-2000 autosampler (Hitachi), a model D-2500 integrator (Hitachi), and a 4.6 x 150 mm YMC-Pack Ph A-402 column (YMC, Tokyo, Japan). The mobile phase consisted of 0.24% phosphoric acid-acetonitrile (68:32, v/v) and was delivered at a flow rate of 0.7 ml/min. Temocaprilat was detected at a wavelength of 233 nm. A calibration curve was generated from 0.5 to 100 μ M by processing the authentic standard

substance through the entire procedure. Clofibric acid (Sigma) was used as an internal standard. Temocapril and temocaprilat were kindly obtained from Dr. Toshihiko Ikeda, Analytical and Metabolic Research Laboratories, Sankyo Co., Tokyo, Japan. The substrate concentration of temocapril for kinetic study ranged from 24 μ M to 300 μ M.

Specific activities of CES toward all substrates used were expressed in terms of the amount of substrate hydrolyzed in 1 min under specified conditions. Enzyme kinetic parameters were estimated using a computer program (DeltaGraph ver 4.5, SPSS Inc., Chicago, IL) designed for non-linear regression analysis as described previously [40]. Each mean kinetic value was the average of three individual experiments with ± S.D. Student's *t*-test was performed to determine significance of difference between two groups. *P* values less than 0.05 were taken to be significant.

Inhibition assay by using specific IgG

Inhibition of hydrolase activity by using a specific IgG was performed according to the procedure described previously [17] with slight modification. Control Ms (n = 3) and DEHP Ms (n = 3) were incubated with control or specific IgG (either anti-CES D1 IgG or anti-CES RL1 IgG) (0.75 mg) for 30 min at 37 °C, and the mixtures were left for 24 hr at 4 °C. Then nProtein A Sepharose 4 Fast Flow (Amersham Bioscience) was added to the mixture. After incubation on ice for one hour, the mixture was centrifuged for 10 min at 20,000 x g. The supernatant was removed and used for a determination of hydrolase activity as described above.

N-terminal sequences of mouse CES1

N-terminal amino acid sequences of mouse CES1 were determined by using a Hitachi C-8500 automatic amino acid analyzer (Hitachi). Amino acids were sequenced by automated Edman degradation using a model 470A gas-phase sequencer (Applied Biosystems, Foster City, CA) with an on-line Spectra-Physics Model SP8100 PTH amino acid analyzer (Applied Biosystem) as described previously [14].

Antibody screening of cDNA library

Antibody screening of a cDNA library was performed as described previously [19]. A ZAP cDNA library was constructed from DEHP-treated C57BL/6 mouse liver and was screened by anti-CES RL1 antibodies. Binding of this rabbit primary antibody to fusion proteins on nitrocellulose overlay was detected with peroxidase-conjugated goat anti-rabbit IgG (Amersham Bioscience). Binding of the second antibody was visualized with diaminobenzidine. cDNA fragments inserted into phage DNA of positive clones were isolated by *EcoRI* digestion and subcloned into the pBlueskript SK (-) vector. The nucleotide sequences were determined using a Dye Terminator Cycle Sequencing-Quick Start Kit and CEQ 2000 DNA Analysis System (Beckman Coulter, Fullerton, CA, U.S.A.) and were confirmed by sequencing at least twice in each direction. The cDNA clone obtained was named mCES1.

Baculovirus-mediated expression of mCES1 in Sf9 cells

The recombinant mCES1 was expressed in Sf9 cells by using a BAC-TO-BAC Baculovirus Expression System (Invitrogen, Calsbad, CA., U.S.A.) in accordance with the directions of the manufacturer. The cDNA in the cloning vector was subcloned into the pFAST BAC1 vector using *EcoRI* and alkaline phosphatase. The pFAST BAC1 vector containing mCES1 was transformed into DH10Bac cells, and this was followed by transposition of the inserts into bacmid DNA. Likewise, non-recombinant bacmid DNA (mock) was also prepared. The recombinant and mock bacmid DNAs were separately transfected into Sf9 cells with CELL FECTIN reagent (Invirogen), and the virus was harvested 72 hr later. The cells were centrifuged at 1,700 x g for 10 minutes to separate cells and virus. The supernatant containing the virus was stored at 4°C in the dark with 5% fetal bovine serum until used for infection. Cells were routinely infected with the virus and were harvested 72 hr after infection, washed twice with phosphate-buffered saline, and stored –80 °C until used. Lysates were prepared by disrupting the cells with a sonicator until the cells were completely lysed as determined by microscopy. Cytosol of Sf9 cells expressing mCES1 and that of Sf9 cells infected with mock virus were prepared by subjecting the cell lysate

to centrifugation (105,000 x g for 60 min at 4°C), and they were named mCES1/Sf9 and mock/Sf9, respectively.

Preparation of mouse tissue homogenates and esterase activity staining after non-denaturing polyacrylamide gel electrophoresis (PAGE)

Three 8-week-old C57BL/6 male mice (Japan SLC, Inc., Shizuoka, Japan) were sacrificed, and nine tissues (brain, thymus, lung, heart, liver, kidney, small intestine, epididymal adipose tissue and testis) were removed from each mouse. Tissue samples of equal weights were pooled, and the homogenate was prepared using a Potter-Elvehjem homogenizer in SET (0.25 M sucrose, 1 mM EDTA and 10 mM Tris, pH 7.4) buffer at 4°C. The protein concentration was determined as described above. Esterase activity staining after non-denaturing PAGE was performed according to the method of Mentlein et al. [41]. α-Naphtylacetate was obtained from Tokyo Kasei (Tokyo, Japan). Different amounts of homogenate were used in this method to adjust band intensity: 20 μg of brain, 15 μg of thymus, 7 μg of lung, 10 μg of heart, 1 μg of liver, 5 μg of kidney, 5 μg of small intestine, 2.5 μg of adipose tissue, and 10 μg of testis. mCES1/Sf9 was used as a positive control.

Total RNA preparation and reverse transcription-polymerase chain reaction (RT-PCR)

Three 8-week-old C57BL/6 male mice (Japan SLC) were sacrificed, and removed tissue samples of equal weights were pooled. Total RNA was extracted from each tissue (brain, thymus, lung, heart, liver, kidney, small intestine, epididymal adipose tissue and testis) using TRIzol reagent (Invitrogen). To prevent contamination with genomic DNA, the extracts were treated with DNase I (Takara Shuzo, Shiga, Japan). Subsequently, first-strand cDNA was synthesized from 2 μg of each RNA by Ready-To-Go RT-PCR Beads with an oligo (dT) primer (Amersham Bioscience). For certification of synthesis of equal amounts of cDNA, PCR was performed (94 °C for 15 s, 49 °C for 20 s, 68 °C for 40 s and 35 cycles) using a set of primers for detection of *mouse glyceraldehyde-phosphate dehydrogenase* (GAPDH) gene expression: sense, 5'-TGCACCACCAACTGCTTA-3'; and anti-sense, 5'-GGATGCAGGGATGATGTTC-3'. Another set of primers (sense, 5'-GGCATCAACAAGCAAGAGTTTGGC-3'; and anti-sense, 5'-CTTTTTGGTGAGGTGATCTGTCCC-3') was used for PCR (94 °C for 15 s, 54 °C for 20 s, 68 °C for 35 s and 32 cycles) to detect *mCES1* gene expression. The pFAST BAC1 vector containing mCES1 cDNA was used as a template for a positive control. The PCR product was purified by a Wizard SV Gel and PCR Clean-up System (Promega, Madison, WI, U.S.A.) and was confirmed to be a fragment of mCES1 cDNA by DNA sequencing. The DNA sequence was determined as described above.

Other methods

SDS-polyacrylamide gel electrophoresis (SDS-PAGE) was performed with 10% acrylamide gel, and Western blotting was performed by using a Vecrastain Elite ABC kit (Vector Laboratories, Inc., Burlingame, CA, U.S.A.) according to manufacturer's directions.

Mouse CES isozymes, CES ML1 and CES ML2, were purified by the same method as that used for the purification of mouse CES1 (papers in preparation).

Chemicals used in this study were of reagent grade and obtained from commercial sources.

I-I-III Results

Induction of hydrolase activity in mouse liver microsomes by DEHP

Exposure of C57BL/6 mice to DEHP in their diet resulted in significant induction of hydrolase activity in mouse liver microsomes (Fig. 1). Compared with Control Ms, DEHP Ms showed 3.0-fold ($P < 0.05$) and 2.8-fold ($P < 0.05$) increases in the level of PNPA hydrolase activity and temocapril hydrolase activity, respectively.

Purification of mouse CES1 from DEHP-treated mouse liver microsomes and N-terminal amino acid sequences

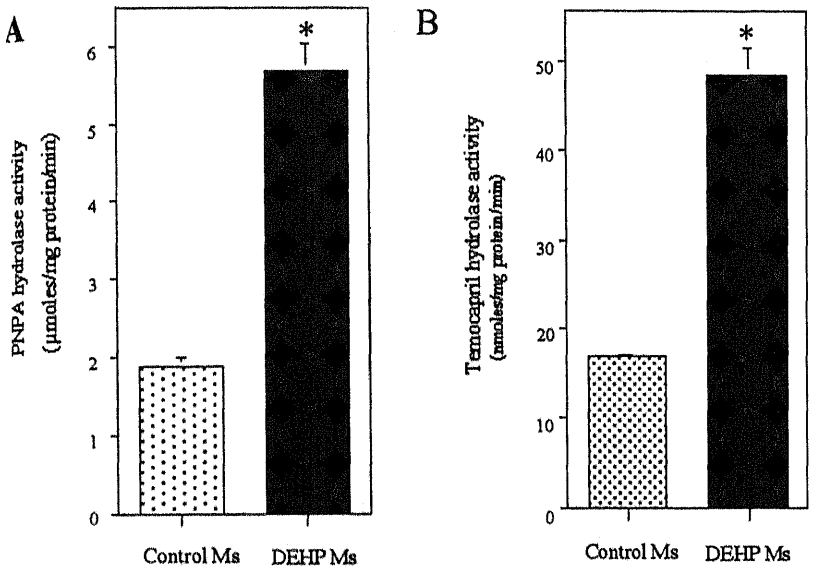

Fig. 1. Induction of carboxylesterase activity in DEHP-treated mouse liver microsomes. A, PNPA hydrolase activity; B, temocapril hydrolase activity. The sample number of Control Ms or DEHP MS was three. Each value is represented as the mean of three independent assays (± S.D.). * indicates statistically significant difference compared with the Control Ms ($P<0.005$).

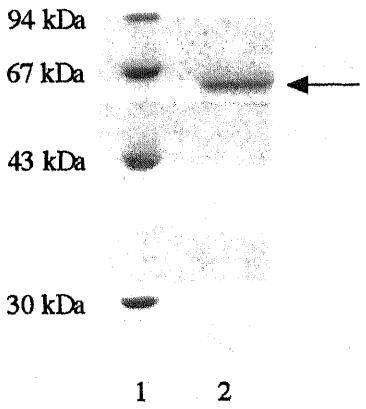

Fig. 2. Purification of mouse CES1 from DEHP-treated mouse liver microsomes. SDS-PAGE of purified preparations resulted in a single band. Lane 1, protein marker (94 kDa, phosphorylase b; 67 kDa, bovine serum albumin; 43 kDa, ovalbumin; 30 kDa, carbonic anhydrase). Lane 2, purified preparations (250ng). An arrow indicates the purified mouse CES1.

Our purification procedures gave a purified CES isozyme indicated by a single band in SDS-PAGE (Fig. 2), and we tentatively named it mouse CES1. The isoelectronic point of mouse CES 1 was 5.8, which was estimated by chromatofocusing. Mouse CES1 was present as a trimer in Sephadex G-150 column chromatography (data not shown), and the molecular weight of a subunit of mouse CES1 was approximately 60 kDa, estimated by a plot of relative mobility vs. log of the molecular weight of the standards. Binding of mouse CES1 to Con A-Sepharose indicated that mouse CES1 was a glycoprotein. The amino acid sequence of mouse CES1 was determined for the first 20 N-terminal amino acids, as shown in the box in Figure 5.

Substrate specificity of mouse CES1

Specific activities of mouse CES1 towards some xenobiotics were examined. The level of activity of mouse CES1 towards PNPesters was found to be dependent on the carbon chain length. When the carbon chain length of PNPesters was three (PNPP) or four (PNPB), the activities towards PNPP and PNPB were almost the same (179 and 157 μmoles/mg protein/min, respectively), while both of them were much higher than that to PNPA (80.9 μmoles/mg protein/min), the carbon chain length of which was two. Mouse CES1 showed butanilicaine hydrolase activity (17.2 μmoles/mg protein/min) in addition to temocapril hydrolase activity (197 nmoles/mg protein/min). Kinetic parameters for these substrates could not be determined due to the limited amount of purified enzyme available.

Specific immunocrossreactivity of anti-CES D1 antibodies with mouse CES1

To obtain antibodies specific to mouse CES1, we performed antibody screening by Western blotting (Fig. 3). Two purified mouse CES isozymes (termed CES ML1 and CES ML2) were used in addition to mouse CES1 and mCES2 [20] for the screening. Among CES antibodies, anti-CES D1 antibodies showed specific immunocrossreactivity with mouse CES1 (Fig. 3A, upper column), while anti-CES P1 antibodies recognized all four CES isozymes (Fig. 3A, lower column), although the recognition of mCES2 was weak. Anti-CES RL1 antibodies could recognize both mouse CES1 and CES ML1 but not CES ML2 or mCES2 (data not shown). Anti-CES D1

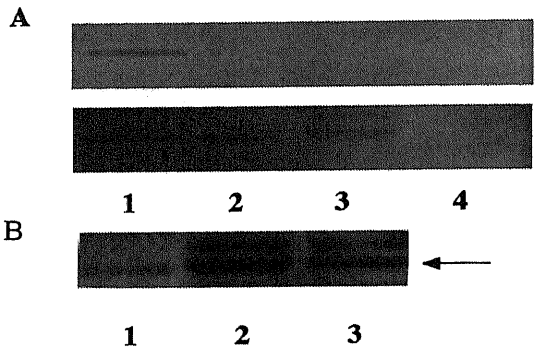

Fig. 3. Specific immunocrossreactivity of anti-CES D1 antibodies with mouse CES1. Western blotting was performed to identify antibodies that specifically recognize mouse CES1. The arrow indicates the band for mouse CES1. A, Anti-CES D1 and anti-CES P1 antibodies were used in the upper panel, in the middle panel, and in the lower panel, respectively. 1, purified mouse CES2 (0.5 μg), 2, purified mouse CES ML1 (0.5 μg), 3, purified mouse CES ML2 (0.5 μg), 4, purified mCES1 (0.5 μg). B, Anti-CES D1 antibodies were used. 1, purified mouse CES1 (0.5 μg), 2, solubilized fraction of DEHP Ms (0.3 mg), 3, Control Ms (0.3 mg).

antibodies could detect mouse CES1 in both Control Ms and DEHP Ms, and the intensity of the band in DEHP Ms was stronger than that in Control Ms (Fig. 3B). Anti-CES D1 antibodies also detected an unknown protein with a slower migration point.

Effects of specific IgG on temocapril hydrolase activity in mouse liver microsomes

After the IgG fraction had been purified from whole antibodies, we observed the effects of specific IgGs, anti-CES D1 IgG or anti-CES RL1 IgG, on temocapril hydrolase activity (Fig. 4). The levels of activity in Control Ms and DEHP Ms obtained from assays using control IgG were adjusted to 100% in each group. Inhibition by anti-CES D1 IgG caused 66.6% ($P < 0.05$) and 46.9% ($P < 0.05$) reductions in the level of temocapril hydrolase activity in Control Ms and DEHP Ms, respectively. On the other hand, inhibition by anti-CES RL1 IgG resulted in 93.7% ($P < 0.05$) and 94.6% ($P < 0.05$) reductions in the activity level in Control Ms and DEHP Ms, respectively.

Antibody screening of cDNA library

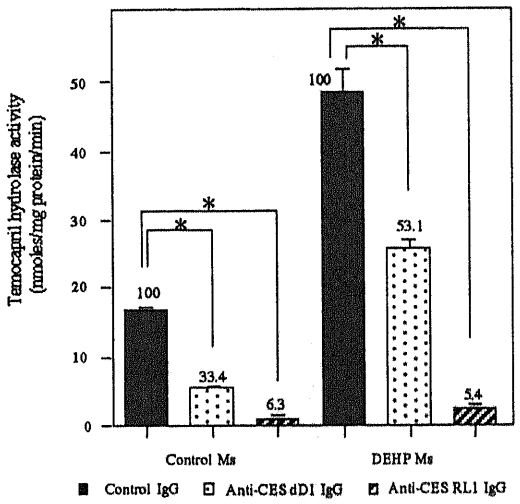

Fig. 4. Effects of anti-CES IgGs on temocapril hydrolase activity in Control Ms or DEHP Ms. Control IgG (0.75 mg), anti-CES D1 antibodies (0.75 mg), and anti-CES RL1 antibodies (0.75 mg) were used in the solid bar, dotted bar, and hatched bar, respectively. The sample number of Control Ms or DEHP MS was three. Each value is the mean of three independent assays (± S.D.). The number above each bar is relative % of activity when that of control IgG in each group (Control Ms or DEHP Ms) is set to 100%. * indicates statistically significant difference compared with the results of control IgG in each group (P<0.005).

As a result of cDNA library screening by anti-CES RL1 antibodies, 27 positive clones were isolated from 9.6 x 10^4 plaques tested. Among them, a 1946-bp cDNA clone was found to contain an open reading frame encoding an amino acid polypeptide followed by a termination codon (TAG) and then by 206 nucleotides of a 3'-noncoding sequence including a poly (A) tail (data not shown). This cDNA clone was named mCES1. The deduced amino acid sequence of mCES1 is shown in Figure 5. It contained a structurally important Cys residue (Cys99), catalytic triad (Ser204, Glu336 and His449), oxyanion hole loop (Gly124 and Gly125) and HXEL-motif (His562, Val563, Glu564, and Leu565), which are specific sequences conserved in the mammalian CES family [1]. The deduced amino acid sequence of mCES1 also contained two N-linked glycosylation sites (Asn62, Thr63 and Thr64, and Asn472, Leu473 and Ser474).

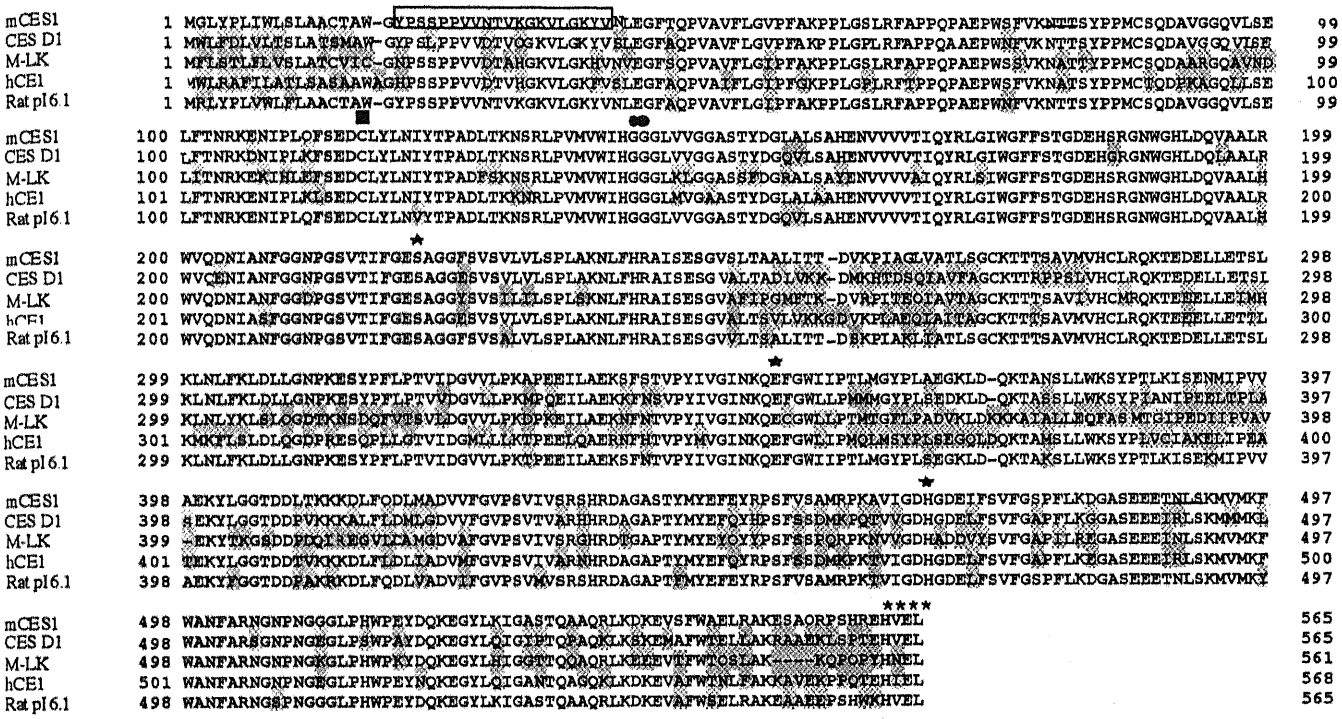

Fig. 5. Comparison of the deduced amino acid sequence of mCES1 with those of other CES1 isozymes. Shadows indicate differences in amino acid residues. The box indicates the same sequence as that of purified mouse CES1 identified. Stars indicate residues composing a catalytic triad. Square indicates structurally important Cys residues. Circles indicate two Gly residues important for oxianion hole loop formation. Asterisks indicate endoplasmic retention signal motifs. Underlines indicate N-linked glycosylation sites.

Baculovirus-mediated expression of mCES1 in Sf9 cells and carbon chain length specificity of the recombinant mCES1protein

Western blotting showed that the recombinant mCES1 protein was recognized by anti-CES D1 antibodies and that the molecular weight of a subunit was the same as that of purified mouse CES1 (Fig. 6A). Esterase activity staining after non-denaturing PAGE also showed that the recombinant CES1 protein possessed α-naphtylacetate hydrolase activity, and the migration rate of the protein was the same as that of purified mouse CES1 (Fig. 6B). On the other hand, a specific protein was not detected in mock/Sf9 either by Western blotting or esterase activity staining after non-denaturing PAGE. In esterase activity staining after non-denaturing PAGE, the accessory band found at a faster migration point indicated by an asterisk was thought to be a monomeric form of mCES1 [42].

To analyze the effect of carbon chain length of the substrate on hydrolase activity of the recombinant mCES1, we used PNPesters that contained various carbon chain lengths (from two to twelve) as substrates (Fig. 6C). The level of specific activity in mCES1/Sf9 was the highest at the length of four. mCES1/Sf9 also showed high levels of activity at lengths from two to five. However, the level of activity decreased as the carbon chain of PNPesters became longer, and when the substrate was PNPL, the activity level in mCES1/Sf9 was almost the same as that in mock/Sf9. According to the results of Western blotting and esterase activity staining after non-denaturing PAGE, mock/Sf9 showed a significantly low level of activity towards PNPesters.

Substrate specificity of recombinant mCES1 protein

Kinetic parameters of PNPA, temocapril and

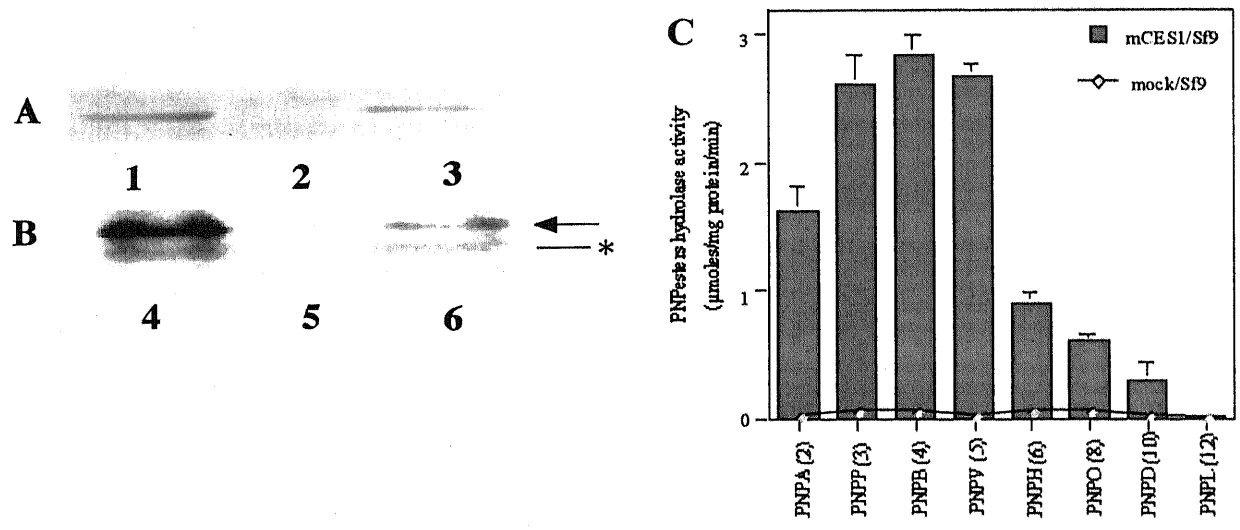

Fig. 6. Validation of recombinant mCES1 expression in Sf9 cells and chain length specificity for PNPester hydrolase activity. Western blotting (in panel A) and esterase activity staining after non-denaturing PAGE (in panel B) were performed to demonstrate the expression of mCES1 in Sf9 cells. Lanes 1 and 4, mCES1/Sf9 (5 μg and 7.2 μg, respectively); lanes 2 and 5, mock/Sf9 (5 μg and 26 μg, respectively); lanes 3 and 6, purified mouse CES1 (0.7 μg and 70 ng, respectively). Panel C shows the hydrolase activities of mCES1/Sf9 (bar chart) and mock/Sf9 (polygonal line) for PNPesters that contain carbon chains of various lengths, indicated in parentheses after the substrate name.

butanilicaine hydrolase activity in mCES1/Sf9 were analyzed. Since the levels of activity towards PNPA, temocapril and butanilicaine in mock/Sf9 were significantly low, if any, the background activity in mCES1/Sf9 was negligible. *Km* value and *Vmax* values of recombinant mCES1 to PNPA were 21.3 ± 3.05 μM and 2.72 ± 0.09 μmoles/mg protein/min, respectively. As purified mouse CES1 did, recombinant mCES1 showed capabilities to hydrolyze temocapril as well as butanilicaine. The *Km* value and *Vmax* value to temocapril were 389 ± 62.4 μM and 9.64 ± 1.28 nmoles/mg protein/min, and those to butanilicaine were 518 ± 19.0 μM and 430 ± 17.1 nmoles/mg protein/min, respectively.

Tissue expression profiles of mCES1 mRNA and protein

RT-PCR and esterase activity staining after non-denaturing PAGE were performed to obtain tissue expression profiles of mCES1 mRNA and protein, respectively. The results of PCR using mouse *GAPDH* gene-specific primers showed that genomic DNA did not mingle with mouse tissue cDNAs (Fig. 7A) and that the cDNAs were synthesized in equal amounts (Fig.7B). PCR using *mCES1* gene-specific primers revealed that mCES1 mRNA expression was present in the thymus, lung, heart, liver, kidney, small intestine, adipose tissue and testis (Fig. 7C). Expression of mCES1 mRNA was not detected in the brain. Nucleotide sequences of all of the PCR products showed 100% homology with that of mCES1 cDNA. In accordance with the results of RT-PCR, esterase activity staining after non-denaturing PAGE showed that activity of mCES1 protein was present in the thymus, lung, heart, liver, kidney, adipose tissue and testis (Fig. 7D). There was no band observed in the lane of the brain and small intestine at the same position as that of mCES1 protein. As in the case of esterase activity staining for which results are shown in Figure 6B, we found an accessory band at a faster migration point, which is thought to be a monomeric form of mCES1 [42], indicated by an asterisk.

I-I-IV Discussion

The enzyme responsible for temocapril hydrolysis in mouse liver microsomes has not been identified. In our preliminary work, a CES-

specific inhibitor [43], bis (*p*-nitrophenyl) phosphate, strongly inhibited temocapril hydrolase activity in mouse liver microsomes (by more than 90%) (data not shown). It has also been reported that temocapril can be a good substrate for hCE-1 [6, 39]. The temocapril hydrolase activity level of mCES2 expressed in Sf9 cells was under the detectable level (data not shown), though we have recently reported that one of the CES isozymes induced by DEHP treatment is mCES2 [20]. Thus, it is thought that the large increase in the level of temocapril hydrolase activity in liver microsomes of mice treated with DEHP was due to the induction of a mouse CES1 isozyme(s), and we identified the mouse CES1 isozyme by purification, cDNA cloning and functional expression in Sf9 cells as described below. The identification of the mouse CES1 isozyme is important for the study of drug metabolism since the mouse CES1 isozyme exhibits striking similarities to the human CES1 isozyme.

As predicted, significant contribution of mouse CES1 to temocapril hydrolase activity in both Control Ms and DEHP Ms was demonstrated by inhibition assays using specific antibodies (Fig. 4). The assays also demonstrated that 1) another mouse CES isozyme(s) is involved in temocapril hydrolysis in liver microsomes, 2) unidentified CES isozyme(s) was also induced by DEHP treatment, and 3) almost all of the temocapril hydrolysis activity in mouse liver microsomes is due to CES isozymes, including mouse CES1. Collectively, these results indicated that mouse CESs play an important role in ester-prodrug metabolism. Other mouse CES isozymes involved in temocapril hydrolysis remain unidentified. However, anti-CES RL1 antibodies could recognize CES ML1 as well as mouse CES1 (data not shown); thus, one possibility is that CES ML1 also contributes to temocapril hydrolysis in mouse liver microsomes. Further experiments are needed to determine other CES isozymes involved in temocapril hydrolysis and to determine whether they are induced by DEHP.

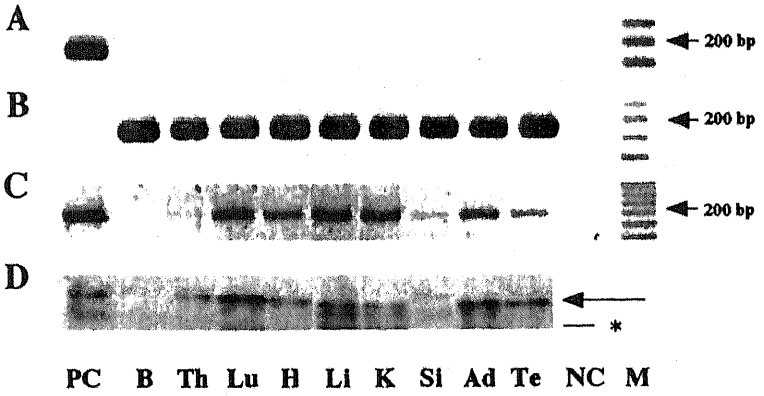

Fig. 7. Tissue expression profiles of mCES1 mRNA and protein. Panels A ~ C show the results of RT-PCR, and panel D shows the results of esterase activity staining after non-denaturing PAGE. PC, positive control; B, brain; Th, thymus; Lu, lung; H, heart; Li, liver; K, kidney; Si, small intestine; Ad, adipose tissue; Te, testis; NC, non-template control; M, DNA size marker. In panel A, mouse *GAPDH* gene-specific primers were used and mouse tissue RNA was used as a template. Mouse liver cDNA prepared in a previous study (Furihata et al., 2003) was used as a positive control. In panel B, mouse GAPDH mRNA expression was detected by using mouse tissue cDNAs as templates. In panel C, mCES1 mRNA expression was detected by using mouse tissue cDNAs as templates. mCES1 cDNA in the pFASTBAC1 vector was used as a positive control. Panel D shows mCES1 protein activity. Purified mouse CES1 (70 ng) was used as a positive control. Various amounts of mouse tissue homogenates were used: 20 μg of brain, 15 μg of thymus, 7 μg of lung, 10 μg of heart, 1 μg of liver, 5 μg of kidney, 5 μg of small intestine, 2.5 μg of adipose tissue, and 10 μg of testis homogenates. An arrow indicates the position of mCES1, and an asterisk indicates the accessory band.

Given that mouse CES1 was involved in DEHP-induced temocapril hydrolase activity in mouse liver microsomes, the next step was characterization of purified mouse CES1. Biochemical characteristics of purified mouse CES1 are very similar to those of mammalian CESs [1]. We should emphasize that purified mouse CES1 was present as a trimer, which is a specific characteristic of CES1A subfamily members. This subfamily includes hCE-1, CES D1 [19] and CES RH1 (also called pI6.1 or ES-10) [29, 44] (Fig. 8). All of these members have been shown to form trimers, whereas other family members behave as monomers [1]. The N-terminal amino acid sequence and immunological properties of purified mouse CES1 provided further experimental data showing that mouse CES1 is similar to other CES1A subfamily isozymes. The N-terminal amino acid sequence of mouse CES1 showed 100% homology to that of CES RH1/pI6.1, 85% homology to that of CES

D1, and 80% homology to that of hCE1 (Fig. 5). The finding that antibodies against CES D1 could specifically recognize mouse CES1 suggested that structural properties of these CES isozymes are similar. Taken together, the results suggest that mouse CES1 belongs to the CES1A subfamily.

Following protein characterization, the next issue was identification of the nucleotide sequence encoding mouse CES1. After we had submitted the nucleotide sequence of the obtained cDNA clone, mCES1, to DDBJ, EMBL and GeneBank nucleotide sequence databases (AB023631), another group reported cDNA coding mouse triacylglycerol hydrolase (mTGH) (AF378751) [36]. Except for one nucleotide in the region coding signal peptide, the nucleotide sequence of mTGH showed perfect homology to that of mCES1 (data not shown). In addition, other biochemical properties of mTGH [36] are very similar to those of mCES1 characterized in this study; thus, mCES1 and mTGH are considered to be the same enzymes with different names. This accordance is not surprising since recent studies have suggested that CESs are involved in fatty acid ester metabolism [19, 20, 22, 45] and should be useful information for elucidating physiological functions of CESs that remain unknown.

Overall homologies of the deduced amino acid sequence of mCES1 to CES1A subfamily isozymes were higher (92.7% to CES RH1/pI6.1, 79.6% to CES D1, and 77.6% to hCE1) than those to CES1B subfamily isozymes (71.3% to Hydrolase C, 70.3% to M-LK, and 69.4% to CES RL1), and mCES1 showed poor homology to CES2 isozymes (less than 50%, data not shown). Therefore, mCES1 is thought to encode a mouse CES1A subfamily isozyme.

The deduced amino acid sequence of mCES1 contained the same sequence as the N-terminal amino acid sequence of purified mouse CES1, indicating that mCES1 encodes mouse CES1. The results of a series of experiments using recombinant mCES1 supported this speculation.

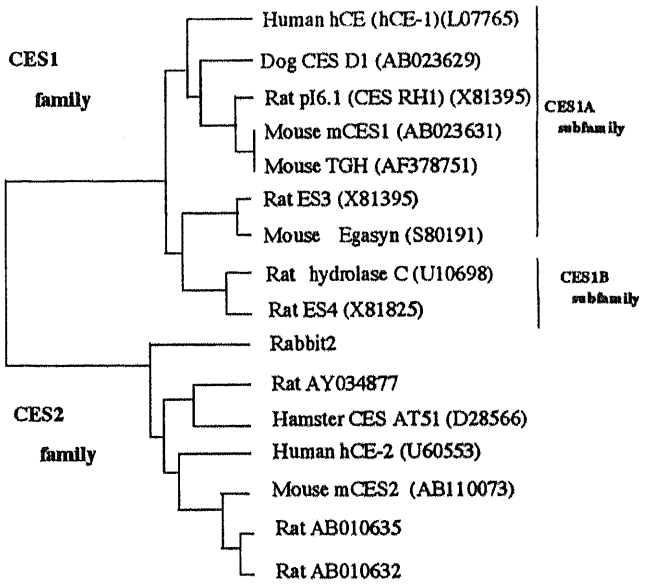

Fig. 8. Phylogenic tree of the CES family. The phylogenic tree was created using a simple unweighted pair group method of analysis (UP-GMA) dendrogram. The trivial name, species and gene bank accession number for their cDNA are shown.

Recombinant mCES1 protein exhibited identical biochemical characteristics, such as molecular weight or hydrolytic activity towards temocapril and butanilicaine, to those of purified mouse CES1. Based on all of our data, it is concluded that mCES1 encodes mouse CES1, belonging to the CES1A subfamily as shown in Figure 8.

Considering our finding that mCES1 was greatly involved in temocapril metabolism, tissue expression profiles of mCES1 should be clarified. RT-PCR was not a perfect quantitative method for mRNA expression. Nevertheless, the amplification levels of the specific band were apparently different between some tissue samples. Expression of mCES1 in the lung and kidney is noteworthy since these tissues are important for extrahepatic drug metabolism. It is notable that overall expression profiles of mCES1 are very similar to those of hCE-1, which is expressed in the brain, heart, lung, liver, and testis [2, 46], although there are a few discrepancies in their expression profiles, such as the case in the brain. Together with our other results, it is considered that mCES1 and hCE-1 are very similar enzymes. This may reflect functional similarities of these two enzymes in drug metabolism and fatty acid ester metabolism.

Given that mCES1 is an important CES1 isozyme involved in drug metabolism like hCE-1,

we should refer to mechanisms by which DEHP induced mCES1 since the induction of drug metabolism enzymes has considerable significance in pharmacokinetics and pharmacological actions of drugs metabolized by the enzymes. DEHP, a peroxisome proliferator (PP), has been shown to cause hepatomegaly and peroxisome proliferation, and eventually hepatocarcinogenesis, in rodents [47]. Recent studies have shown that many effects of DEHP in the rodent liver were mediated by peroxisome proliferator-activated receptor alpha (PPARα) [48]. Thus, it can be speculated that the induction of mCES1 by DEHP is mediated by PPARα, and it has been reported that the *mCES1* promoter has a PPAR response element (PPRE)-like motif [49]. However, the participation of PPARα in the regulation of *mCES1* gene expression is controversial. Hosokawa et al. [30, 31] reported that oral administration of clofibrate or perfluorinated fatty acids to rats for 3 days or 5 days, respectively, resulted in an increase in the level of CES RH1/pI6.1 expression. On the other hand, Dolinsky et al. [50] has recently reported that two weeks of clofibrate feeding did not significantly affect mCES1 expression in wild-type or PPARα-null mice. Poole et al. [51] showed that the changes in expression level of CES RH1/pI6.1 caused by PP treatment were time- and compound-dependent. The alteration of mCES1 expression level by PP in the liver may result from an adaptive secondary effect, and further studies are needed to understand the molecular mechanisms of PP by which mCES1 is induced.

In this study, we identified a mouse CES1 isozyme, mCES1, that was induced by DEHP. Purification, cDNA cloning and baculovirus-mediated expression of mCES1 revealed that mCES1 plays an important role in temocapril metabolism and that it belongs to the CES1A subfamily. Collectively, our results showed that mCES1 is very similar to hCE-1. Therefore, mCES1 is thought to be one of the critical determinants for pharmacokinetics and pharmacological actions of ester prodrugs as well as ester drugs. This work provides useful information for study of metabolism and dispositions of ester-prodrugs as well as ester-drugs. Elucidation of the substrate specificity of mCES1 and the mechanisms by which the *mCES1* gene is regulated is our next challenge.

I-II

Purification, molecular cloning, and functional expression of inducible liver acylcarnitine hydrolase in C57BL/6 mouse, belonging to the carboxylesterase multigene family

I-II-I Introduction

A variety of chemicals have been identified as peroxisome proliferators and it is known that they can alter a series of gene expressions associated with lipid metabolism [52]. In rodents, treatment with a peroxisome proliferator resulted in proliferation of peroxisome with drastic changes in the lipid condition, ultimately promoting hepatomegaly and hepatocarcinigenesis. It has been reported that treatment of DEHP caused remarkable depression in serum cholesterol and triglyceride levels in rats [53]. Mice treated with DEHP exhibited significant reduction in the amount of epidydimal addipose tissue and liver lipid storage (Furihata, T., Hosokawa, M., Satoh, T., and Chiba, K., unpublished observation). Mentlein et al. [21, 32] have reported that two rat CESs, characterized as acylcarnitine hydrolases, were induced by clofibrate administration [21, 32, 54]. Hosokawa et al. [30] have also reported that microsomal palmitoyl-CoA hydrolase, identical to rat CES RL1, was induced by clofibrate. These findings suggest that CESs contribute to the pharmacological and toxicological actions of peroxisome proliferators in lipid metabolism through their hydrolytic activity towards various endogenous fatty acid esters. Thus, it is important to identify and characterize the CES isozyme that was induced by peroxisome proliferators to understand the functions of the CESs in lipid metabolism.

In the previous section, we described that one of the induced CES isozymes was mCES1. In addition, the results of the preliminary experiments suggested that other CES isozymes were induced by DEHP treatment, and the CES isozyme(s) remains to be identified. Here, we purified acylcarnitine hydrolase induced by DEHP from mouse liver microsomes, cloned cDNA encoding the hydrolase, and expressed the clone in Sf9 cells. Based on the results, we conclude that DEHP-inducible acylcarnitine hydrolase is a member of the CES family that has not yet been characterized.

I-II-II Materials and Methods

Animals

Adult male C57BL/6 mice (Japan SLC Inc., Shizuoka, Japan) of 5 weeks and of 8weeks were used in this study. Procedures for treatment of 2% (w/w) DEHP to mice and preparation of liver microsomes were described in the section of I-I-II. Protein concentrations were determined by using a Bio-Rad Dc Protein Assay kit (Bio-Rad Laboratories).

Purification of inducible acylcarnitine hydrolase from DEHP-treated C57BL/6 mouse liver microsomes

DEHP-treated male C57BL/6 mouse liver microsomes were used in this experiment. To measure the enzymatic activity of inducible acylcarnitine hydrolase, pooled fractions were assayed with palmitoyl-*dl*-carnitine as a substrate. Microsomes were solubilized in 100 mM Tris-HCl buffer, pH 8.0, containing 0.5% cholic acid, at a final protein concentration of 2.30 mg/ml. The solution was stirred for 60 min at 4°C and then centrifuged at 105,000 x g for 60 min. The soluble fraction was applied to a column (3.0 x 8.0 cm) of Whatman DE-52 (Maidstone) that had been equilibrated with 10 mM Tris-HCl buffer, pH 8.0. The column was washed with the same buffer and then eluted with a stepwise NaCl gradient in 10 mM Tris-HCl buffer, pH 8.0. The peak

fraction was applied to a column (1.0 x 30 cm) of chromatofocusing gel PBE 96 (Amersham Biosciences) that had been equilibrated with 25 mM Bis-Tris-HCl buffer, pH 6.5. The enzyme was eluted with 270 ml of Polybuffer 74 (Amersham Biosciences), diluted at a ratio of 1:8, and adjusted to pH 4.0 with HCl. Then, the active fraction was applied to a column (1.5 x 5.0 cm) of ConA-Sepharose (Amersham Biosciences) that had been equilibrated with 20 mM Tris-HCl buffer (pH 7.6) containing 0.1 M NaCl, 0.1 mM $MgCl_2$ and 0.5 mM $CaCl_2$. The column was washed with 20 mM Tris-HCl buffer (pH 7.6) containing 0.5 M NaCl, 0.1 mM $MgCl_2$ and 0.5 mM $CaCl_2$. The fractions that were not bound to the ConA-Sepharose column was applied to a column (3.0 x 8.0 cm) of Hypatite C (hydroxylapatite) that had been equilibrated with 5 mM potassium phosphate buffer, pH 7.0. The column was washed with the same buffer and then eluted with a linear gradient of 5 – 90 mM potassium phosphate buffer, pH 7.0. The purified enzyme was tentatively named ACH M1 and could be stored at – 80°C for several months without loss of enzyme activity.

Preparation antibodies

Antibodies against ACH M1 were raised in male Japanese White rabbits (2.5-3.0 kg in body weight) according to the previously described procedure [29]. Anti-CES RL1 antibodies and anti-CES RL4 antibodies used in this study were prepared as described previously [14].

Inhibition assay by using specific IgG

Inhibition of hydrolase activity by using an anti-ACH M1 IgG was performed as described in the section I-I-II. All assay tubes were brought to the same final concentration of IgG with control IgG. Microsomes (0.2 mg) were solubilized with 0.5% cholic acid in 10 mM Tris-HCl buffer (pH 8.0) and were incubated with IgG (0.1 mg to 0.3 mg). The mixtures were left 3 hours at 4°C and then centrifuged at 10,000 x g for 5 min. The resulting supernatants were used for assay of hydrolase activity.

Peptide sequence of ACH M1 by mass spectrometry

Mass spectrometry of tryptic peptides was performed as follows. Protein band from SDS-PAGE was excised from Zn stained gel. In gel digestion of protein with sequencing grade modified trypsin (Promega, Madison WI) was performed essentially as described [55]. The resultant proteolytic peptides were analyzed by nano-LC tandem mass spectrometry (MS/MS) to generate peptide sequence information. A Q-TOF-2 hybrid mass spectrometer (Micromass, Manchester, UK) equipped with a nanoelectrospray ion source was used for nano-LC/ESI MS/MS experiment. The mass spectral data was searched against mouse ACH M1 sequence and SwissProt database using the ProteinLynx (Micromass) and Mascot software (Matrix Science, London, UK). The purified protien was analyzed from at least two different preparations.

Total RNA preparation and cDNA synthesis

C57BL/6 mice at 8 weeks of age were used. Total RNA was extracted from mouse liver and cDNA was synthesized as described in the section of I-I-II.

cDNA cloning and sequencing of mouse acylcarnitine hydrolase

The PCR amplification was carried out to obtain the full length of mouse liver acylcarnitine hydrolase cDNA using mouse liver cDNA described above as a template. The following primers were used: the sense, 5'-ATCTTAGCAGCACAGACTTAGGACT-3' and antisense, 5'-AACACATTTTTTTTGATACAGGGTA-3'. The amplified DNA fragments were sub-cloned into the pCR Blunt II TOPO vector (Invitrogen). The nucleotide sequences were determined as described in the section of I-I-II.

Expression of mouse acylcarnitine hydrolase in Sf9 cells

Expression of acylcarnitine hydrolase using baculovirus was carried out as described in the section of I-I-II. Expression of the hydrolase was analyzed by Western immunoblotting and hydrolase activity toward acylcarnitine, *p*-nitrophenylacetate and α-naphthylacetate.

Enzyme assay

The determination of the hydrolytic activity toward *p*-nitrophenylacetate (PNPA) (Nacalai Tesque, Kyoto Japan) was described in the section of I-I-II. The hydrolytic acitivities toward acylcarnitines and acylglycerides were determined by an enzymatic determination of released free fatty acid (NEFA C-test, Wako Chemicals, Tokyo, Japan) according to the method of Mentlein et al. [54]. The substrate concentration of palmitoyl-*dl*-carnitine for kinetic study ranged from 5 to 400 μM. The hydrolysis of decanoyl-CoA and palmitoyl-CoA was assayed in 30 mM Hepes buffer (pH 7.4) at 30°C by colorimetric determination (412 nm) of free thiol groups by reaction with 5,5'-dithiobis-(2-nitrobenzoic acid) as previously described [14].

Procedures for the determination of emocapril hydrolase activity was described in the section I-I-II.

Methylprednisolone hemisuccinate (MPHS) and methylprednisolone (MP) were purchased from Sigma. The MPHS hydrolase activity was determined essentially according to the method of Hattori et al. [56]. MPHS was dissolved in 1% dimethylformamide water. MPHS hydrolase activity was assayed in 50 mM citrate-phosphate buffer (pH 5.5), and methylprednisolone (MP), a metabolite of MPHS, was analyzed by using the following HPLC method. The HPLC system consisted of a model L7100 pump (Hitachi, Tokyo, Japan), a model L7400 UV detector (Hitachi), a model L7200 autosampler (Hitachi), a model D7500 integrator (Hitachi), and a COSMOSIL 5C18-MS-II 4.6 x 250 mm column (Nacalai Tesque). The mobile phase consisted of 0.05 M phosphate buffer (pH 7.0)-acetonitrile (65:35, v/v) and was delivered at a flow rate of 0.9 ml/min. MP was detected at a wavelength of 254 nm. A calibration curve was generated from 0.25 to 75 μM by processing an authentic standard substance through the entire procedure. Fluoxymesterone was used as an internal standard. The substrate concentration of MPHS for kinetic study ranged from 5 to 400 μM.

Temocapril hydrolase activity was assayed as described in the section I-I-II.

Palmitoyl-*dl*-carnitine, decanoyl-*dl*-carnitine, 1-monocaprylin, 1-monocapryn, 1-monolaurin, 1-monomyristin, 1-monopalmitin, 1-monoolein and 1-oleoyl-2-acetyl-*sn*-glycerol, decanoyl-CoA, palmitoyl-CoA, MPHS, MP, and fluoxymesterone were purchased from Sigma. Temocapril and temocaprilat were kindly obtained from Dr. Toshihiko Ikeda, Analytical and Metabolic Research Laboratories, Sankyo Co., Tokyo, Japan.

Specific activities of CES toward all substrates used were expressed in terms of amount of substrate hydrolyzed in 1 min under specified conditions. Enzyme kinetic parameters were estimated as described in the section of I-I-II

Other methods

Table 1. Purification of induced acylcarnitne hydrolase from DEHP-treated C57BL/6 mouse liver microsomes

Purification Step	Volume ml	Total protein mg	Total activity unit	Specific activity units/mg	Purification fold	Yield %
Microsomes	120	958	8824	7.53	1.0	100
Solubilized fraction	225	495	7830	15.8	2.1	88.7
DE52 240 mM NaCl	35	51.5	854	16.6	2.2	9.68
Chromatofocusing	4.9	1.37	195	142.1	14.9	2.21
Hydroxyapatite (Hypatite C)	6.6	0.57	110	192.4	25.5	1.25

Table 2. Kinetic parameters of purified ACH M1 for the hydrolysis of palmitoyl-*dl*-carnitine and *p*-nitrophenylacetate

Substrate	Concentration range (μM)	*Km* (μM)	*Vmax* (μmoles/mg/min)
Palmitoyl-*dl*-carnitne	100 - 500	98.8	1.67
p - Nitrophenyl acetate	10 - 600	392	353

SDS-polyacrylamidegel electrophoresis (SDS-PAGE), Western blotting, esterase activity staining after non-denaturing PAGE was performed as described in the section of I-I-II.

Mouse CES 1 isozyme, CES ML1, was purified by the same method as that used for the purification of acylcarnitine hydrolase except for the use of a ConA-Sepharose column instead of Hypatite C (hydroxylapatite).

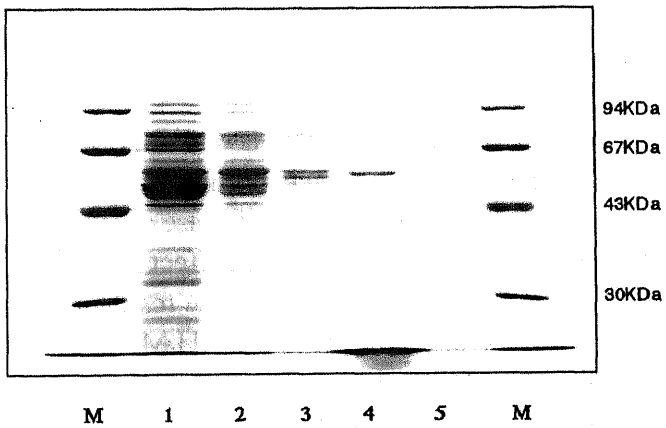

Fig.1. Analysis of proteins on SDS-PAGE in liver microsomes and purified preparations of ACH M1 according to purification steps. 1, microsomes; 2, solubilized microsomes; 3, DE52 240 mM NaCl eluate fractions; 4, chromatofocusing; 5, hypatite C (hydroxylapatite); M, Standard protein for relative molecular mass, phosphorylase b (94K), bovine serum albumin (67K), ovalbumin (43K), carbonic anhydrase (30K).

I-II-III Results

Effects of DEHP on acylcarnitine hydrolase activity in C57BL/6 mouse liver microsomes

Palmitoyl-*dl*-carnitine hydrolase activity of DEHP-treated C57BL/6 mouse liver microsomes was 20.9 nmoles/mg/min, while that of control microsomes was 3.2 nmoles/mg/min. Exposure of C57BL/6 mice to DEHP in their diet resulted in an approximately 7 fold increase in the activity of mouse liver microsomes.

Purification of inducible acylcarnitine hydrolase from DEHP-treated C57BL/6 mouse liver microsomes

Acylcarnitne hydrolase (ACH M1) was purified 25.5 fold with a yield of 1.25% by this purification method (Table.1). The hydrolase peak was eluted by 240 mM NaCl from DE-52 ion-exchange column chromatography at pH 4.5, and then the peak fractions were applied to a column of chromatofocusing gel. The active fractions were eluted out from the gel to apply them to a ConA-Sepharose column. However, the hydrolase peak fractions at pH 4.5 were not bound to the ConA-Sepharose column. Thus, the pH 4.5 fractions were applied to a Hypatite C (hydroxylapatite) column, and the hydrolase was eluted by

potassium phosphate gradient. The progress of acylcarnitine hydrolase purification was monitored by SDS-PAGE. The purified preparations exhibited a single band on SDS-PAGE (Fig. 1). A plot of relative mobility versus log of the molecular weight of the protein standards indicated a molecular weight of 60 kDa.

Substrate specificity of purified ACH M1

The purified ACH M1 showed hydrolytic activity toward palmitoyl-*dl*-carnitine. It also showed catalytic activity toward PNPA and α-naphthylacetate, which are typical CES substrates. The kinetic parameters of purified ACH M1 for the hydrolysis of palmitoyl-*dl*-carnitine and PNPA are listed in Table 2.

Immunological characters of ACH M1

In liver microsomes from DEHP-fed mice, anti-ACH M1 antibodies completely eliminated the induced palmitoyl-*dl*-carnitine hydrolase activity, while the control antibodies did not affect the activity (Fig. 2). On the other hand, the residual activity with the inhibition of anti-ACH M1 antibodies was almost the same as that of control antibodies in non-treated mouse liver microsomes.

Since purified ACH M1 possessed hydrolase activities toward CES substrates, the immunocross-reactivity of ACH M1 was assessed using two different anti-rat CES antibodies: anti-CES RL1 antibodies, which can recognize mouse CES1 family, and antibodies against rat CES RL4, which can recognize mouse CES2 family. Western immunoblotting showed that anti-rat CES RL4 antibodies were immunocross-reactive with purified ACH M1, while anti-rat CES RL1 antibodies were not (Fig. 3). As shown in Fig.4, both anti-CES RL4 antibodies and anti-ACH M1 antibodies inhibited the activity of ACH M1 but did not affect the activity of a purified mouse CES1 mixture, two purified mouse CES 1 family

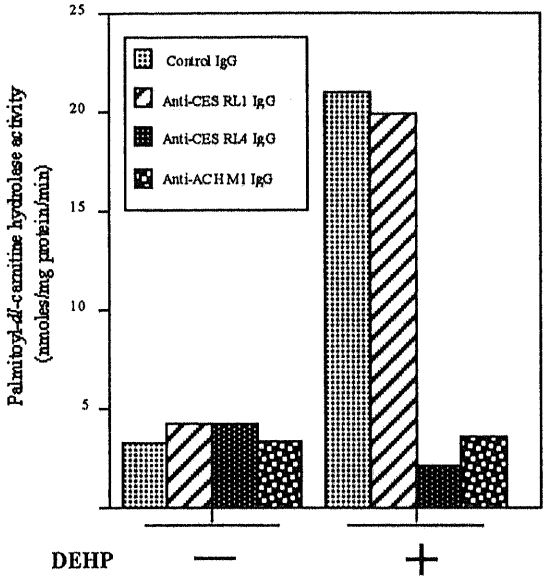

Fig.2. Inhibition of microsomal palmitoyl-*dl*-carnitine hydrolase activity by anti-rat CES and anti ACH M1 antibodies. Microsomes (0.2 mg) were solubilized with 0.5% cholic acid in 10 mM Tris-HCl buffer (pH 8.0) and were incubated with IgG (0.3 mg).

isozymes, mCES1 and CES ML1. On the other hand, the activity of the purified mouse CES1 mixture was inhibited completely by anti-CES RL1 antibodies, but anti-CES RL4 antibodies had no effect on the activity.

The effect of anti-CES RL4 antibodies toward microsomal acylcarnitine hydrolase activity was examined. Both anti-ACH M1 antibodies and anti-CES RL4 antibodies completely abolished the induced palmitoyl-*dl*-carnitine hydrolase activity in DEHP-fed mouse liver microsomes but failed to reduce the activity in non-treated mouse liver microsomes.

Peptide sequence of ACH M1 by mass spectrometry

ACH M1 protein band that was separated by SDS-PAGE was characterized by the LC/ESI MS/MS methods and the twelve peptides fragments of purified ACH M1 were identified. The database seaches revealed that these peptides showed 100% identical with those of the deduced amino acid sequence of mouse carboxylesterase 2 (BC015290) as shown in Table 3.

cDNA cloning of mouse ACH M1

The cDNA encoding mouse ACH M1 was obtained from cDNA of DEHP-treated mouse liver by PCR amplification. The specific primer was designed on the basis of the nucleotide sequence of the mouse CES2 family (BC015290). The obtained cDNA, referred to as mCES2, contained an in-frame initiation codon (ATG) and a termination codon (TAG). The cDNA was 1,747-bp long with an open reading frame of 1,686-bp encoding a polypeptide of 561 amino acid residues, which was identical to that encoded by BC015290.

Expression of mCES2 using baculovirus in Sf9 cells

The clone mCES2 was inserted into baculovirus and successively transfected into Sf9 cells. The homogenate of the cells infected with the recombinant virus showed a high level of PNPA hydrolase activity (11.2 μmole/mg protein/min). This level of activity was 243 times as high as that of mock baculovirus infected cells (data not shown). In tracing the activity according to the differential centrifugation procedure, more than 80% of the total hydrolase activity was recovered from the cytosols. The remaining activity was scattered in other fractions. Western immunoblot analysis using anti-CES RL4 identified a major immunoreactive protein produced by the recombinant virus in the cytosols (Fig. 6A). This protein co-migrated with the purified ACH M1, the estimated molecular mass of which was 60 kDa. On the other hand, mock baculovirus produced no protein that co-migrated with the purified ACH M1 detected by Western immunoblotting. A similar result was also

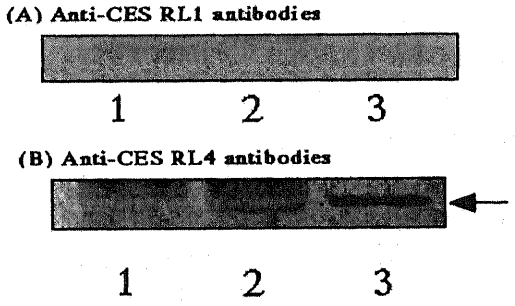

Fig.3. Western immunoblotting of ACH M1 using anti-rat CES antibodies. 1, control mouse liver microsomes (10 μg); 2, DEHP-treated mouse liver microsomes (10 μg); 3, purified ACH M1 (100 ng). Arrows indicate the purified preparations.

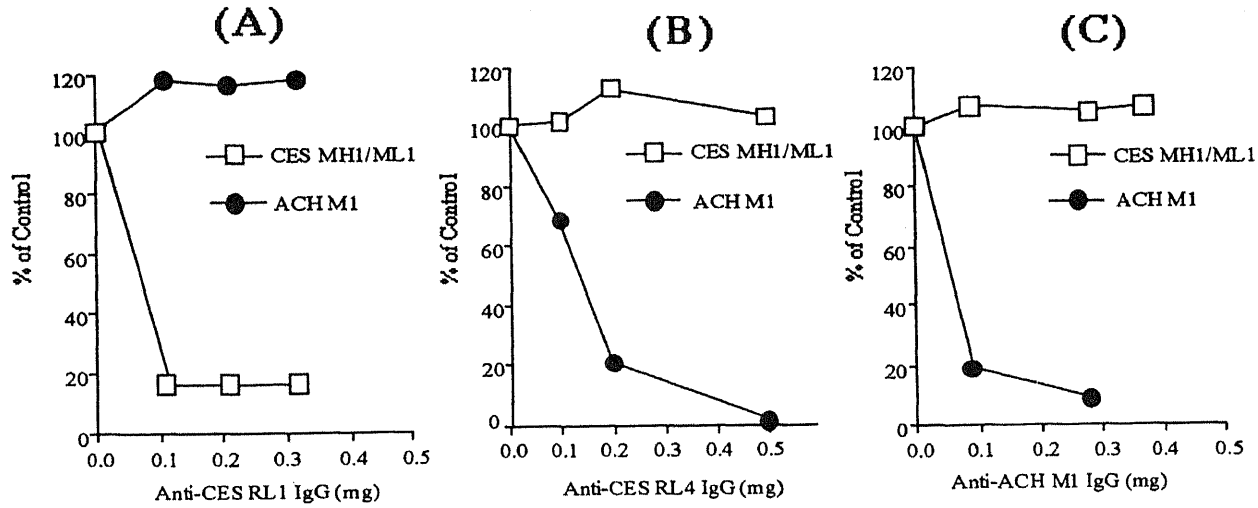

Fig.4. Effects of various antibodies on *p*-nitrophenylacetate hydrolase activity of ACH M1 and CES isozymes purified from C57BL/6 mice liver microsomes. A, anti-CES RL1 IgG; B, anti-CES RL4 IgG; C, anti-ACH M1 IgG; CES MH1/ML1, the mixtrue of purified CES MH1 and CES ML1.

obtained from esterase activity staining after non-denaturing PAGE (Fig. 6B). The recombinant protein showed a-naphtylacetate hydrolase activity on the gel at the same migration with purified enzyme, suggesting that the molecular size and the isoelectronic point (pI) of both proteins were equal.

Substrate specificity of recombinant mCES2

Hydrolase activity was analyzed using the cytosols of Sf9 cells expressing recombinant mCES2 (mCES2/Sf9). The *Km* value of the mCES2/Sf9 for PNPA (309 μM) was similar to that of purified ACH M1, while the kinetic parameters of palmitoyl-*dl*-carnitine hydrolase activity could not be calculated because of the high level of activity of mock/Sf9. mCES2/Sf9 nevertheless possessed a much higher level of acylcarnitne hydrolase activity than did mock/Sf9, and it preferentially hydrolyzed decanoyl-*dl*-carnitine (Table. 4). We also determined the hydrolytic activities towards other endogenous fatty acid derivatives (Table. 4). mCES2/Sf9 exhibited the hydrolytic activity toward palmitoyl-CoA and decanoyl-CoA. It also showed the activity toward various monoglycerides. In both cases, mCES2 preferred to hydrolyze medium-chain fatty acid esters. Interestingly, mCES2 showed a higher level of activity toward 1-oleoyl-2-acetyl-*sn*-glycerol than 1-monoolein. As for xenobiotic chemicals, mCES2 showed significantly high hydrolase activity to MPHS, while it did not to temocapril.

Table 3. Peptides identified by LC/MS/MS for purified ACH M1. The peptides from purified ACH M1 was compared with the deduced amino acid sequence of BC015290.

Peptide number	Peptide sequence	Peptide position in the deduced amino acid sequence of BC015290
1	NTHTGQIQGSLIHVK	37-51
2	FAPPEAPEPWSGVR	75-88
3	LGVLGFFSTGDQHAR	181-195
4	GNWGYLDQAAALR	196-208
5	WVQQNIAHFGGNPDR	209-223
6	LSGCEAMDSQALVR	279-292
7	GKSEAEILAINK	296-307
8	MIPAVVDGEFFPR	311-323
9	ENLQAVLK	368-375
10	SHAPVYFYEFQHPPSYFK	431-448
11	YWANFAR	492-498
12	LQFWTK	537-542

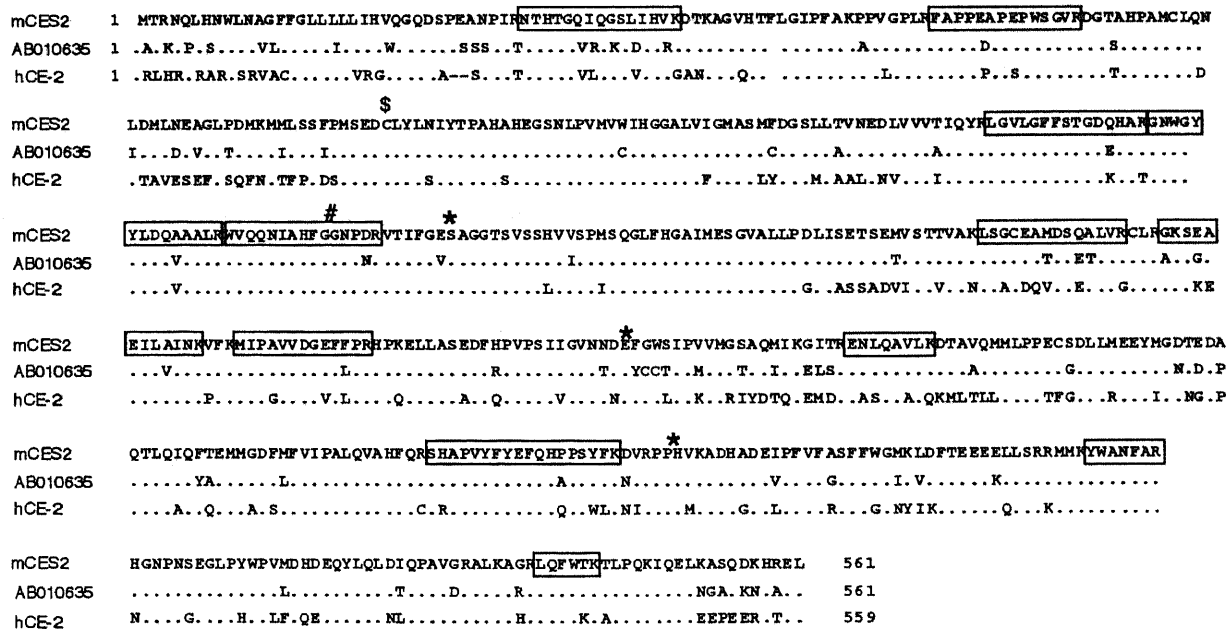

Fig. 5. Comparison of mCES2 deduced amino acid sequences with those of rat (AB010635) and human CES hCE-2. *, catalytic triad; #, oxyanion hole loop; $, conserved cysteine residue; underline, endoplasmic reticulum retention motif; box, the peptides identical to those of ACH M1 which were identified by mass spectrometry.

I-II-IV Discussion

In order to identify the peroxisome proliferator-inducible acylcarnitine hydrolase in mouse liver microsomes, we purified and characterized the acylcarnitine-hydrolyzing enzyme present in DEHP-treated C57BL/6 mouse liver microsomes. The results showed that a hydrolase, purified from DEHP-treated mouse liver microsomes and that was designated ACH M1, exhibited the high levels of palmitoyl-*dl*-carnitine hydrolase activities and of PNPA hydrolase activity (Table 2). Experiments on inhibition of the hydrolase activity using anti-ACH M1 antibodies indicated that ACH M1 did not contribute to the basal level of palmitoyl-*dl*-carnitine hydrolase activity in mouse liver microsomes but played a major role in DEHP-induced activity (Fig. 2). Therefore, ACH M1 appears to be an inducible type of acylcarnitne hydrolase.

The immunological characterization showed that anti-rat CES2 isozyme (CES RL4) antibodies could detect ACH M1 and inhibited its hydrolase activity, whereas anti-rat CES1 isozyme (CES RL1) antibodies failed to recognize ACH M1 (Figs.2-4). Furthermore, the peptide fragmemnts of ACH M1 identified were found to completely cover 26% of the total deduced amino acid sequence of mouse carboxylesterase 2 (BC015290) (Table 3). Therefore, the purification and characterization of ACH M1 purified in the present study suggest that it is thought to be a member of the CES2 family.

To identify the *ACH M1* gene, cDNA cloning was performed. We cloned mCES2 of which the deduced amino acid sequence was completely identical to BC015190. The deduced amino acid sequence of mCES2 contained several motifs characteristics of CES isozymes and other serine hydrolases [1, 2, 57, 58] (Fig.5). For example, it contained 4 Cys residues that are highly conserved in serine hydrolases and may function as specific disulfide bonds. The sequence also possessed

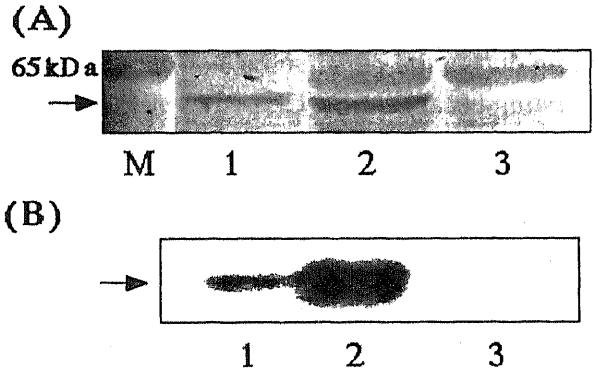

Fig.6 Expression of mouse liver mCES2 in Sf9 insect cells infected with recombinant baculovirus as determined by Western immunoblotting and nondenaturing gel electrophoresis with staining for esterase activity. (A), Western immunoblotting analysis using anti-CES RL4 antibodies. M, protein marker; 1, purified ACH M1 (100 ng); 2, mCES2/Sf9 (20 μg); 3, Mock/Sf9 (20 μg). (B), Esterase activity staining after non-denaturing PAGE. 1, purified ACH M1 (45 μg); 2, mCES2/Sf9 (10 μg); 3, Mock/Sf9 (10 μg). Arrows indicate the purified preparations.

Table 4. Determination of hydrolase activity of mCES2/Sf9 and mock/Sf9 towards various fatty acid esters. Values are the means ± S.D. of 3 determinations. N.D., not detectable.

Substrate	Concentration (μM)	Specific activity [a]	
		mCES2/Sf9	Mock/Sf9
Palmitoyl-*dl*-carnitne	500	126.8±11.3	80.3±2.2
Decanoyl-*dl*-carnitne	500	136.0±14.5	87.7±4.0
Palmitoyl-CoA	40	36.1±0.6	15.2±2.2
Decanoyl-CoA	40	34.3±3.1	10.9±0.7
1-monocaprylin	400	76.9±4.0	N.D.
1-monocaprin	400	58.2±5.6	N.D.
1-monolaurin	400	31.6±4.5	N.D.
1-monomyristin	400	35.7±4.7	N.D.
1-monopalmitin	400	25.4±0.006	N.D.
1-monoolein	400	26.2±3.6	N.D.
1-oleoyl-2acetyl -*rac*-glycerol	400	43.3±1.8	N.D.
Methylprednisolone hemisuccinate	400	43.3±1.8	N.D.
Temocapril	180	N.D.	N.D.

a, the activities to palmitoyl-*dl*-carnitine and decanoyl-*dl*-carnitine were expressed as pmoles/mg protein/min. The activities to other substrates were expressed as nmoles/mg protein/min.

common structures of the serine hydrolase superfamily, Ser^{204}, Glu^{321} and His^{428}, which comprise a catalytic triad, and Gly^{124}-Gly^{125}, which may be a part of the oxyanion hole. These residues are highly conserved in CES isozymes, acetylcholine-esterases, and butyrylcholinesterases. N-X-S/T motif, a putative N-glycosylation site found in most mammalian CES genes, however, did not exist in the deduced amino acid sequence

of mCES2. This was in accordance with the fact that ACH M1 did not bind to the Con-A Sepharose column during the purification step. This is very interesting because most CES isozymes are high-mannose-type glycosylated proteins and there have been a report that glycosylation is essential for maximal catalytic activity of human CES isozyme [1, 12]. However, glycosylation is not required for the catalytic activity of ACH M1.

Figure 5 shows a comparison of the deduced amino acid sequence of mCES2 with those of other CES 2 family isozymes, AB010635 [59] and hCE-2 [4]. As expected, the deduced amino acid sequence of mCES2 showed a higher degree of similarity to those of the CES2 family than to those of other CES families. A comparison of all of the amino acid sequences showed that AB010635, hCE-2, AT51 [60] and rabbit 2 [61] are 85.7, 70.9, 72.3 and 69.4% identities to mCES2, respectively. Recently, we have described that CES isozymes were divided into four groups based on the sequence homologies [1]. There is about 70% identify within a family and about 50% identify between families. This classification is also supported by phylogenic analysis. Figure 8 shows that the phylogenic tree containing some mammalian CES isozymes was created using a simple unweight pair group method of analysis (UPGMA) dendrogram in this study. There are two families of CESs according to this analysis. As expected, mCES2 belong to CES2 family in this analysis, and is close to rat CES2 isozymes (AB010635, AB010632).

In the expression system using baculovirus, recombinant mCES2 mostly existed in the cytosols. The reason why recombinant mCES2 was localized in the cytosols despite the fact that it possessed a C- terminal endoplasmic reticulum retention signal, HXEL motif [42, 62], is currently unknown. Intracellular localization of recombinant mCES2 was different from that expected, but its molecular weight, molecular size, pI amd immuno-crossreactivity were identical to those of

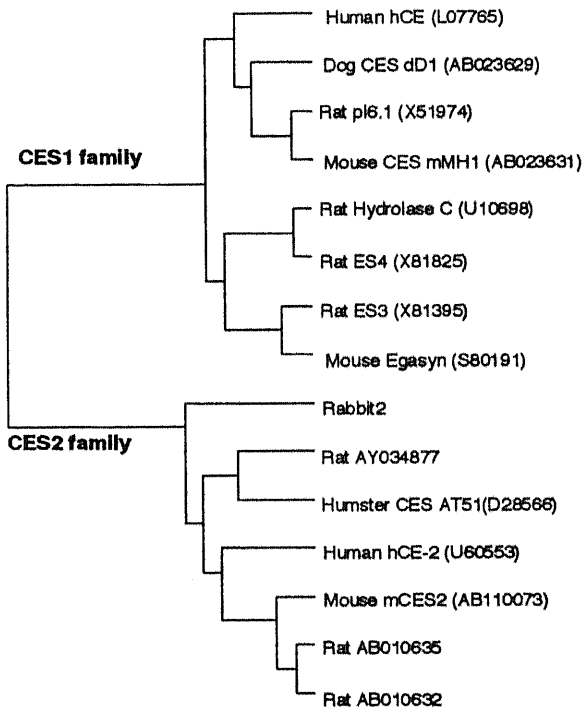

Fig.8 Phylogenic tree for CES families. The phylogenic tree was created using a simple un-weight pair group method of analysis (UPGMA) dendrogram. The trivial name, species and gene bank accession number for their cDNA are noted. References for the cDNA sequence was shown as follows: hCE, (34); CES dD1, (4); pI6.1, (43); Hydrolase C, (44); ES4, (11); ES3, (45); Egasyn, (46); Rabbit2, (38); AY034877, (35); CES AT51, (37); hCE-2, (36); AB010635, (35). mCES2 was reported in the present study. Others were not published.

purified ACH M1 (Table 3, Fig.5, 6). In addition, the recombinant mCES2 could cleave medium- and long-chain acylcarnitines (Table.4). Together, these results strongly indicate that ACH M1 is encoded by mCES2. It has been shown that most CES isozymes can hydrolyze several substrates, and mCES2 also exhibited broad substrate specificities. Among endogeneous substrates, mCES2 preferentially hydrolyzed acylglycerols. Thus, in the basal level of expression, mCES2 may function as a microsomal acylglecerol hydrolase. The hydrolase activity of mCES2 to acylglycerol seems subject to the level of esterification of glycerol since the level of hydrolase activity toward 1-oleoyl-2-acetyl-*sn*-glycerol is higher that that to 1-monoolein. Since most CES isozymes act as drug metabolizing enzyme, we determined the hydrolase activity to prodrugs. As expected, mCES2 can hydrolyze

ester-prodrug, MPHS; thus mCES2 is also thought to function a drug metabolising enzyme. Detailed amalysis for substrate specificities of mCES2 are definitely needed to clarify the roles of mCES2 in drug metabolism.

It is very difficult to speculate the physiological significance of the existence and induction of mCES2 in the endoplasmic reticulum since mCES2 shows promiscuous substrate specificity to endogeneous fatty acid esters. One possible function of mCES2 is that, as suggested by Mentlein et al. [21], mCES2 may detoxify membrane-lysing concentrations of acylcarnitine in hepatocytes with the treatment of peroxisome proliferator. Paul et al. [63] showed that clofibrate greatly increased carnitine and acylcarnitine concentrations in the liver (by 6 and 5 fold, respectively). Another possible function of mCES2 is control of very low-density lipoprotein (VLDL) secretion from the liver. It has recently been reported that triacylglycerol utilized for the assembly of a VLDL complex was synthesized from diacylglycerol and acyl-CoA, and that microsomal acyl-CoA was generated from acylcarnitine by carnitne acyltransferase in intraluminal spaces of microsomes [64]. mCES2 might hydrolyze the acylcarnitine, acyl-CoA and acylglycerol, eventually repressing the VLDL secretion.

In conclusion, we have purified and chacaterized an ACH M1 from DEHP-treated mouse liver microsomes, and we cloned the cDNA encoding ACH M1, named mCES2, and expressed it in Sf9 cells and characterized it. The results of the present study suggest that mCES2/ACH M1 is an inducible mouse liver microsomal acylcarnitine hydrolase and it belonged to the member of the CES2 family that can hydrolyze medium- and long-chain acylcarnitines as well as acyl-CoA, acylglycerol and prodrug. This mCES2/ACH M1 may play an important role in fatty acid metabolism amd drug metabolism through its broad substrate specificity.

I-III

Dexamethasone-induced methylprednisolone hemisuccinate hydrolase: Its identification as a member of the rat carboxylesterase 2 family and its unique existence in plasma

I-III-I Introduction

Much interest has been taken by both clinicians and researchers in the induction of expression of drug-metabolizing enzymes by various chemicals, including dexamethasone, which is one of the potent inducers of various drug metabolizing enzymes. It has been shown that dexamethasone can strongly induce cytochrome P450s (CYPs) in rodents and human [65, 66] which results in the alteration of pharmacokinetics and pharmacodynamics of a co-administrated drug that is metabolized by the CYP [67, 68]. As for CESs, it has been reported that dexamethasone caused a slight increase in human CES isozymes in human primary hepatocytes [16]. In addition, dexamethasone possesses a potent and interesting ability to affect CES expression in the rat liver. Hattori et al. [56, 69] reported that methylprednisolone hemisuccinate (MPHS) was hydrolyzed to methylprednisolone *via* CES in rat liver microsomes and that several clinically used glucocorticoids, including dexamethasone, caused a remarkable increase in the level of this hydrolytic activity. In contrast to the report of induction of CES activity, some researchers have shown that the level of microsomal PNPA hydrolase activity was significantly decreased in rat liver microsomes [16, 70, 71]. This apparent contradiction in the same animals is probably due to the different methods for determination of CES activity by using different CES substrates; thus, it is hypothesized that the CES isozyme contributing to PNPA hydrolysis in rat liver microsomes is different from the one contributing to MPHS hydrolysis. However, the rat CES isozymes responsible for MPHS hydrolysis in rat liver microsomes have not been identified.

The purpose of this study was to identify the dexamethasone-induced CES isozyme that can hydrolyze MPHS in the rat liver. The results revealed that the dexamethasone-induced CES isozyme belongs to the CES2 family (rCES2) and possesses different biochemical properties from those of known rat CES1 isozymes. We also identified the gene encoding rCES2 by cDNA cloning and functional expression in Sf9 cells. Furthermore, we found that rCES2 was present in plasma and that the amount of rCES2 protein in plasma was increased by dexamethasone accompanying an increase in the level of MPHS hydrolase activity.

I-III-II Materials and Methods

Animals, dexamethasone treatment and preparation of tissue samples

Adult male Sprague-Dawley rats (Japan SLC Inc., Shizuoka, Japan) of 7 weeks in age were used in this study. The rats were housed in a 1800 - 0600 h dark/0600 – 1800 h light cycle with free access to chow and water. One group of rats (n = 3) was given dexamethasone (Wako Pure Chemicals, Osaka, Japan) in corn oil by intraperitoneal injection at a dose of 5 mg/kg body weight for 4 consecutive days, and another group (n = 3) was given corn oil in the same way. The rats were sacrificed on day 5 after injection, and the livers were removed, weighed and perfused with 1.15% KCl. Microsomes were isolated by differential centrifugation as described previously [29] and were resuspended in SET buffer (0.25 M sucrose, 1 mM EDTA and 10 mM Tris, pH 7.4). Blood was also collected from the aorta of each rat with a syringe under diethyl ether anesthesia, and plasma was obtained by centrifugation

(1,500 x g for 10 min) of the blood specimens. These samples were stored at -80°C until used. Control (corn oil) and dexamethasone-treated rat liver microsomes are referred to here as Control Ms and Dex Ms, respectively, and, similarly, control (corn oil) and dexamethasone-treated rat plasma are referred to here as Control Plasma and Dex Plasma, respectively. Protein concentrations were determined by using a Bio-Rad Dc Protein Assay kit (Bio-Rad Laboratories, Hercules, CA, U.S.A.). Glutamate-oxaloacetate transaminase (GOT) and glutamate-pyruvate transaminase (GPT) activities were measured by using a GOT-UV TEST Wako and a GPT-UV TEST Wako (Wako Pure Chemicals), respectively. All subsequent procedures were performed at 0 - 4°C.

SDS-polyacrylamide gel electrophoresis (SDS-PAGE), Western blotting and esterase activity staining after non-denaturing PAGE

SDS-PAGE was performed with 10% acrylamide gel. After the electrophoresis, either coomassie brilliant blue staining (Quick-CBB kit; Wako Pure Chemicals) or Western blotting (Vectastain Elite ABC kit; Vector Laboratories, Inc., Burlingame, CA, U.S.A.) was performed. In both cases, the procedure was performed according to the manufacturer's directions. Specific antibodies used in Western blotting were anti-CES RH1 antibodies, anti-CES RL1 antibodies and anti-CES RL4 antibodies, which were previously prepared [29, 72]. Anti-β-actin antibodies and secondary antibodies for them were purchased from Sigma (St. Louis, MO, U.S.A).

Esterase activity staining after non-denaturing PAGE was performed as described in the section I-I-II.

In these experiments, purified rat CES isozymes were used as positive controls [29, 72].

Determination of hydrolase activity

MPHS hydrolase activity was determined essentially according to the method of Hattori et al. [56] as described in the section I-II-II.

Hydrolysis of PNPA was determined colorimetrically in 50 mM Tris-HCl buffer (pH 8.0) at 30 °C by measuring the amount of *p*-nitrophenol released as described in the section I-I-II. The substrate concentration of PNPA for determination of hydrolytic activity was 500 μM.

Specific activities of CES towards two substrates used were expressed in terms of the amount of substrate hydrolyzed in 1 min under specified conditions. Enzyme kinetic parameters were estimated using a computer program (DeltaGraph ver 4.5, SPSS Inc., Chicago, IL) designed for non-linear regression analysis as described previously [20]. Each mean kinetic value was the average of three individual experiments with ± S.D. Student's *t*-test was performed to determine significance of difference between two groups. P values less than 0.05 were taken to be significant.

Inhibition assay by using specific IgG

The IgG fractions of rabbit antiserum or control serum were purified from whole antibodies as described in the section I-I-II.

Immunoprecipitation with specific IgG was performed as described in the section I-I-II. Either anti-CES RL4 IgG (0.1 mg) or control IgG (0.1 mg) was used. After the incubaton with IgG and protein G agaronse, the supernatant was removed and used for a determination of MPHS hydrolase activity as described above. Inhibition assay was also performed for Control Plasma and Dex Plasma in the same way except for the solubilization by cholic acid.

Immunoprecipitation and determination of amino acid sequence of dexamethasone-induced carboxylesterase by nano-electrospray ionization tandem mass spectrometory (nano-ESI/MS/MS) analysis

Solubilized Dex Ms and Dex Plasma were incubated with anti-CES RL4 IgG for 12 h at 4 °C and centrifuged at 18,000 x g for 30 min. After washing with 10 mM Tris-HCl buffer, the precipitates were dissolved in solubilization buffer containing SDS. The samples were incubated in a water bath for 60 min at 60 °C and subjected to SDS-PAGE. Then, the separated proteins were visualized by coomassie brilliant blue as described above. The single band separated was taken out from the gel. Peptide sequnece of the protein was determined by nano-ESI/MS/MS analysis (consigned to

Exigen; Tokyo, Japan).

Determination of amino acid sequence of purified CES RL4

Purified CES RL4 (100 μg) was digested with endoproteinase Glu-C (V8 protease) (Sigma) in 100 mM Tris-HCl buffer (pH 8.0) containing 0.1 % SDS. The mixture was incubated for 3 h at 37 °C and then subjected to reverse-phase HPLC described above. The column used was a TSK octadecyl-4 PW (TOSOH, Tokyo, Japan). An eluted peptide was sequenced by automated Edman degradation using a model 470A gas-phase sequencer (Applied Biosystems, Foster City, CA) with an on-line Spectra-Physics Model SP8100 PTH amino acid analyzer (Applied Biosystem) as described previously [14].

Total RNA preparation and reverse transcription-polymerase chain reaction (RT-PCR)

Total RNA was extracted from each liver sample (control liver: n = 3, dexamethasone-treated liver: n = 3) using TRIzol reagent (Invitrogen, Calsbad, CA) as described in the section I-I-II. For certification of synthesis of equal amounts of cDNA, PCR was performed (94 °C for 15 s, 49 °C for 20 s, 68 °C for 40 s and 35 cycles) using a set of primers for detection of *rat glyceraldehyde-phosphate dehydrogenase* (GAPDH) gene expression: sense, 5'-TGCACCACCAACTGCTTA-3'; anti-sense, 5'-GGATGCAGGGATGATGTTC-3'. Another set of primers (sense, 5'-CAAGAGTGGAGCAGAGATTC-3'; anti-sense, 5'-GTACTTCATCATCCGCCTAC-3') was used for PCR (94 °C for 15 s, 55 °C for 30 s, 68 °C for 45 s and 36 cycles) to detect AB010635 gene expression. The PCR product was purified by using a Wizard SV Gel and PCR Clean-up System (Promega, Madison, WI). The nucleotide sequences of the products were determined by using a Dye Terminator Cycle Sequencing-Quick Start Kit and CEQ 2000 DNA Analysis System (Beckman Coulter, Fullerton, CA) and were confirmed by sequencing at least twice in each direction.

cDNA cloning of AB010635

PCR amplification was carried out to determine the coding region of AB010635 cDNA using rat liver cDNA described above as a template. The following primers were used: sense, 5'-TAGCCCGACGAACTGAGAACTG-3'; antisense, 5'-CCACACTCTGTTCCTTTCACCA-3'. The amplified DNA fragments were subcloned into the pCR-Blunt II TOPO vector (Invitrogen). The nucleotide sequences were determined as described above and were confirmed by sequencing at least twice in each direction.

Expression of AB191005/AB010635 in Sf9 cells

Expression of AB191005/AB010635 by using a BAC-TO-BAC Baculovirus Expression System (Invitrogen) was carried out in accordance with the directions of the manufacturer as described in the section I-I-II. Cytosolic fractions of Sf9 cells transfected with mock baculovirus and those expressing AB191005/AB010635 were prepared by subjecting the cell lysate to centrifugation (105,000 x g for 60 min at 4 °C) and were used for the assays.

I-III-III Results

Effects of dexamethasone on carboxylesterase activity in rat liver microsomes

Intraperitoneal injection of dexamethasone for 4 consecutive days resulted in a marked increase in the level of MPHS hydrolase activity (24.5 fold increase, $P<0.005$), while the level of hydrolase activity towards PNPA was decreased ($P<0.005$) (Fig. 1). These changes are in good agreement with previously reported results [56, 70]. In respect to physiological effects of dexamethasone, rats given dexamethasone exhibited hepatomegaly accompanying increases in GOT and GPT activity levels, although these increases were not statistically significant and were not correrated with the level of increase in MPHS hydrolase activity in microsomes (data not shown).

Identification of carboxylesterase induced by dexamethasone in rat liver microsomes

To identify the dexamethasone-induced CES isozyme, esterase activity staining after non-denaturing PAGE was performed. As shown in Fig. 2A, induced esterase activity was detected at the same migrated position as that of purified CES RL4. The protein induced by dexamethasone was also detected by Western blotting using CES RL4 specific antibodies at the same migrated position as that of purified CES RL4 (Fig. 2B). These results indicated that dexamethasone induced a CES isozyme that was closely related to CES RL4 in terms of molecular weight of a subunit, isoelectronic point and immunocrossreactivity. It was also found that the level of expression of the dexamethasone-induced CES isozyme was very low in normal conditions. As for other CES isozymes, the results showed that expression of both CES RH1 (also named ES-10, pI6.1 or hydrolase A) and CES RL1 (also named ES-4 or hydrolase B) were repressed, in consistent with previous results. The activity band of CES RL1 appeared as a doublet in Fig. 2A. Sanghani et al. [59] obtained the same results

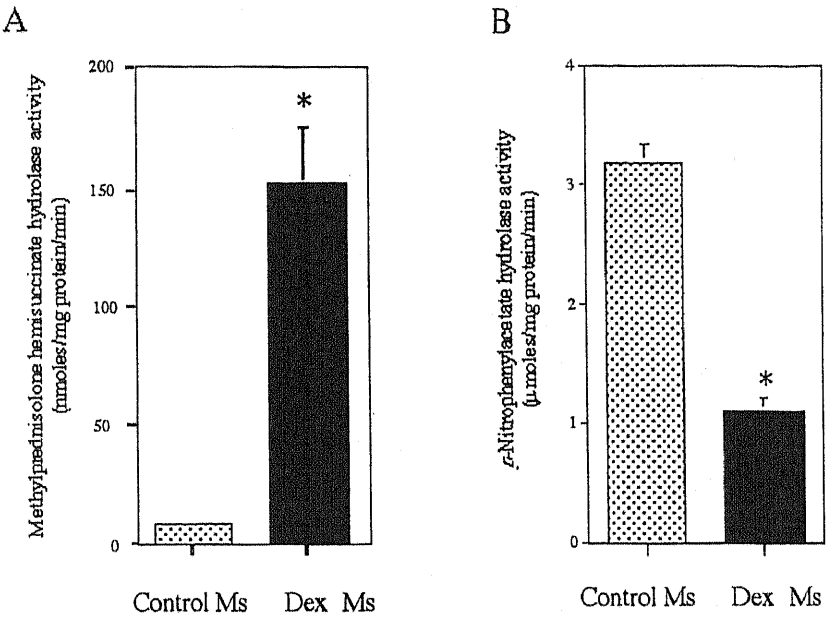

Figure 1. Effects of dexamethasone on microsomal CES activities in rat liver. A, MPHS hydrolase activity; B, PNPA hydrolase activity. The sample number in each group was three. Each value is the mean of three independent assays (± S.D.). * indicates statistically significant difference compared with Control Ms (P<0.005).

and concluded that both bands were originated from ES-4 by liquid chromatography ESI/MS analysis.

The results described above implied that the dexamethasone-induced CES isozyme was identical to CES RL4. To determine this possibility, amino acid sequences of both proteins were analyzed. A peptide fragment containing 25 amino acid residues of CES RL4 (including two undefined residues, N-

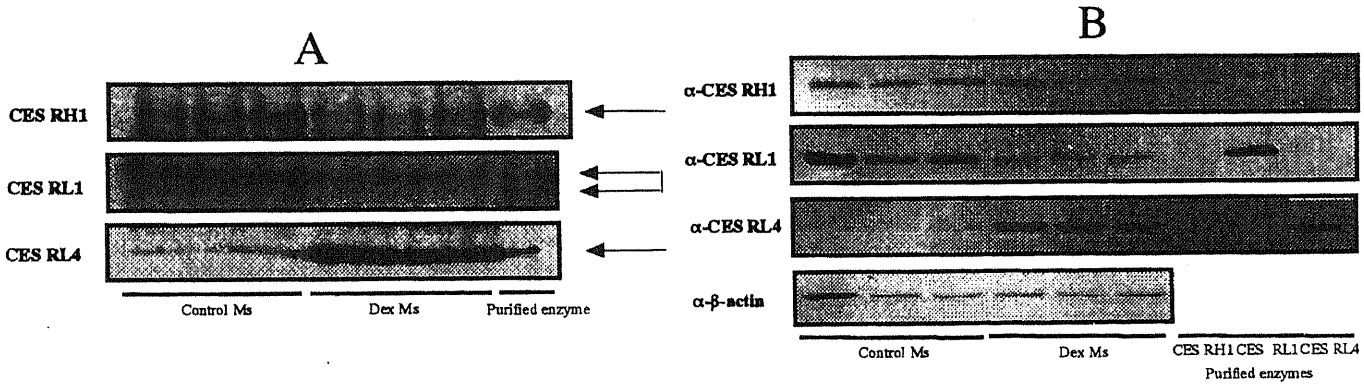

Figure 2. Identification of dexamethasone-induced CES isozyme in rat liver microsomes. The sample loaded in each lane is indicated below the panel in A and B. A, Esterase activity staining after non-denaturing PAGE. The amount of microsomal proteins loaded in each lane was 5 μg. The name of the CES isozyme detected in each panel is shown on the left side of the panel, and an arrow(s) indicates the corresponding activity band(s). Purified CES isozymes (CES RH1, CES RL1, and CES RL4, 100 ng each) were used as positive controls. B, Western blotting. The amount of microsomal proteins loaded in each panel was 2.5 μg. Anti-CES RH1 antibodies, anti-CES RL1 antibodies, and anti-CES RL4 antibodies were used to detect the expression of the corresponding CES isozyme as indicated on the left side of each panel. Anti-β-actin antibodies were used to detect β-actin protein for verification that a similar amount of protein was loaded in each lane. Purified CES isozymes (CES RH1, CES RL1, and CES RL4, 100 ng each) were used as positive controls.

QHAPXYFKNVRPXHVKADHADEVPF-C) was identified, and several peptide fragments derived from the dexamethasone-induced CES isozyme were identified. A database search revealed that the amino acid sequence of these peptide fragments obtained from CES RL4 and dexamethasone-induced CES isozyme were identical to that of AB010635 (Fig. 5A). These findings indicated that CES RL4 and dexamethasone-induced CES isozyme are probably the same protein. The dexamethasone-induced CES isozyme is therefore hereafter named CES RL4.

Inhibition of MPHS hydrolase activity in rat liver microsomes by anti-CES RL4 IgG

Inhibition assays were performed using anti-CES RL4 IgG to determine whether CES RL4 is responsible for the increase in the level of MPHS hydrolase activity in rat liver microsomes induced by dexamethasone. As shown in Fig. 3, anti-CES RL4 IgG significantly inhibited MPHS hydrolase activity in both Control and Dex Ms (decreases to 53.8% and 21.8% of that of control IgG, respectively). Collectively, the results were in good agreement with those obtained by Western blotting and esterase activity staining. The findings showed that the increase of the level of MPHS hydrolase activity in Dex Ms resulted from the induction of CES RL4. We also determined the contribution of CES RL4 to hydrolysis of PNPA in Dex Ms. In contrast to the finding of strong inhibition of MPHS hydrolase activity, the effect of anti-CES RL4 IgG on microsomal PNPA hydrolase activity was small (decrease to 82.7% of that of control IgG).

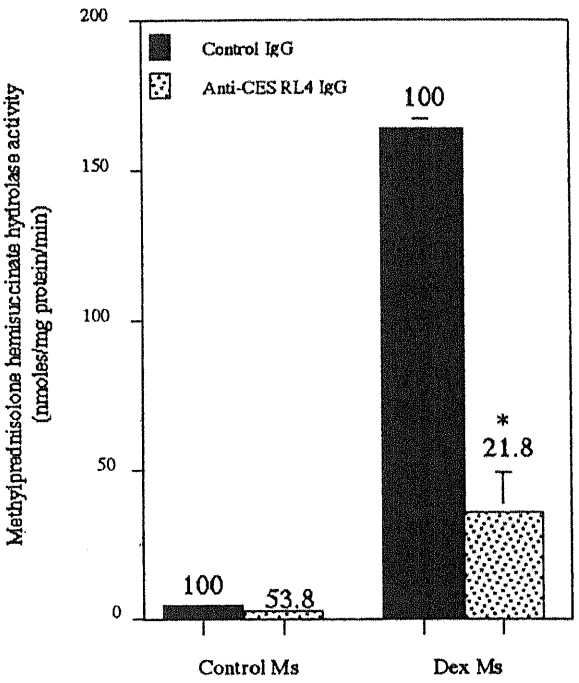

Figure 3. Effects of anti-CES RL4 IgG on MPHS hydrolase activity in rat microsomes. Control IgG (0.1 mg) and anti-CES RL4 IgG (0.1 mg) were used in the assays for which results are shown by a solid bar and a dotted bar, respectively. The sample number of Control Ms or Dex MS was three. Each value is the mean of three independent assays (± S.D.). The number above each bar is relative % of activity when that of control IgG in each group (Control Ms or Dex Ms) is set to 100%. * indicates statistically significant difference compared with the results of control IgG in each group ($P<0.005$).

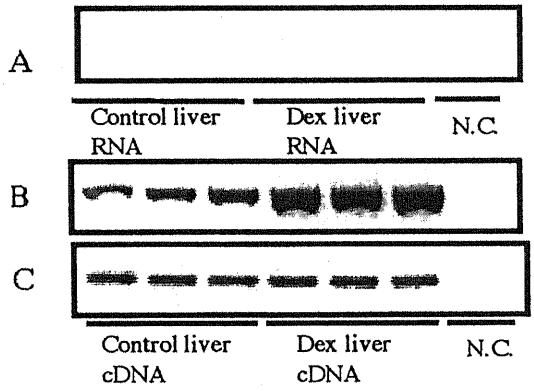

Figure 4. Induction of AB010635 mRNA expression by dexamethasone in rat liver. RT-PCR analysis was performed by using total liver RNA from each rat in panel A and liver cDNA from each rat in panel B. The name of the sample used in each lane is indicated below the panel. N.C. indicates non-template control. A, detection of genomic DNA of the *GAPDH* gene; B, detection of AB010635 cDNA; and C, detection of GAPDH cDNA.

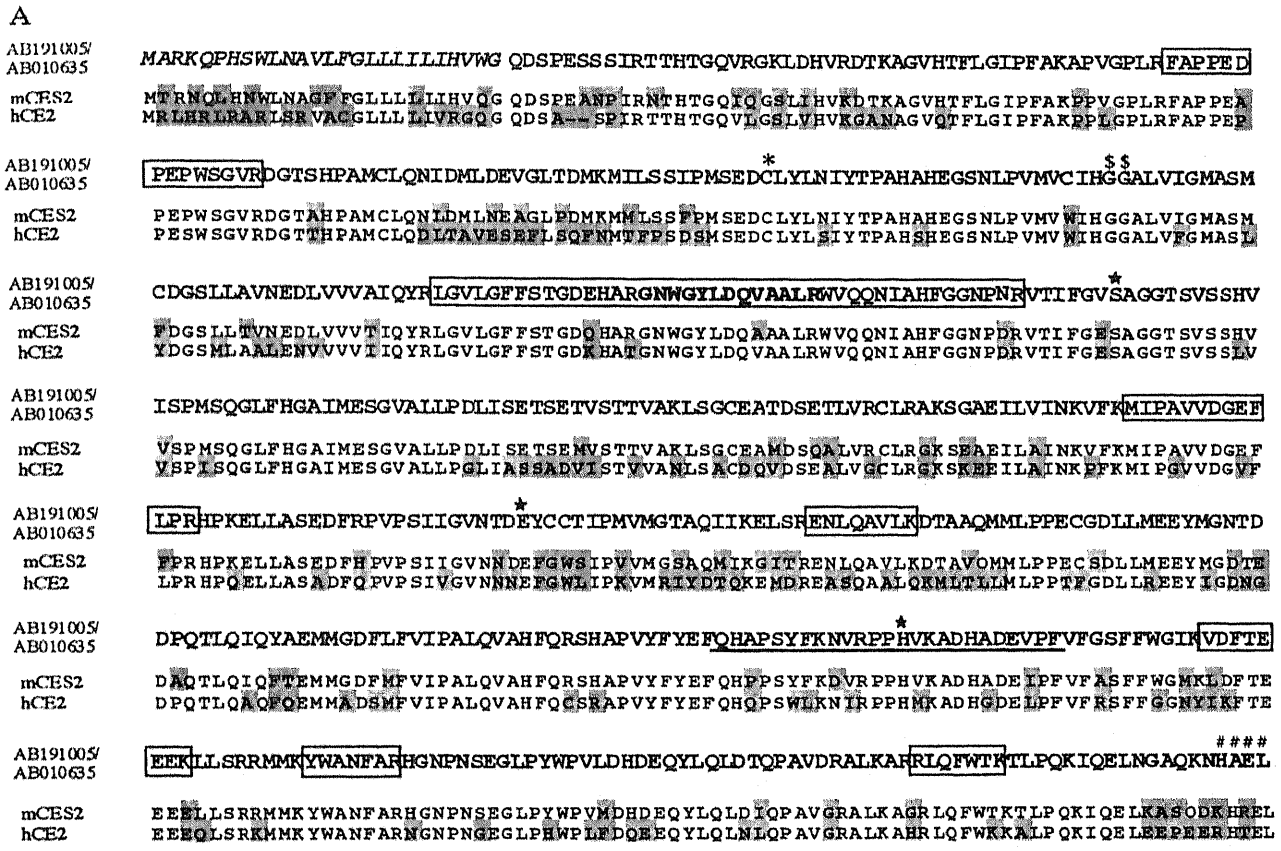

Figure 5. Classification of AB191005/AB010635 as a member of the CES2 family. A, Comparison of the deduced amino acid sequence of AB010635 with those of human and mouse CES2 isozymes. Shadows indicate differences in amino acid residues. Italic letters indicate the signal peptide (1-26) predicted by computer analysis (Signal IP 3.0 Server; http://www.cbs.dtu.dk/services/SignalP/). * indicates conserved Cys (125) residue, and stars indicate three amino acids composing a catalytic triad, Ser (230), Glu (347), and His (459). $ indicates two Gly residues (150 and 151) involved in an oxyanion hole loop, and four residues at the carboxyl-terminal (His-Ala-Glu-Leu, 557-561), indicated by #, are thought to function as an endoplasmic reticulum retention signal. No putative glycosylation site was found. Numbers in parentheses indicate the relative position of the corresponding amino acid residue with respect to the first Met residue. An underline indicates the peptide identified by amino acid sequence analysis of purified CES RL4. Boxes indicate the peptides identified by amino acid sequence analysis of dexamethasone-induced CES isozyme in liver microsomes, and bold letters indicate the peptide of the dexamethasone-induced CES isozyme in plasma. B, phylogenic tree of human and rodents CES isozymes. Trivial names, animals, and accession numbers are shown from left to right.

Induction of AB010635 mRNA expression by dexamethasone in rat liver

The results of protein analysis described above presented the possibility that expression of AB010635 mRNA was induced in dexamethasone-induced rat liver. RT-PCR is not a completely quantitative method for evaluation of mRNA expression; nevertheless, the results of RT-PCR using specific primers for AB010635 showed that the amount of

AB010635 mRNA was obviously greater in dexamethasone-treated liver than in control liver (Fig. 4B). Both dexamethasone-treated liver cDNA and control liver cDNA are free from genomic DNA contamination (Fig. 4A) and are synthesized in equal amounts (Fig. 4C). The nucleotide sequences of PCR products were confirmed as fragments of AB010635 cDNA by direct DNA sequence. In this confirmation, one nucleotide of the products was found to be mismatched to that of AB010635 (at position +1093).

cDNA cloning of AB191005/AB010635 and its expression in Sf9 cells

The protein of which partial amino acid sequence is identical to that of AB010635 has been detected in
rat liver microsomes [59], but it has not been characterized. There has been no report of AB010635 cDNA being expressed in eukaryotes. Thus, to confirm that AB010635 encodes CES RL4, cDNA cloning was performed. The nucleotide sequence of the obtained cDNA clone showed perfect homology to AB010635 except for two nucleotides (C1093T and C1548T). The former one was also found in the results of RT-PCR analysis as described above. These substitutions were also found in the data of the Rat Genome Project (http://www.sanger.ac.uk/). We submitted the nucleotide sequence of our cDNA clone to Genebank, EMBL and DDBJ (Accession no. AB191005). These nucleotide changes are not accompanied by amino acid alteration.

The deduced amino acid sequence of AB191005/AB010635 is shown in Fig. 5A with

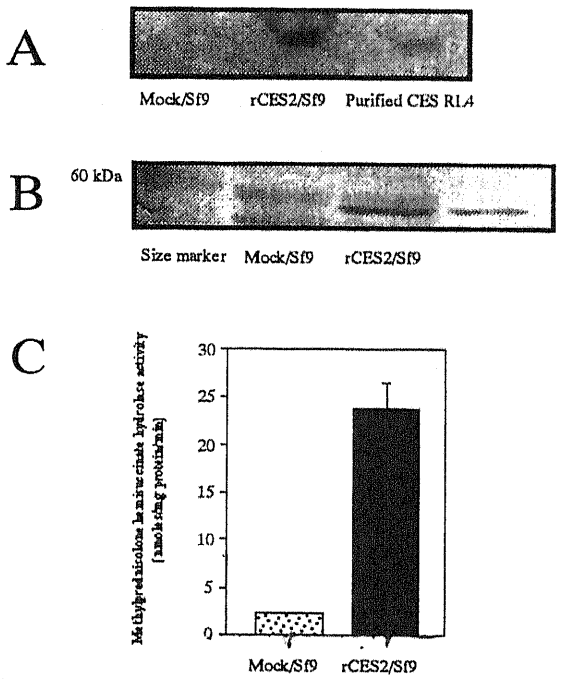

Figure 6. Characterization of recombinant rat CES expressed in Sf9 cells. Mock/Sf9, cytosolic fraction of Sf9 cells transfected with empty baculovirus. rCES2/Sf9, cytosolic fraction of Sf9 cells expressing rCES2. A, Esterase activity staining. Cytosolic proteins of Sf9 cells (10 μg) were loaded in each lane. Purified CES RL4 (100 ng) was used for comparison. B, Western blotting using anti-CES RL4 antibodies. Cytosolic proteins of Sf9 cells (15 μg) were loaded in each lane. Purified CES RL4 (100 ng) was used for comparison. An arrow indicates the band recognized by anti-CES RL4 antibodies. C, determination of MPHS hydrolase activity. Each value is the mean of three independent assays (± S.D.).

comparison to human CES2 isozyme (hCE-2, [4]) and mouse CES2 isozyme (mCES2, [20]). The sequence contained several conserved amino acid residues among CES isozymes and an endoplasmic reticulum (ER) retention signal at the carboxyl-terminal, but no glycosylation motif was found (Details are given in the legend of Fig. 5A.). The sequence of AB191005/AB010635 showed high similarity to those of other CES2 isozymes, especially to that of mCES2, suggesting that AB191005/AB010635 belongs to the CES2 family (Fig. 5B). Thus, AB191005/AB010635 is hereafter called rCES2.

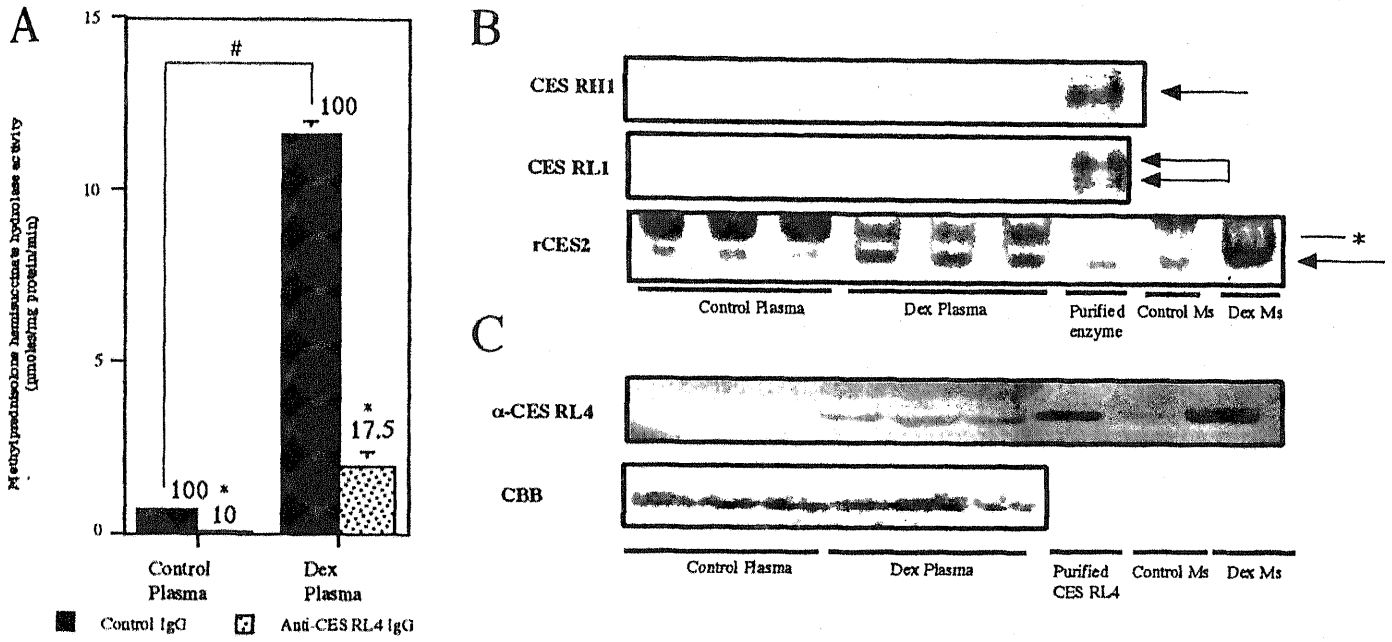

Figure 7. Detection of rCES2 protein in rat plasma and increase in its amount by dexamethasone. A, Determination of MPHS hydrolase activity and its inhibition by anti-CES RL4 IgG. Control IgG (0.1 mg) and anti-CES RL4 IgG (0.1 mg) were used in the assays for which results are shown by a solid bar and a dotted bar, respectively. The sample number of Control Plasma or Dex Plasma was three. Each value is the mean of three independent assays (± S.D.). The number above each bar is relative % of activity when that of control IgG in each group (Control Plasma or Dex Plasma) is set to 100%. * indicates statistically significant difference compared with the results of control IgG in each group ($P<0.005$). # indicates statistically significant difference compared between the results of Control Plasma and Dex Plasma ($P<0.005$). B, esterase activity staining after non-denaturing PAGE. The sample loaded in each lane is indicated below each panel. Plasma proteins (10 μg) were used, and purified CES isozymes (CES RH1, CES RL1, and CES RL4, 100 ng each) were used as positive controls. Pooled Control Ms and Dex Ms (3.0 μg) were also used as references. C, Western blotting. Plasma proteins (20 μg) were loaded in each panel. Anti-CES RL4 antibodies were used to detect rCES2 protein as indicated on the left side of the upper panel. An approximately 80-kDa plasma protein was visualized by coomassie brilliant blue staining for verification that a similar amount of protein was loaded in each lane. Purified rCES2 (100 ng) was used as a positive controls. Pooled Control Ms and Dex Ms (3.0 μg) were also used as references.

When the recombinant bacmid DNA was transfected into Sf9 cells, the cells expressed the recombinant protein as determined by Western blotting and esterase activity staining after non-denaturing PAGE (Fig. 6A and B). The recombinant rCES2 exhibited the same biochemical properties as those of purified CES RL4 in terms of molecular weight of a subunit, pI, and immunocrossreactivity. The recombinant proteins were recovered from the cytosolic fraction as in the case with other CES isozymes expressed in Sf9 cells [5, 20]. The hydrolase activity level of recombinant protein towards PNPA was very low (1.6 fold compared to that of mock/Sf9, results not shown) according to the results of inhibition assays. The recombinant rCES2 possessed a high level of MPHS hydrolase activity (Fig. 6C), and the kinetic parameters (*Km* and *Vmax*) of the activity were 76.6 ± 0.02 μM and 28.8 ± 3.0 nmoles/mg protein/min, respectively, these values being comparable to those of purified CES RL4 (*Km* = 120.0 ± 2.0 μM and *Vmax* = 4.3 ± 0.4 μmoles/mg protein/min).

Together with other results, these data show that rCES2 encodes CES RL4. CES RL4 should be called rCES2 in accordance with the nomenclature system suggested by Hosokawa and Satoh [1], although the system is currently under establishment.

Detection of rCES2 in rat plasma

Hattori et al. [56] reported that treatment of rats wit h dexamethasone caused induction of MPHS hydrolase activity not only in liver microsomes but also in plasma, although the nature of the induced protein was not determined. In our experiments, accordingly, the level of MPHS hydrolase activity in Dex Plasma was increased to 15.5 fold (P<0.005) compared with that in Control Plasma (Fig. 7A). Esterase activity staining after non-denaturing PAGE and Western blotting showed that, as in the case of microsomes, the induced protein migrated to the same position as

rCES2 (Fig. 7B and C). On the other hand, other CES members, CES RH1 and CES RL1, did not exist in either Control Plasma or Dex Plasma. The activity bands (indicated by an asterisk in Fig. 7B) observed in plasma samples were attributed to plasma CES isozyme (hydrolase S), since it has been reported that mRNA expression of this plasma CES isozyme was suppressed by dexamethasone [16]. When an inhibition assay using anti-CES RL4 IgG was performed, the MPHS hydrolase activities in Control Plasma and Dex Plasma were strongly inhibited (decrease to 10% of control IgG, $P<0.005$, and to 17.5% of control IgG, $P<0.005$, respectively) (Fig. 7A). To identify the CES isozyme that exists in plasma, immunoprecipitation and amino acid sequence analysis was performed by using Dex Plasma as describe above. The amino acid sequence of a peptide fragment originating from dexamethasone-induced plasma CES isozyme was identical to that of rCES2 (Fig. 5).

I-III-IV Discussion

Identification of the enzyme that metabolizes a drug is important to understand the biological fate of the drug after administration, and induction of expression of the enzyme strongly influences the pharmacokinetics and pharmacodynamics of the drug. From these points of view, this study, in which we identified dexamethasone-induced MPHS hydrolase as a member of the CES2 family, provides three major topics for discussion: 1) biochemical properties of rCES2 as a drug-metabolizing enzyme, 2) rCES2 existence in plasma, and 3) the mechanism by which rCES2 is induced.

MPHS is a widely used drug for the treatment of systemic lupus erythematosus and in renal transplantation and medical emergencies, and the hydrolysis of MPHS is critical for this drug to exert its pharmacological actions. To the best of our knowledge, rCES2 is the first enzyme catalyzing this hydrolysis to be identified. Hattori et al. [56] reported that MPHS hydrolase activity was induced by several glucocorticoids. Such induction of rCES2 may significantly affect pharmacokinetic parameters of its substrate, such as MPHS or CPT-11 (CPT-11 is a substrate for rCES2, unpublished observation, A. Fujii, M. Hosokawa, T. Furihata, and K. Chiba). There are currently no experimental data that support this idea, but it is important to test the idea since it has been reported that MPHS pulse treatment resulted in a decrease in the area under the curve and an increase in clearance of cyclosporin through induction of hepatic cytochrome P450 (CYP) 3A activity in the rat [73].

A comparison of the biochemical properties of rCES2 and those of rat CES1 isozymes shows that they are strikingly different. Regarding the preferential substrates, CES RH1 and CES RL1 do not seem to be involved in the hydrolysis of MPHS in the rat liver. On the other hand, the contribution of rCES2 to PNPA hydrolysis is very low. In addition, temocapril is a substrate for CES RH1 but not for rCES2 (unpublished observation, T. Furihata, M. Hosokawa, A. Fujii, and K. Chiba). This difference is probably due to the different structure of rCES2 from those of CES1 isozymes, as the results of comparison of their deduced amino acid sequences, immuno-crossreactivity, and esterase activity staining after non-denaturing PAGE indicate. The results obtained in this study, together with the findings discussed below, provide important information for study of pharmacokinetics of ester-(pro)drugs that can be substrates for rCES2, including MPHS, as well as for study of prodrug design.

The next issue to discuss is how rCES2 exists in plasma. Needless to say for the case of dexamethasone treatment, the results of both esterase activity staining after non-denaturing PAGE and inhibition assays indicate that the active form of rCES2 is present in plasma even under normal conditions, although rCES2 protein

was hardly detected by Western blotting probably due to the very small amount of rCES2. What makes rCES2 exist in plasma? As shown in Fig. 5, the deduced amino acid sequence of rCES2 has a HXEL motif in the C-terminal region, which is a variant of the consensus eukaryotic ER retention signal of KDEL [74]. Therefore, rCES2 is firstly thought to exist in the lumen of the ER as other CESs do. Together with the fact that the levels of plasma GOT and GPT activities were increased by dexamethasone treatment, one possibile explanation of how rCES2 can exist in plasma is that hepatocyte necrosis, exacerbated by dexamethasone, ultimately results in the leakage of rCES2 protein. However, this is unlikely since other CES isozymes did not leak into Dex plasma even if they were still present in the dexamethasone-treated liver and the degree of hepatotoxity caused by dexamethasone in each rat was not correlated with the level of the corresponding plasma rCES2 activity. Another possibile explanation of the existence of rCES2 in plasma is its active release from hepatocytes. Although we did not perform any experiments to determine this possibility, it has been shown that the release of rCES2 into plasma was significantly inhibited by monensin, which could inhibit the release of secretory proteins by disrupting the Golgi apparatus [56, 75]. If this hypothesis is true, at least in part, the active release of rCES2 would be of biochemical interest as well as clinical interest. Since the possibility of passive release of rCES2 resulting from hepatocyte necrosis can not be ruled out, further studies are needed to determine how rCES2 can exist in plasma.

Finally, we focus on the question of how rCES expression is induced by dexamethasone. Given the fact that the amount of rCES2 mRNA in the liver was apparently increased when dexamethasone was administered, there are likely to be two mechanisms for rCES2 induction. One is enhanced intracellular stability of rCES2 mRNA since it has been demonstrated that dexamethasone can stabilize mRNA of the several genes [76, 77], and the other is the enhanced transcription of the *rCES2* gene triggered by specific transcription factors. For the latter case, the involvement of glucocorticoid receptor (GR) in rCES2 induction was likely to occur. We can not determine which is the major mechanism accounting for rCES2 induction at present. However, several experiments to examine this are in progress in our laboratory, and we expect that results of those experiments will shed light on the question.

In conclusion, we identified a dexamethasone-induced CES isozyme that can hydrolyze MPHS in the rat liver and plasma as a member of the CES2 family, rCES2. The different biochemical properties of rCES2 from those of known rat CES1 isozymes, including its unique existence in plasma, will be useful information for studies aimed at elucidation of functions of CESs in drug metabolism. In addition, we also identified the gene encoding rCES2 by cDNA cloning and functional expression in Sf9 cells. Since we demonstrated that the level of the corresponding mRNA expression was markedly increased, the identification of the coding gene is valuable for studies aimed at elucidation of the molecular mechanisms by which dexamethasone induces rCES2 expression.

Chapter II

Molecular characterization of the mouse *carboxylesterase 2* gene promote

II-I

Synergistic role of specificity proteins and upstream stimulatory factor 1 in transactivation of the mouse *carboxylesterase2/microsomal acylcarnitine hydrolase* gene promoter

II-I-I Introduction

We have reported that an inducible acylcarnitine hydrolase in mouse liver microsomes, termed mouse carboxylesterase 2 (mCES2), belongs to the CES2 family in the previous section (I-II) [20]. mCES2 showed a significant contribution to acylcarnitine hydrolysis in DEHP-treated mouse liver microsomes and is therefore thought to play some important roles in lipid metabolism in the ER. It has been reported that, as observed in mitochondria or peroxisomes, the carnitine/acylcarnitne system exists in microsomes to supply the intraluminal space with acyl-CoA, which is widely used in the formation of various fatty acid esters. Abo-Hashema et al. [64] presented evidence of microsomal triacylglycerol (TAG) synthesis via a lipolysis-esterification pathway, the critical point in very low-density lipoprotein assembly [78], involving carnitine acyltransferases (CATs). In their works, microsomal TAG synthesis was found to be dependent on the presence of both extraluminal carnitine and intraluminal CoASH, and glybencramide, an inhibitor of liver microsomal CAT [79], was found to greatly reduce the amount of luminal synthesis of TAG. Results of additional works supporting the results of their study have recently been reported by Washington et al. [80]. Since mCES2 can hydrolyze various acylcarnitine and acyl-CoA, the expression level of mCES2 might significantly affect the rate of TAG synthesis in the ER by modulating the amount of acyl-CoA generated from acylcarnitine by intraluminal CAT. Therefore, determination of the mechanisms by which *mCES2* gene expression is regulated would be an important step toward elucidation of how mCES2 is involved in TAG synthesis as well as other fatty acid ester metabolisms within the ER.

Experimental data to elucidate molecular mechanisms controlling *CES* gene expression are limited. The mouse CES1 isozyme showed a developmental expression pattern in the liver, and it has been suggested that specificity protein (Sp) 1 and Sp3 interacting with the mouse *CES1* promoter region could be involved in the ontogenic profile of the mouse *CES1* gene expression [49]. Other investigators showed that sterol regulatory element-binding protein (SREBP) 2 and Sp1 could bind to the promoter regions of the rat CES1 isozyme and human CES1 isozyme, respectively [81, 82]. With regard to the CES2 family, it has recently been reported that an approximately 1.6-kbp fragment of the 5'-flanking region of the human *CES2* gene was isolated and found to contain three functional promoters [83]. However, transcriptional factors interacting with the promoters have not been identified. No other information about the mechanisms regulating the *CES2* gene transcription is currently available.

The aim of this study was to determine the molecular mechanisms controlling *mCES2* gene expression. First we obtained the tissue expression profiles of mCES2 mRNA and protein. Given the fact that mCES2 is ubiquitously expressed, we characterized the promoter region of the *mCES2* gene and analyzed the mechanisms regulating the basal promoter activity. The results showed that three transcriptional factors synergistically contribute to the promoter activity of the *mCES2* gene. This study provides useful information for further studies aimed at elucidation of the molecular mechanisms controlling *mCES2* gene expression.

II-I-II Maetrial and Methods

Preparation of mouse tissue homogenates and esterase activity staining after non-denaturing polyacrylamide gel electrophoresis (PAGE).

Procedures for preparation of tissue homogenate were described in the section I-I-II. The homogenate of Sf9 cells expressing mCES2 was used as a positive control [20].

Total RNA preparation and reverse transcription-polymerase chain reaction (RT-PCR).

Procedures for total RNA extraction and RT-PCR were described in the section I-I-II. A set of primers (sense, 5'-TTCAAGGATGTCAGACCACC-3'; and anti-sense, 5'-AACACATTTTTTTTGATACAGGGTA-3') was used for PCR (94 °C for 15 s, 55 °C for 20 s, 68 °C for 40 s and 35 cycles) to detect *mCES2* gene expression. PCR conditions are shown in the parentheses. A plasmid vector containing mCES2 cDNA [20] was used as a template for a positive control. The PCR product was purified by a Wizard SV Gel and PCR Clean-up System (Promega, Madison, WI, U.S.A.) and was confirmed to be a fragment of mCES2 cDNA by DNA sequencing. The DNA sequence was determined using a Dye Terminator Cycle Sequencing-Quick Start Kit (Beckman Coulter, Fullerton, CA, U.S.A.) and a CEQ2000 DNA Analysis System (Beckman Coulter). The results were confirmed by sequencing at least twice in each direction.

Mouse upstream stimulatory factor (USF) 1 cDNA was obtained from the liver cDNA by PCR using the following primers: sense, 5'-CGCCTCGGATGAGCCCC-3'; and anti-sense, 5'-ATGGGGTTAGCCTGTTGCTC-3'. The isolated cDNA was inserted into the pCR-Blunt II TOPO vector (Invitrogen) and the nucleotide sequence was determined as described above.

Isolation of the 5'-flanking region of the mCES2 gene.

Mouse genomic DNA was extracted from the liver of a 5-week-old C57BL/6 male mouse (Japan SLC) by DNAzol Reagent (Invitrogen). The 5'- flanking region of the *mCES2* gene was isolated by PCR with the sense primer 5'-CCCATTGTGTGTCCAGTATCAC-3' (-1385) and the anti-sense primer 5'-GCTCTCAGTCCTAAGTCTGTGC-3' (+60) using the genomic DNA as a template. The relative 5'-positions of primers with respect to the transcription start site determined in this study are shown in parentheses. The primers were designed on the basis of results of the Mouse Genome Project (http://www.sanger.ac.uk). The amplicon was subcloned into the pCR-Blunt II TOPO vector, and the nucleotide sequence was determined as described above.

Determination of the transcription start site of the mCES2 gene.

The method of RNA ligase-mediated and oligocapping rapid amplification of 5' cDNA ends (RLM 5'-RACE) was used to determine the transcription start site of the *mCES2* gene (GeneRacer kit, Invitrogen). This method ensures the capture of only full-length 5' ends of specific transcripts via elimination of truncated messages from the amplification process. Total RNA from mouse liver was treated with calf intestinal phosphatase and tobacco acid pyrophosphatase according to the directions of the manufacturer. After selective ligation of an RNA oligonucleotide to the 5'-ends of decapped mRNA, first-strand cDNA was synthesized. Using the supplied sense primer and the *mCES2* gene-specific primer designed, 5'-AGCAGCAGCCCGAAGAACCC-3' (+121), touchdown PCR amplification was performed (94 °C for 2 min followed by 5 cycles of 94 °C for 30 s, 66 °C for 90 s, 5 cycles of 94 °C for 30 s, 64 °C for 90 s, and 25 cycles of 94 °C for 30 s, 63 °C for 30 s and 68 °C for 90 s) by using high-fidelity DNA polymerase (KOD plus, TOYOBO, Tokyo, Japan). The product was subcloned into the pCR-Blunt II TOPO vector and sequenced as described above.

Plasmid construction.

The *mCES2* gene promoter region was removed from the cloning vector and inserted into the pGL3-Basic vector (Promega) by *Xho* I and *Kpn* I digestion. The plasmid is referred to as p–1385/+60. Seven deletion constructs were generated by nested PCR of the primary clone using the following sense primers: 5'-

TGTGACCTCGCATAACTATCAT-3' (p-966/+60), 5'-CAAAGCACAGGAGTCTTGAAGC-3' (p-363/+60), 5'-AGAGAGAACAGAAGCAGCAGAG-3' (p-163/+60), 5'-GCCATTGGCTCCTATCACT-3' (p-120+60), 5'-TTCACCCGTCACACAATG-3' (p-69/+60), and 5'-TTAAATAGCTGCCTGTGC-3' (p-29/+60). The antisense primer used was the same as that used in the genome cloning. All constructs are named and are shown in parentheses. The obtained 5' deletion fragments were transferred into pGL3-Basic vectors as described above.

To introduce mutations into the reporter plasmids, complimentary primers harboring a few mutations were designed for each target site as follows: 5'-GTCACACAATGTTTCCACCTACACCCT-3' and 5'-AGGGGTGTAGGTGGAAACATTGTGTGAC-3' for the GC box, 5'-TCCTATGACTAGTGACTAATTACTGTTCC-3' and 5'-GGAACAGTAATTAGTCACTAGTCATAGGA-3' for the E box, and 5'-GCAGCAGAGGCTCCTTTCCCCTACCTCC-3' and 5'-GGAGGTAGGGGAAAGGAGCCTCTGCTGC-3' for the NFκB element. Inverse PCR amplification was performed by using KOD PLUS and using p-163/+60 as a template. PCR products were treated with *Dpn* I to digest the residual template plasmid and were applied to the transformation. The mutations introduced were confirmed by DNA sequencing as described above. All mutational constructs are named as follows: pGCmt for the GC box mutant, pEmt for the E box mutant, pNFmt for the NFκB element mutant, pGCEmt for the GC box and E box mutant, pGCNFmt for the GC box and NFκB element mutant, pENFmt for the E box and NFκB element mutant, and pAllmt for the GC box, E box and NFκB element mutant.

An Sp1 mammalian expression vector, pCMVSp1, and *Drosophila* Sp3 expression vector, pPacUSp3, were generous gifts from Dr. Robert Tjian (University of California, Berkeley, Berkeley, U.S.A.) and Dr. Guntram Suske (Philipps-Universitat Marburg, Marburg, Germany), respectively. To construct an Sp1 *Drosophila* expression vector, the coding region of Sp1 [84, 85] was amplified by PCR and subcloned into the pCR -Blunt II TOPO vector. The sense primer was 5'-CACCATGGATCCCTCGA-3', and the anti-sense primer was 5'-TGCCTGATCTCAGAAGCC-3'. Then the coding region of Sp1 was inserted into pAc5.1/V5-His (Invitrogen) (pAcSp1). Likewise, mUSF1 cDNA was subcloned into pAc5.1/V5-His (pAcUSF1) by *EcoR*I digestion coupled with alkaline phosphatase treatment to enable it to be expressed in *Drosophila* cells. DNA sequencing as described above confirmed the orientations and the nucleotide sequences of these constructs.

Cell cultures

Hepa1-6 cells and COS7 cells were obtained from Riken Cell Bank (Tsukuba, Japan). Both cell lines were maintained at 37°C with 5% CO_2 in Dulbecco's modified Eagle's medium (D-MEM) (Invitrogen) supplemented with 10% (v/v) heat-inactivated fetal bovine serum and 50 units/mL penicillin and with 50 μg/mL streptomycin. *Drosophila* SL2 cells, purchased from American Type Culture Collection (Rockville, MD, U.S.A.), were grown at 24°C without CO_2 in *Drosophila* Schneider's medium (Invitrogen) supplemented with 10% fetal bovine serum and 50 units/mL penicillin and with 50 μg/mL streptomycin.

Transient transfections and dual luciferase assays

Hepa1-6 cells were plated at a density of $0.8x10^5$ cells/well in a 24-well dish one day before transfection. When the cells had reached 60 to 80 percent of confluence, they were transiently transfected with 200 ng of the reporter plasmids and 4 ng of phRL-TK vector (Promega) using Lipofectamine (Invitrogen) and PLUS Reagent (Invitrogen) according to manufacturer's protocol. At 3 hr after transfection, the medium was removed and the cells were cultured for a further 24 hr in complete supplemental D-MEM. Then the cells were washed with phosphate-buffered saline (PBS) and were harvested. The cells were lysed with passive lysis buffer (PLB) (Promega), and luminescence from transfected cell lysates was determined using a Dual-Luciferase Reporter Assay System (Promega) and a TD-20/20 luminometer (Promega) according to manufacturer's directions. Results were expressed as relative ratio (firefly luciferase activity /*renilla* luciferase activity). Experiments were performed in triplicate, and each value presented is the mean (± S.D) from three independent assays.

COS7 cells were plated at a density of $1.3x10^6$ cells/dish in a 100-mm dish one day before transfection. When the cells had reached 60 to 80 percent of confluence, they were transiently transfected with 5 μg of pCMVSp1 using the same reagents as those used for Hepa1-6 cells. The medium was removed 3 hr after transfection and the cells were cultured for a further 72 hr in complete supplemental D-MEM. The cells were harvested and the nuclear extracts were prepared as described below.

SL2 cells were plated at a density of $5x10^5$ cells/well in a 24-well plate. At 18 h after plating, the cells were transfected with 150 ng of the reporter plasmid and various amounts of a mixture of expression plasmid (pAcSp1, pPacUSp3, and/or pAcUSF1) using Cellfectin reagent (Invitrogen) according to the provided protocol. The total amount of DNA of the mixture was adjusted to 300 ng by adding an empty pAc5.1/V5-His vector. Complete growth medium was added to each well 5 hr after transfection. The cells were harvested 48 hr after addition of the medium. After being washed with PBS, the cells were lysed with PLB and single luciferase activity was determined using the same system as that described above. The luciferase activity was normalized by total protein concentration determined by using a Bio-Rad *Dc* Protein Assay Kit. Experiments were performed in duplicate, and each value presented is the mean (± S.D) from three independent assays.

Student's *t*-test was performed to determine significance of difference between the groups in mutation analysis. Similarly, ANOVA was performed to determine significance of synergism between the groups in co-transfection assays. *P* values less than 0.05 were taken to be significant.

Nuclear extraction, electrophoretic mobility shift and supershift assays.

Nuclear extracts were prepared from the cultured cells by using a CelLytic Nuclear Extraction Kit (Sigma-Aldrich Co., St. Louis, MO., U.S.A.) according to manufacturer's directions. Hepa1-6 cells or COS7 cells were washed twice with ice-cold PBS and collected. After extracting nuclear contents, the protein concentrations were determined as described in the previous section. The nuclear extracts were stored at -80°C until use.

Probe double-stranded (ds) DNA was generated by annealing the complementary oligonucleotides listed in Table s1. Consensus and mutated consensus oligonucleotides for the Sp family, USFs, CCAAT/enhancer binding proteins (C/EBP) and nuclear factor kappa B (NFκB) were designed by the directions of Santa Cruz Biotechnology (Santa Cruz, CA., U.S.A.). dsDNA was end-labeled with [γ-^{32}P]dATP (Amersham Bioscience) using T4-polynucleotide kinase (Promega). Each binding reaction mixture contained 10 mM Tris-HCl (pH 7.5), 50 mM NaCl, 1 mM $MgCl_2$, 0.5 mM EDTA, 0.5 mM dithiothreitol, 4% glycerol, 0.5 μg poly(dI-dC)/poly(dI-dC), and 1-2 μg each of the nuclear extracts. The reaction mixtures were pre-incubated on ice for 10 min prior to the addition of a [γ-^{32}P]-labeled probe. Samples were kept for a further 20 min at room temperature with the probe, and the mixtures were electrophoresed with 6% polyacrylamide gel in 0.5x 45 mM Tris-borate buffer with 1 mM EDTA at 4 °C. Gels were dried and autoradiographed by BASS 2000 II (Fuji Film, Tokyo, Japan).

Competition experiments were carried out as described above except that cold competitive dsDNA (Table s1) was added to the binding reaction mixture at a 50-fold excess of the probe amount before addition of the probe. For supershift assays, 2 μg of antibodies against Sp1 (sc-59x, Santa Cruz Biotech), Sp3 (sc-644x, Santa Cruz Biotech), USF1 (sc-229x, Santa Cruz Biotech), NFκB p65 (sc-109x, Santa Cruz Biotech) or AP1 (sc-45x, Santa Cruz Biotech) was added to the binding reaction mixture at room temperature for 30 min prior to addition of the probe.

All results are representative of two or three independent experiments.

Chemicals used in this study were of reagent grade and obtained from commercial sources.

II-I-III RESULTS

Tissue expression profiles of mCES2 mRNA and protein.

At the start of this study, we obtained tissue expression profiles of mCES2 mRNA and protein by performing RT-PCR and esterase activity staining after non-denaturing PAGE, respectively. The results of PCR using mouse *GAPDH* gene-specific primers showed that mouse tissue cDNAs were free of contamination with genomic DNA (Fig. 1A) and were synthesized in equal amounts (Fig.1D). PCR using *mCES2* gene-specific primers revealed limited expression of mCES2 mRNA in the liver, kidney and small intestine (Fig. 1B). When template cDNAs were increased to 12-fold excess amounts of those used in the experiment for which the results are shown in Figure 1B, mCES2 mRNA expression was also detected in the thymus, adipose tissue, brain, lung and testis (Fig. 1C). There was no band observed in the heart. Nucleotide sequences of all of the PCR products showed 100% homology with that of mCES2 cDNA. Consistent with the results of RT-PCR, a strong activity band was detected in the liver, kidney and small intestine and a weak activity band was detected in the thymus by esterase activity staining after non-denaturing PAGE (Fig. 1E). The band detected on the lane of the small intestine was a doublet with slightly different migration.

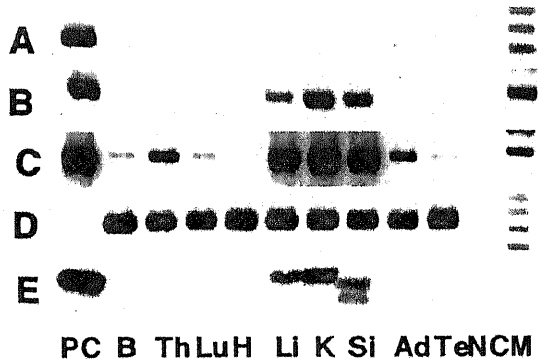

Figure 1. Tissue expression profiles of mCES2 mRNA and protein. Panels A ~ D show the results of RT-PCR, and panel E shows the results of esterase activity staining after non-denaturing PAGE. PC, positive control; B, brain; Th, thymus; Lu, lung; H, heart; Li, liver; K, kidney; Si, small intestine; Ad, adipose tissue; Te, testis; NC, non-template control; M, DNA size marker. In panel A, mouse *GAPDH* gene-specific primers were used and mouse tissue RNA was used as a template. Mouse liver cDNA prepared in our previous study [3] was used as a positive control. In panels B and C, mCES2 mRNA expression was detected. Mouse tissue cDNA was used as a template. mCES2 cDNA in the pFAST BAC1 vector [3] was used as a positive control. In panel C, template tissue cDNA was increased to a 12-fold excess amount of that used in panel B. In panel D, mouse GAPDH mRNA expression was detected. Mouse tissue cDNA was used as a template. In panel E, mCES2 protein activity was detected. Various amounts of mouse tissue homogenates were used to adjust band intensity: 20 μg of brain, 15 μg of thymus, 7 μg of lung, 10 μg of heart, 1 μg of liver, 5 μg of kidney, 5 μg of small intestine, 2.5 μg of adipose tissue, and 10 μg of testis homogenates.

Isolation of the mCES2 5'- flanking region.

To understand the mechanism by which *mCES2* gene transcription is regulated, the 5'-flanking region of the *mCES2* gene was isolated from the C57BL/6 mouse genomic DNA by PCR amplification. The obtained nucleotide sequence is shown in Fig. 2A, together with the sequence around the translation start site obtained from the results of RLM-RACE and cDNA cloning of mCES2 [20]. When the nucleotide sequence of the clone was compared to the results of the genome project, a thymine nucleotide deletion was found in the clone at position -978 with respect to the transcription start site (+1), which was determined in this study. Regions homologous to known *cis* elements were identified using searching programs for transcription factor binding sites (http://www.gene-regulation.com/ and http://www.drkazu.com/KENKYUU.htm/). The results showed that there were a GC box, an E box and an NFκB element in precedence to a translation start codon in addition to other elements scattered throughout the sequence, such as binding sites for hepatocyte nuclear factors or C/EBPs. A TATA box, however, was not found.

Determination of the transcription start site of the mCES2 gene.

A

```
-1385 CCCATTGTGT GTCCAGTATC ACTGTCAGGA TTCCATTCTG GGTAGATTTC AAGAAGAAGC TGGCATCGAC AACTGTGACT TGCTCCACTG

-1295 GTATATTGAC TCCACTCCTT ATTAGAATGA ACTGGCATAT CACATATAGA GCACAAATGG GGATAACCCT TCAGTAAGAG TCCGTGTAAC
                                                                          C/EBPα

-1205 TGTTTAATAT TGCTACTTAG AAGAGTGCCC CTATTTTTCT CAATTTTACC TGTGTTTCTC TCCATAGTAC CTCCATGGTA TTCCCTATAA
      HNF3β                          C/EBPβ

-1115 GTGCCAAGCT CTGATCCAGG AGCACGGTAT AGTTCTAGTC AATCTTAGCA CAACATCTGA GAAGCACATG AGGCACTCAT CCACAAAGAG

-1025 AGAAAACTGC TGTGTTGCTG AGATTGAGAA AGGTGTAAGG ATGGTTCTTT TTTTTTTTAT GTGACCTCGC ATAACTATCA TAAATTTTAC
                          C/EBPβ                 HNF3β                                  CdxA

 -935 AGTGAGTATA AGGGAATAGG ACGTGGGTGG TCGAAGCTCC TTGTTGATTC AATGAAGAAC TCATTCCTAG ATTCATTAAA CTAGCAAGGT

 -845 TTGCAGTATG ATGGTTCACC CTTCCAAGAG ATGCTAGCAT ACTTAAAGAC TGGGTAGCAG CAGTAAGAAG GCCTATTCCT GTTGCAGGCA

 -755 GGTTACACCC ATGACCCTGT AAATCCCCAC TGAAAAATGA CTGCTGAAAT GACTTGGACA TTGTAGAACT ATGTCTTTTC TATTTTATAG
                          MZF1

 -665 ATTAAAAAAA AATGTTTTAA AACAGGGCCA AAAAGAAAGC ACAAGCTAGA AAGCAAGGTT AATTGCTACA AAAATGGTAA TGGCAAGAAG
                                                                HNF-1      YY1

 -575 AAAGATCAAT AAGGACCATA GAATCTATTC AAGCTGAGAG CCAGCAGTTA GGGGAAGAGA GAGGGAAAGA AGGGACTGTG ACCTTTAAAG
                                    Ap-4                                          ER

 -485 CACCAGAGTA TCCATGTGTC TTGTTAAAAC AAGTGTGACT TAATAGGGAA ACTGTCCATG CAGATCCTAA GATAATTGTA GGAACCAGGG

 -395 ACTCGGGAAG CAGGCTCAGT AAACTGAGTC TTCAAAGCAC AGGAGTCTTG AAGCTGAGGT TACACTCAGA GCTTCTGCAC TTGCCTGATT

 -305 CTCCTGTGAC ATCTTGACTA TGACCTTCTC ACAGAAGCAC TCTGGCTTCT CCTGTTACAG CTTTCTGGCC AGGTGAGGAG ACAGGGTTCC
                                                                          ∂EF1

 -215 TGGTATCCCA GACAAGTTCC AGAATTCATG CTGTGCCTTT CCAGGAGGCC AGAGAGAGAA CAGAAGCAGC AGAGGGGACT TTCCCCTACC
                                                                GR                NFκB

 -125 TCCTGGCCAT TGGCTCCTAT CACTTCTGAC TAATTACTGT TCCTGCAATG AGAACTTTCA CCCGTCACAC AATGGCCCCA CCTACACCCT
                E box          +1                          C/EBP                  GC box

  -35 TTTGGTTTAA ATAGCTGCCT GTGCAAGGTT CACTCCTTAT GCTTCCTGTT TGTGAAACTT GGTCATCTTA GCAGCACAGA CTTAGGACTG

  +55 AGAGCTGATC ATGACACGGA ACCAACTACA TAACTGGCTG AATGCTGGGT TCTTCGGGCT
```

B

```
mCES2       AGAACTTTCA CCCGTCACAC AATGGCCCCA CCTACACCCT TTTGGTTTAA
RLM-RACE    **************************************CGACTGGAG CACGAGGACA

                                                    +1
mCES2       ATAGCTGCCT GTGCAAGGTT CACTCCTTAT GCTTCCTGTT TGTGAAACTT
RLM-RACE    CTGACATGGA CTGAAGGAGT AGAAACTTAT GCTTCCTGTT TGTGAAACTT

                                                              +65
mCES2       GGTCATCTTA GCAGCACAGA CTTAGGACTG AGAGCTGATC ATGACACGGA
RLM-RACE    GGTCATCTTA GCAGCACAGA CTTAGGACTG AGAGCTGATC ATGACACGGA

mCES2       ACCAACTACA TAACTGGCTG AATGCTGGGT TCTTCGGGCT GCTGCT....
RLM-RACE    ACCAACTACA TAACTGGCTG AATGCTGGGT TCTTCGGGCT GCTGCT....
```

The RLM 5'-RACE method was used to determine the transcription start site of the *mCES2* gene. DNA sequencing analysis of a PCR product showed that it contained a partial nucleotide sequence of the *mCES2* gene ligating to the adopter sequence. The partial sequence started at 65 bp upstream from the translation start codon (Fig. 2B). The data showed that this relative position was the transcription start site of the *mCES2* gene, and this position is hereafter referred to as +1 (indicated by the arrow in Fig. 2A).

C

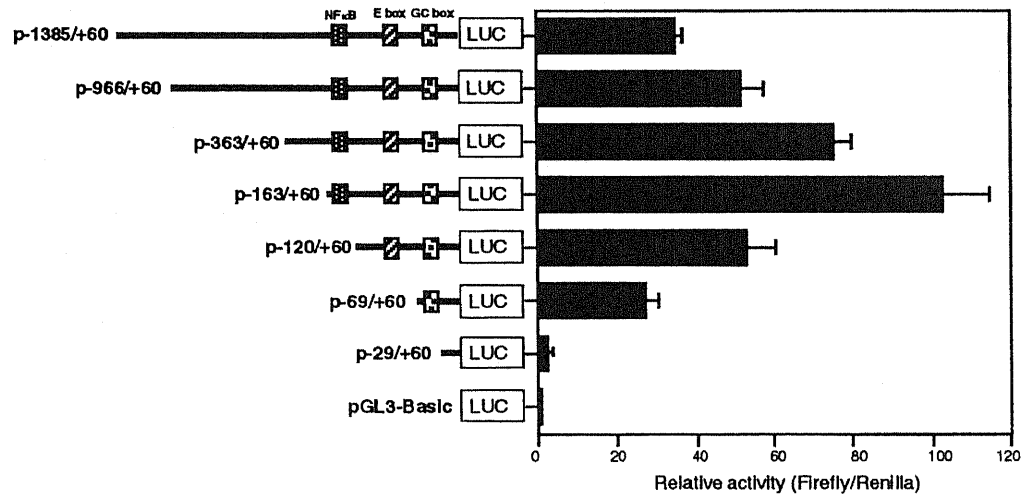

Figure 2. Characterization of the mCES2 gene promoter. A, nucleotide sequences of the 5'-flanking region of *the mCES2* gene. The nucleotide sequence shown here is based on the combination of results of three kinds of experiments: results of mouse genomic DNA cloning shown in this paper (from –1385 to +60), results of RLM-RACE shown in this paper (from –1 to +114), and results of cDNA cloning of mCES2 reported in [3] (from +30 to +114). Possible transcription factor binding sites are underlined. A GC box and an E box are indicated by squares. The arrow indicates the transcription start site (designed as +1) determined in this study, and the double underlines indicate the translation start codon. The relative positions with respect to the transcription start site are shown on the left side of the sequence. B, determination of the transcription start site of the *mCES2* gene. Alignment of nucleotide sequences of the *mCES2* gene and cDNA clone obtained from RLM-5'-RACE. Bold letters show the identical nucleotides in the two sequences. The numbers indicate the relative position to the point of ligation, which should be the transcription start site (+1). *mCES2*, nucleotide sequence of the 5'-untranslated region of the *mCES2* gene determined by mouse genomic DNA cloning performed in this study and cDNA cloning of mCES2 reported in [3]; RLM-RACE, nucleotide sequence of the obtained cDNA clone; underline, translation start site (+65); double underline, oligonucleotide sequence used for adopter. C, deletion analysis of the 5'-flanking region of the *mCES2* gene. Luciferase genes regulated by various lengths of the *mCES2 5'* deletion fragments (200 ng) were transiently transfected into Hepal-6 cells. A GC box, an E box, and an NFκB element are boxed. Names of constructs are shown on the left side. Explanations of deletion constructs are given in Experimental. Each value is the mean (± S.D) of relative activity (Firefly/*Renilla*) of three separate experiments, each performed in triplicate.

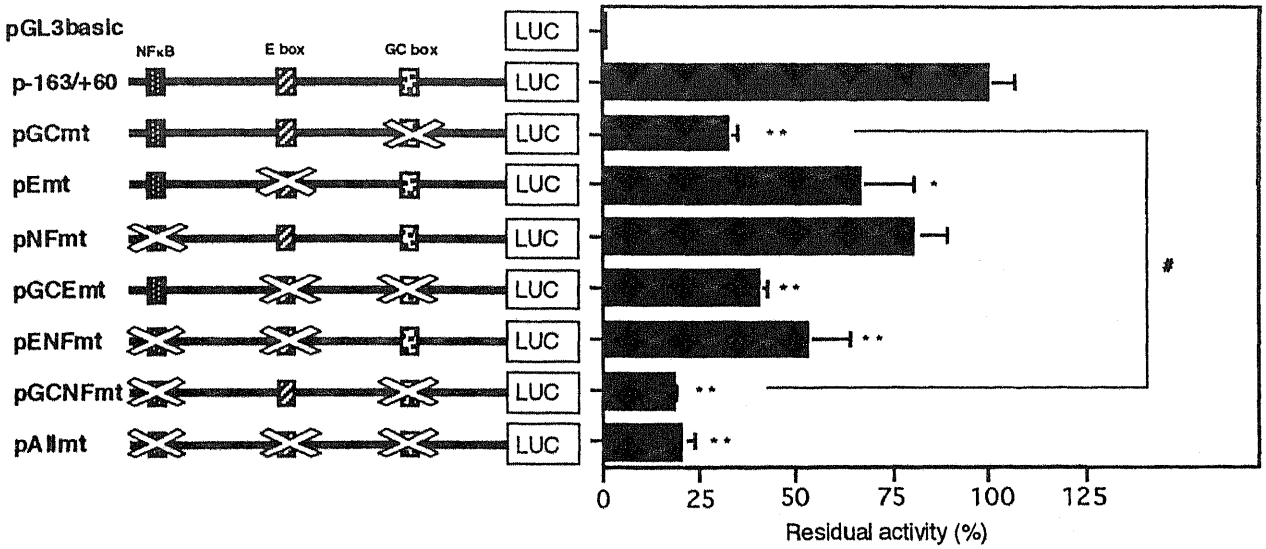

Figure 3. Mutation analysis of the 5'-flanking region of the *mCES2* gene. Luciferase genes regulated by the *mCES2* promoter constructs harboring various mutations (200 ng) were transiently transfected into Hepa1-6 cells. A GC box, an E box, and an NFκB element are boxed, and mutations are indicated by crosses. Explanations of mutation constructs are given in Experimental. Luciferase activity was determined as relative activity (Firefly/*Renilla*), and each value is the mean (± S.D) of residual activity (%) of the control (p-163/+60) of three separate experiments, each performed in triplicate. * and ** indicate statistically significant differences compared with the control (p-163/+60) ($P<0.05$ and $P<0.005$, respectively). # indicates a statistically significant difference between pGCmt and pGCNFmt ($P<0.05$).

Identification of the major cis elements responsible for transcriptional activity of the 5'-flanking region of the mCES2 gene.

Deletion analysis and mutation analysis were performed to examine the transcriptional activity of the 5'-flanking region of the *mCES2* gene and to identify the elements that contribute to its transcriptional activity. Seven deletion constructs were transiently transfected into mouse hepatoma cells (Hepa1-6 cells). Deletion analysis showed that the highest level of transcriptional activity was in p-163/+60 (Fig. 2C) and that the level of activity was gradually reduced as the fragment became longer or shorter. Deletion of the region from –163 to –121, which contained the NFκB element (p-120/+60), resulted in a reduction of the level of transcriptional activity by 50%. Further deletion of the region from -120 to –70, which contained the E box (p-69/+60), resulted in a reduction of the level of activity to one fourth of the highest level observed in p-163/+60. The activity was almost abolished by deletion of the region from -69 to –30, in which the GC box was located (p–29+60).

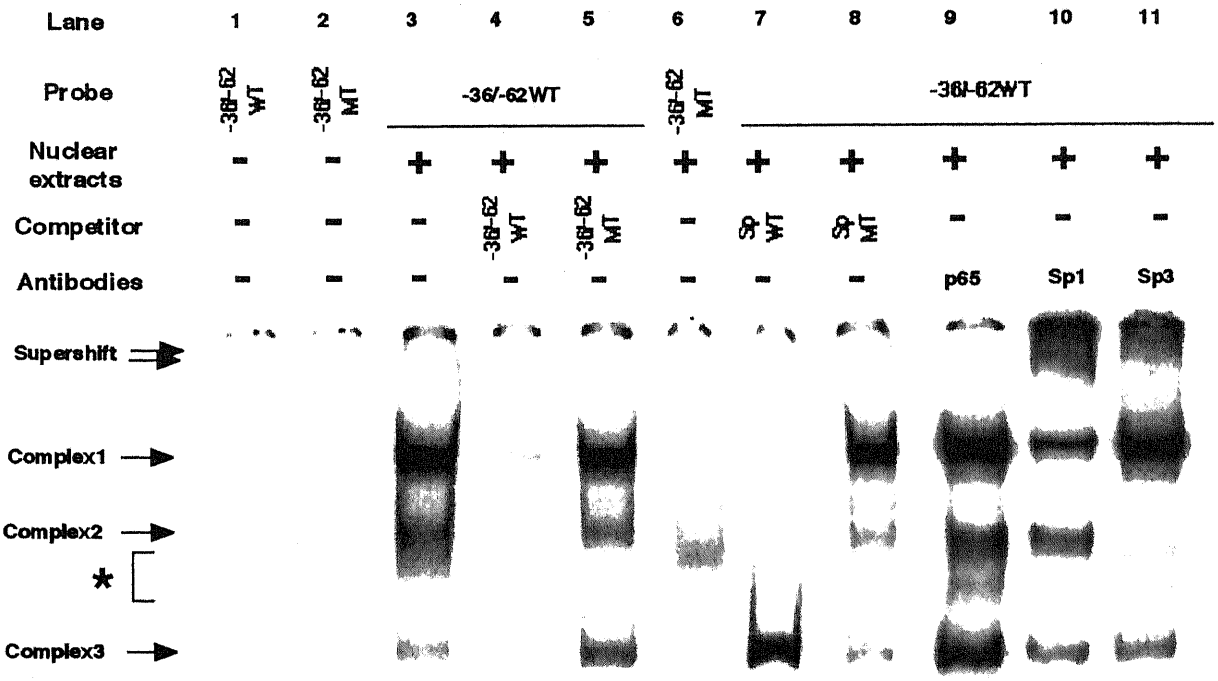

Figure 4. Identification of nuclear proteins interacting with the GC box in the *mCES2* gene promoter. The probes and competitors are listed in Table s1. Symbols (-) and (+) indicate the absence and presence of nuclear extracts or competitor, respectively. DNA-protein complexes are indicated by arrows and are named. Asterisk indicates unknown complexes. EMSAs were performed using the following probes: -36/-62WT in lanes 1, 3 - 5, and 7 -11 and -36/-62MT in lanes 2 and 6. Oligonucleotide competitors were added with 50-fold excess amounts of the following probes: -36/-62WT in lane 4, -36/-62MT in lane 5, SpWT in lane 7, and SpMT in lane 8. Supershift assays were performed using antibodies specific for Sp1 or Sp3. Anti-Sp1 antibodies (2 μg) were added to the reaction mixtures in lane 10, and anti-Sp3 antibodies (2 μg) were added to the reaction mixtures in lane 11. Anti-p65 antibodies (2 μg) were used as a negative control (lane 9). The arrows indicate shifted bands. Other experimental procedures are described in Experimental.

The results of mutation analysis were similar to those obtained from deletion analysis of the 5'-flanking region of the *mCES2* gene (Fig. 3). All of the mutational constructs except for pNFmt showed significant reduction of transcriptional activity compared with that of the intact p-163/+60. The introduction of mutation into the GC box (pGCmt) and the E box (pEmt) caused 68% ($P<0.005$) and 33% ($P<0.05$) reductions in the activity level, respectively, relative to the activity level of p-163/+60. The effects of double mutations on transcriptional activity differed among constructs. Additional mutation in the NFκB element to pGCmt (pGCNFmt) resulted in reduction of the transcriptional activity level (decrease of a further 14%, $P<0.05$). However, the activity level of the double GC box and E box mutant (pGCEmt) was comparable to that of pGCmt. The activity level of the double E box and NFκB element mutant (pENFm) was 53% of that of control (p-163/+60) and was slightly lower than that of pEmt. The activity level of the constructs harboring GC box, E box and NFκB element mutations (pAllmt) was significantly low (20% of the control level, $P<0.005$), but this activity level was almost the same as that of pGCNFmt.

Identification of nuclear proteins interacting with the GC box of the mCES2 gene promoter.

The results of deletion and mutation analyses showed that the 5'-flanking region of –163 to +60 consists a minimal promoter of the *mCES2* gene and that three *cis* elements, GC box, E box and

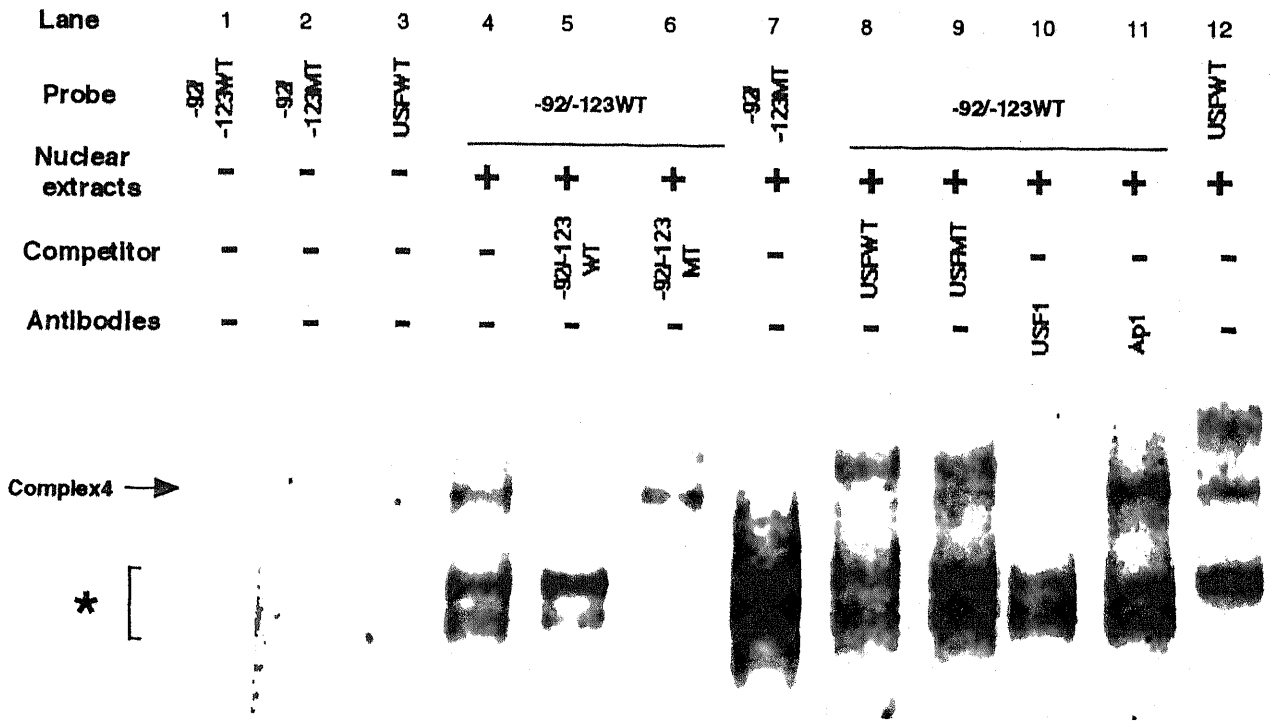

Figure 5. Identification of nuclear proteins interacting with the E box in the *mCES2* gene promoter. The probes and competitors are listed in Table s1. Symbols are explained in the legend of Fig. 4. EMSAs were performed using the following probes: -92/-123WT in lanes 1, 4 - 6, and 8 -11, -92/-123MT in lanes 2 and 7, and USFWT in lanes 3 and 12. Oligonucleotide competitors were added with 50-fold excess amounts of the following probes: -92/-123WT in lane 5, -92/-123MT in lane 6, USFWT in lane 8, and USFMT in lane 9. EMSAs were also performed using antibodies specific for USF1. Anti-USF1 antibodies (2 μg) were added to the reaction mixtures in lane 10. Anti-AP1 antibodies (2 μg) were used in lane 11 as a negative control. Other experimental procedures are described in Experimental.

NFκB element, located within the region were important for transactivation of the promoter. Electrophoretic mobility shift assays (EMSAs) were carried out to determine the nuclear proteins that could interact with these elements. The probes used in EMSAs are listed in Table s1.

Figure 4 shows the results of EMSAs and supershift assays for identification of proteins interacting with the GC box. The probe, -36/-62WT, was incubated with Hepa1-6 nuclear extracts, resulting in the formation of three DNA-protein complexes, termed complex 1, complex 2 and complex 3 (lane 3). There was an unknown factor in the nuclear extracts indicated by an asterisk. All three complexes disappeared when a 50-fold excess amount of –36/-62WT was added as a competitor (lane 4), while a competitor containing a degenerate GC box of the *mCES2* gene, -36/-62MT, did not affect the formation of any of the three complexes (lane 5). The labeled probe –36/-62MT could hardly produce all three complexes (lane 6). Complex 1 and complex 2 were completely competed-out by the addition of SpWT, an Sp family consensus oligonucleotide (lane 7), but not by the addition of SpMT, a mutated Sp family consensus oligonucleotide (lane 8). Neither SpWT nor SpMT could prevent the formation of complex 3 (lanes 7 and 8). To identify the proteins composing the three complexes, supershift assays were performed using anti-Sp1 and anti-Sp3 antibodies. The addition of anti-Sp1 antibodies generated a supershifted band together with a decrease in the amount of complex 1 formed (lane 10), and,

similarly, the addition of anti-Sp3 antibodies completely disrupted the formation of complex 2 accompanied by the generation of a supershifted band (lane 11). Anti-p65 antibodies, used as a negative control, did not influence the formation of any complexes (lane 9). These data show that Sp1 and Sp3 proteins are bound to the GC box of the *mCES2* gene promoter. The formation of complex 3 is not dependent on the canonical GC box but is dependent on the GC box of the mCES2 promoter. Nuclear proteins in complex 3 remain unknown.

Identification of nuclear proteins interacting with the E box of the mCES2 gene promoter.

Next, we examined nuclear proteins that interacted with the E box of the *mCES2 promoter* (Fig. 5). Incubation of the labeled probe –92/-123WT with nuclear extracts resulted in the formation of complex 4 (lane 4).

Formation of complex 4 was not observed in the presence of –92/-123WT as a competitor (lane 5), and this complex was detected in the presence of a competitor containing a mutated E box, –92/-123MT (lane 6). In addition, -92/-123MT could not bind to the nuclear protein forming complex 4 (lane 7). This complex was eliminated by the addition of the competitor USFWT, a USFs consensus oligonucleotide (lane 8), while it was resistant to the competitor USFMT, a mutated USFs consensus oligonucleotide (lane 9). A protein-DNA complex migrating at the same position as that of complex 4 was detected in lane 12 where USFWT was used as a probe. To determine the proteins composing complex 4, EMSAs were performed using antibodies against USF1. Anti-USF1 antibodies prevented the formation of complex 4 (lane 10), while non-related antibodies (anti-AP1 antibodies) did not (lane 11). These results demonstrate that USF1 proteins exist in complex 4.

Identification of nuclear proteins interacting with the NFκB element of the mCES2 gene promoter.

Results of deletion analysis and mutation analysis showed that, even in normal cell culture conditions, the NFκB element is important for the *mCES2* gene promoter to exert its maximum level of transcriptional activity. To identify the constitutive factor(s) bound to the NFκB element of the *mCES2* gene promoter, EMSAs were performed using consensus or mutational probes for Sp family and C/EBPs (Fig. 6A). This is because it has been reported that the upstream regions of *P-selectin* [86], *angiotensinogen* [87], major histocompatibility complex *H2K* [88], and *Cytochrome P450 3A7* [89] genes possess NFκB elements that can bind to a constitutive factor in a sequence-dependent manner (Table s2). The probe –123/-149WT could bind to nuclear proteins, resulting in the formation of complex 5 and complex 6 (lane 3). These complexes were not observed in the presence of the competitor –123/-149WT (lane 4) but were found in the presence of the mutational competitor –123/-149MT (lane 5). The formation of complex 5 was competed away by addition of the competitor SpWT (lane 7) but not affected by the competitor SpMT (lane 8). The competitor NFκBWT slightly diminished the rate of formation of complex 5 and simultaneously abolished the formation of complex 6 (lane 9). No effect of the competitor NFκBMT on the formation of complexes was observed (lane 10). Neither the C/EBP consensus competitor nor its mutant affected the formation of complexes (lanes 11 and 12). When antibodies were added to the reaction mixture, the formation of complex 5 was reduced in the presence of anti-Sp1 antibodies but not in the presence of anti-p65 or anti-Sp3 antibodies (data not shown). To verify the binding of Sp1 to the *mCES2* NFκB element, EMSAs were carried out using nuclear extracts from COS7 cells in which Sp1 was overexpressed (Fig. 6B). The probe –123/-149WT could produce complex 7

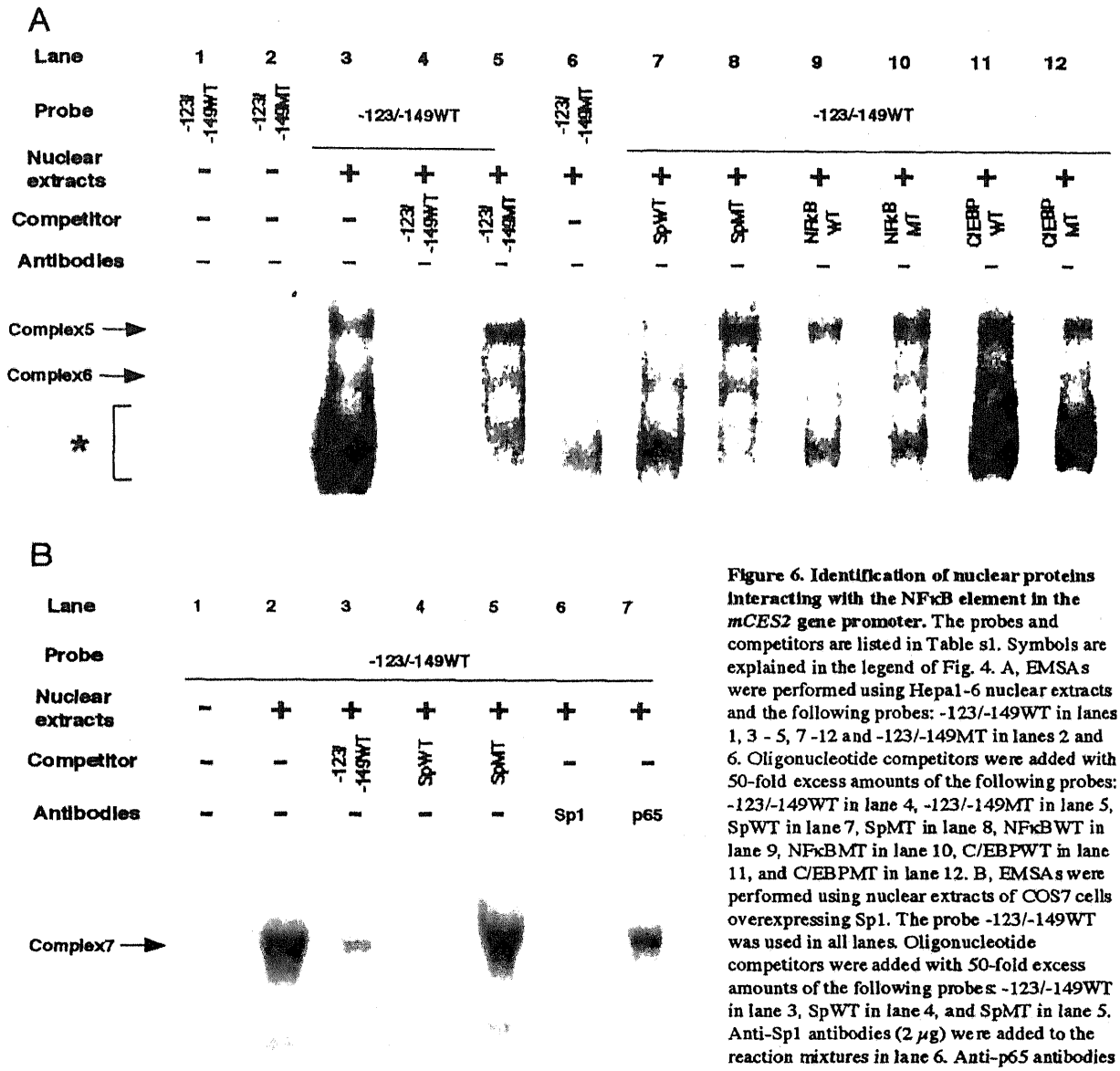

Figure 6. Identification of nuclear proteins interacting with the NFκB element in the *mCES2* gene promoter. The probes and competitors are listed in Table s1. Symbols are explained in the legend of Fig. 4. A, EMSAs were performed using Hepa1-6 nuclear extracts and the following probes: -123/-149WT in lanes 1, 3 - 5, 7 -12 and -123/-149MT in lanes 2 and 6. Oligonucleotide competitors were added with 50-fold excess amounts of the following probes: -123/-149WT in lane 4, -123/-149MT in lane 5, SpWT in lane 7, SpMT in lane 8, NFκBWT in lane 9, NFκBMT in lane 10, C/EBPWT in lane 11, and C/EBPMT in lane 12. B, EMSAs were performed using nuclear extracts of COS7 cells overexpressing Sp1. The probe -123/-149WT was used in all lanes. Oligonucleotide competitors were added with 50-fold excess amounts of the following probes: -123/-149WT in lane 3, SpWT in lane 4, and SpMT in lane 5. Anti-Sp1 antibodies (2 μg) were added to the reaction mixtures in lane 6. Anti-p65 antibodies (2 μg) were added to the reaction mixtures in lane 7. Other experimental procedures are described in Experimental.

with nuclear extracts (lane 2), and this complex was eliminated by the addition of either a self-competitor or SpWT (lanes 3 and 4, respectively). The formation of complex 7 was not disturbed by SpMT (lane 5). Furthermore, complex 7 disappeared in the presence of anti-Sp1 antibodies (lane 6), whereas anti-p65 antibodies did not disturb the formation of complex 7 (lane 7). Together with the results shown in Figure 6A, our data show that Sp1 is involved in the formation of these complexes.

Synergistic transactivation of the mCES2 promoter by Sp1, Sp3 and USF1 in Drosophila SL2 cells.

We finally analyzed the functional capabilities of Sp1, Sp3 and USF1 for transactivation of the *mCES2* gene promoter. p-163/+60 was co-transfected with pAcSp1, pPacUSp3, and/or pAcUSF1 in *Drosophila* SL2 cells, which possess a null background for these transcription factors [90], and luciferase activities were compared (Fig. 7). When transfected alone, Sp1 was shown to be

a strong transactivator of the promoter (2.4-fold increase in promoter activity), while USF1 induced only a weak transactivation (1.4-fold increase in promoter activity) and Sp3 was almost inert. However, in the case of a combination of Sp1 with Sp3 or USF1, the promoter activity level was increased by 3.7 fold ($P<0.01$) and 4.2 fold ($P<0.05$), respectively. The combination of Sp3 and USF1 also showed a synergistic transactivation (increase by 3.5 fold, $P<0.005$). Moreover, potent synergistic transactivation (increase by 8.7 fold) was observed in the case of a combination of all three factors, and this induction level of promoter activity was significantly higher than those obtained with the Sp1/Sp3 combination or the Sp1/USF1 combination ($P<0.005$). These data indicate cooperative transactivation of the *mCES2* promoter by Sp1, Sp3, and USF1.

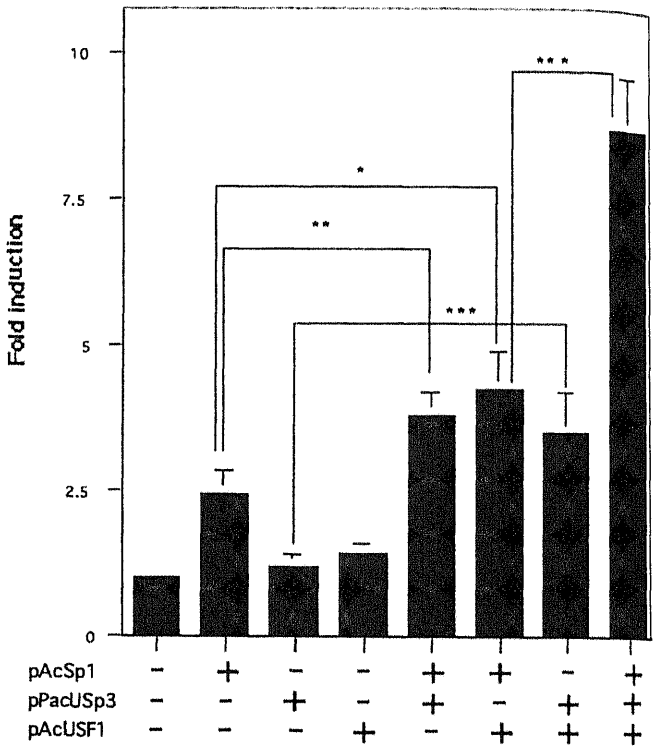

Figure 7. Co-transfection assays of the *mCES2* gene promoter. Luciferase ge regulated by the *mCES2* promoter (150 ng) were transiently co-transfected into *Drosophila* SL2 cells together with 50 ng of pAcSp1, pPacUSp3, and/or pAcUS Total DNA amount was adjusted to 300 ng by using an empty pAc5.1V5/His ve Luciferase activity was determined as relative activity (Firefly/total cellular prot Each value is the mean (± S.D.) of fold induction towards the activity obtained b *mCES2* promoter alone (left column) of three separate experiments, each perfor duplicate. *, ** and *** indicate statistically significant differences between tw transfectants indicated in the figure ($P<0.05$, $P<0.01$, and $P<0.005$, respectively)

II-I-IV Discussion

We have presented here some experimental data showing tissue expression profiles of mCES2 and indicating that Sp1, Sp3, and USF1 contribute to synergistic transactivation of the *mCES2* promoter.

As for the examination of tissue expression profiles of mCES2, RT-PCR is not a completely quantitative method for evaluation of mRNA expression; nonetheless, the amplification levels of specific bands in tissue cDNA were apparently different. Relatively high expression levels of mCES2 in the liver and small intestine are reasonable since it has been demonstrated that the carnitine/acylcarnitne system does work in the ER in these tissues [64, 80]. The reason why mCES2 is expressed in the kidney, thymus, adipose tissue, brain, lung, and testis but is not expressed in the heart is currently unknown. It has been reported that human CES2 is expressed at high levels in the kidney and heart and at low levels in the brain and lung but is not expressed in the thymus [83]. Although physiological functions of these CES2 isozymes remain obscure, the similarities and differences between expression profiles of these CES2 isozymes may mirror functional similarities and species differences of the CES2 family.

The possibility that mCES2 is posttranslationally modified or forms a complex with another protein or other proteins in a small intestine-specific manner should be pointed out. Results of esterase activity staining after non-denaturing PAGE showed that the bands observed in the small intestine were doublet bands with slightly different rates of migration, although all tissue samples were prepared in the same way. However, the doublet bands are thought to result from mCES2 protein since anti-mCES2 antibodies [20] could specifically eliminate both bands (data not shown). Further analysis is needed to determine how mCES2 is expressed in the small intestine, and the results of such analysis may lead

to revelation of novel physiological functions of mCES2.

Our next challenge is to determine how *mCES2* transcription is controlled. An approximately 1.4-kbp fragment of the 5'-flanking region of the *mCES2* gene shows characteristics of a TATA-less promoter, such as the lack of a TATA box but the presence of a GC box and an E box in precedence to the transcription start site. A TATA-less promoter seems to be shared by other members of the CES family, since two previously reported CES promoters also do not have a functional TATA box [49, 91].

The *mCES2* promoter transactivation was controlled by the synergistic action of three *cis* elements, a GC box, an E box and an NFκB element (Figs. 2 and 3), but the degrees of contribution of these elements to the promoter activity were not equivalent. It is noteworthy that the E box could work as a functional *cis* element only when a functional GC box was present in the promoter (Fig. 3, pGCmt vs. pGCE and pGCNFmt vs. pAllmt), indicating that there was potential cooperative interaction between nuclear factors that bound to these two *cis* elements. These nuclear proteins were revealed to be Sp1, Sp3 and USF1 by following experiments.

Sp family proteins and USFs are transcription factors that are ubiquitously expressed and that are involved in transactivation of TATA-less promoter via binding to the GC/GT box and E box (CANNTG), respectively [92-95].Among Sp family proteins, Sp2 is structurally different from other Sp members [96-98] and Sp4 is predominantly expressed in the brain [97, 99]. Sp3 is expressed in all mammalian cells that express Sp1 [96, 98]. Thus, Sp1 and Sp3 were our first choice as candidates for nuclear proteins that interact with the GC box of the mCES2 promoter. On the other hand, we chose USF1 as a candidate for nuclear proteins that bind to the mCES2 E box since USFs are involved in the regulation of many genes that play a role in glucose or fatty acid metabolism, such as those encoding glucokinase [100] and fatty acid synthase [101, 102].

In addition to the GC box, we also determined that Sp1 could bind to the mCES2 NFκB element. Hirano et al. [86] demonstrated that Sp1 can bind to subsets of NFκB elements with high affinities. They proposed that Sp1 might raise the basal expression levels of NFκB-dependent genes in the absence of activated NFκB. Although *mCES2* gene transcription is apparently not NFκB-dependent, their proposition, at least in part, supports our data because the mCES2 NFκB element is necessary for full promoter activity. Further analysis is needed to determine whether NFκB is involved in the regulation of *mCES2* gene transcription.

Sp family and USFs show many heterotypic interactions with different classes of nuclear proteins [103-106]. It has recently been reported that physical and functional interactions between Sp1 and USFs regulate human deoxycytidine kinase promoter activity [107]. Here, we have provided additional experimental data showing the synergistic role of Sp family and USF1 in transactivation of the promoter. Our results of co-transfection assays are in accordance with all other results obtained in the present study. Notable findings are that transfection with USF1 alone only weakly activated the transcription but that was a positive activator in the presence of either Sp1 or Sp3. Although the mechanism by which Sp3 interacts with USF1 is currently unknown, these results are also in good agreement with those indicating that the E box needs the GC box to work as a functional *cis* element (Fig. 3).

Unexpectedly and interestingly, Sp3 could interact with Sp1 to synergistically increase mCES2 promoter activity rather than compete with Sp1, whereas Sp3 alone was unable to drive the transactivation. More surprisingly, Sp3 could cooperatively interact with the Sp1/USF1 complex to further increase mCES2 promoter activity. Regarding the interaction between Sp1 and Sp3,

our results are reminiscent of studies in which transcriptional regulation of the mouse *hepatocyte growth factor (HGF) receptor* gene [108] or the rat *fatty acid synthase* (*FAS*) gene [109] was analyzed. In these studies, Sp1 and Sp3 transcription factors exhibited cooperative functions in gene transcription, and Zhang et al. [108] reported that physical interaction between these factors was demonstrated by co-immunoprecipitation assays. However, others reported that anti-Sp3 antibodies did not co-immunoprecipitate Sp1 or *vice versa* [110]. Transcriptional properties of Sp3 are so complicated [93] that it remains uncertain how Sp3 is involved in the synergism observed in our case. Further analysis is needed to elucidate the mechanism.

It is very intriguing that Sp1 and USF1 are strongly involved in transcriptional regulation of the *mCES2* gene because there has been accumulating evidence of Sp1 and USF1 being mediators for insulin response. The current understanding of Sp1 is that it is not just a basal transcription factor but is also a member of insulin signaling cascades as well as of other signal transductions [111]. Keembiyehetty et al. [112] showed that insulin augments Sp1 expression, enhances its translocation to the nucleus, and increases its glycosylation. In the diet-induced DNase I-hypersensitive site of the *rat FAS* gene promoter, the binding of Sp1 to the GC box, which is juxtaposed with FAS insulin-responsive element 1 (FIRE1), contributed to the binding of NF-Y to FIRE1 [113]. On the other hand, Latasa et al. [114] have elegantly demonstrated *in vivo* that USF binding to the E box is required for SREBP binding and activation of the FAS promoter in refeeding states in mice. There is no information at present on hormonal or nutritional regulation of *mCES2* gene transcription. However, considering our proposition that mCES2 plays an important role in fatty acid (ester) metabolism, we are ready to test the possibility that *mCES2* gene transcription is regulated by insulin or feeding conditions through Sp1 and/or USFs.

In the present study, we have shown tissue expression profiles of mCES2 and parts of the mechanism by which transcription of the *mCES2* gene is regulated. mCES2 is expressed in the liver, kidney, small intestine, brain, thymus, lung, adipose tissue and testis. We have also shown that Sp1, Sp3, and USF1 contribute to synergistic transactivation of the *mCES2* promoter. Although the possibility of involvement of other transcription factors in the regulation of *mCES2* gene expression cannot be ruled out and further studies are needed to fully elucidate the mechanisms, our data indicate that Sp1, Sp3 and USF1 are indispensable factors for transcription of the *mCES2* gene. The results of the present study have provided some clues for understanding the molecular mechanisms regulating *mCES2* gene expression and should be useful for studies aimed at elucidation of physiological functions of mCES2.

II-II
Hepatocyte nuclear factor-4 alpha plays pivotal roles in transactivation and bile acid-mediated repression of the *mouse carboxylesterase 2 gene* promoter

II-II-I Introduction

In the previous section, we have found that mCES2 are expressed in various tissues with the higher level of expression present in the liver, kidney and small intestine. And three transcription factors, Sp1, Sp3 and USF1, can bind to the promoter region of the *mCES2* gene, leading to a synergistic transactivation of the promoter. Although this mechanism may explain ubiquitous tissue expression profiles of mCES2, it is unlikely to contribute to the high level of mCES2 expression in the liver, kidney and small intestine. Therefore, another mechanism controlling this tissue specific transcription would exist.

Hepatocyte nuclear factor-4 alpha (HNF-4α) is a member of the nuclear receptor superfamily [115]. Many nuclear receptors required their specific ligands to strongly stimulate transcription of the target gene, but HNF-4α exerts its ability to activate transcription of the target genes without its ligand. Instead, the ability of transacriptional activation of HNF-4α was modulated by its various ligands, long-chain acyl-CoA thioesters [116]. HNF-4α was specifically expressed in the liver, kidney, small intestine, pancreas, and stomach [115, 117, 118]

HNF-4α has been in the limelight in the studies amid at the elucidation of mechanisms controlling liver differentiation and functions since this nuclear factor has been shown to be involved in the regulation of many genes related to various metabolisms, such as glucose or lipid metabolism, synthesis of blood coagulation factors, and epithelial morphogenesis [119-122]. The roles of HNF-4α in lipid metabolism has been examined by development of mice with the *Hnf-4α* gene null hepatocytes [123] since the disruption of the *Hnf-4α* gene causes embryonic lethal [124]. The mice with the *Hnf-4α* gene null hepatocytes showed the increased level of the lipid accumulation in hepatocytes, concurrently with the decreased levels of the serum cholesterol and triglycerides. The mice also showed the elevated serum bile acid level. Interestingly, recent studies have showed that the orphan nuclear receptor small heterodimer partner (SHP) inhibits HNF-4α-mediated transactivation in the various genes [125-127], indicating that HNF-4α is one of the targets for metabolic switches in response to bile acid signals. Collectively, HNF-4α is thought to be one of the key factors for orchestrating various hepatic functions. These biological characteristics of HNF-4α described above prompted us to test the hypothesis that HNF-4α would be involved in the transcriptional regulation of the *mCES2* gene.

In this study, we have obtained several experimental data indicating that HNF-4α is involved in the regulation of the *mCES2* gene. Furthermore, we have also showed that bile acid can repress mCES2 expression by inhibiting the HNF-4α-mediated transactivation of the *mCES2* gene promoter. These results would be valuable information for the study aimed at the elucidation of the physiological functions of mCES2.

II-II-II Materials and Methods

Cell cultures, total RNA isolation, cDNA synthesis and reverse transcription-polymerase chain reaction (RT-PCR) analysis

Human hepatoma cell line, HepG2 cells, were obtained from the Institute of Development, Aging and Cancer, Tohoku University (Sendai, Japan), and Chinese hamster lung carcinoma, V79 cells, were from American Type Culture Collection (Rockville, MD). Both cell lines were maintained at 37°C with 5% CO_2 in Dulbecco's modified Eagle's medium (D-MEM) (Invitrogen, Carlsbad, CA) supplemented with 10% (v/v) heat-inactivated fetal bovine serum (FBS) and 50 units/mL penicillin and with 50 μg/mL streptomycin. Humam hepatoma cell line, FLC7 cells [128], were kindly provided by Dr. S. Nagamori (Kyorin University, Tokyo, Japan) and were grown at 37°C with 5% CO_2 in D-MEM/ F-12 (Invitrogen) supplemented with 10% (v/v) heat-inactivated FBS and 50 units/mL penicillin and with 50 μg/mL streptomycin. Mouse immortalized hepatocytes, TLR2 cells [129], were obtained from Japan Health Sciences Foundation (Tokyo, Japan) and were grown at 33°C with 5% CO_2 on the type I collagen-coated flask. Culture medium for this cell line was RITC80-7 (Asahi Techno Grass, Funabashi, Japan) supplemented with 2% (v/v) heat-inactivated FBS, insulin-transferin-selenium-X supplement (10 mg/L insulin, 6.7 ng/L sodium selenate, 5.5 mg/L transferin, and 2 mg/L monoethanolamine at final concentrations) (Invitrogen), 10 ng/μL recombinant human epidermal growth factor (Wako), and 50 units/mL penicillin and with 50 μg/mL streptomycin.

Total RNAs of these cell lines were extracted from TRIzol reagent (Invitrogen) and cDNA was synthesized by using Ready-To-Go RT-PCR Beads with an oligo (dT) primer or randam hexamer primer (Amersham Bioscience, Piscataway, NJ, U.S.A.) as described in the section I-I-II. To demonstrate that no genomic DNA was contaminated, PCR amplification was performed using total RNA as a template with a set of primers for detection of the mouse *glyceraldehyde-phosphate dehydrogenase (GAPDH)* gene: sense, 5'-TGCACCACCAACTGCTTA-3'; and anti-sense, 5'-GGATGCAGGGATGATGTTC-3', or a set of primers for detection of the human *β2 microgloburin* gene: sense, 5'-GCTTACATGTCTCGATCCCACTT-3'; and anti-sense, 5'-CCCCCACTGAAAAAGATGAGTATG-3'. To detect the expression of the human *HNF-4α2* gene and the *HNF-4α8* gene, the different sense primers and the shared antisense primer were used as follows; sense for the human *HNF-4α2* gene, 5'-ATGGACATGGCCGACTACAGTGCT-3', sense for the *HNF-4α8* gene, 5'-CTTGGCCATGGTCAGCGTGAACG-3', and common anti-sense, 5'-CGAATGTCGCCGTTGATC-3'. These primers were designed on the basis of the previous reports [130]. Similary, to detect the expression of the mouse *HNF-4α2* gene and the *HNF-4α8* gene, the different sense primers and the shared antisense primer were used as follows; sense for the mouse *HNF-4α2* gene, 5'-GACTCTCTAAAACCCTTGCCG -3', sense for the *HNF-4α8* gene, 5'-GTCATGGTCAGTGTGAACGC-3', and common anti-sense, 5'-GTGATGTTGGCAATCTTCTTTG-3'.

Plasmid construction

Luciferase reporter gene plasmids containing the *mCES2* gene promoter region (p-1385WT/+60, p-163/+60 and p-29/+60) were prepared by inserting the *mCES2* gene promoter to pGL3-basic vector (Promega) as described previously [131]. To make another deletion plasmid in which direct repeat 1 (DR1) element in the *mCES2* promoter was excluded, Kpn I site was introduced within the element by inverse PCR amplification as described previously [131]. The sense primer was 5'-CCTGTGCAAGGTACCCTCCTTATGCTTCCT-3' and the anti-sense primer was 5'-AGGAAGCATAAGGAGGGTACCTTGCACAGG-3'. This mutated plasmid was digested by Kpn I, followed by self-ligation. This plasmid was termed p-9/+60. In the same way, mutation was introduced into the DR1 element of p-1385WT/+60 by using the sense primer, 5'-CTGGCCATTGGCTCCTATCAAAAGTGACTAAT-3', and the anti-sense primer, 5'-ATTAGTCACTTTTGATAGGAGCCAATGGCCAG-3'. This mutated plasmid was termed as p-1385MT/+60.

The cDNA clones of two isoforms of mouse HNF-4α, HNF-4α2 and HNF-4α8, were cloned from mouse liver cDNA and TLR2 cDNA, respectively, by PCR amplification. For the cloning of HNF-4α2 , the sense primer, 5'-GACTCTCTAAAACCCTTGCCG -3', and the anti-sense primer was 5'-CGTGTCACATCTTCTTTGCCA-3' were used. Similary, the sense primer, 5'-

GTCATGGTCAGTGTGAACGC-3', and the anti-sense primer, 5'-ACTAGGTTACTCCCAGGTGCTC-3', were used for the cloning of HNF-4α8. To obtain small heterodimer partner (SHP) cDNA, PCR amplification was perfomed by using rat liver cDNA and the primer sets, 5'-CAAGACACAGACCATGAGCT-3' and 5'-GTCACCTCAACAAAAGCATG-3'. The cDNA clones were inserted into pCR-Blunt II TOPO vector (Invitrogen). Preparation of mouse and rat liver cDNA was described previously [131]. Then the cDNAs were subcloned into pTARGET mammalian expression vector (pHNF-4α2, pHNF-4α8 and pSHP) by EcoRI digestion coupled with alkaline phosphatase treatment to enable it to be expressed in mammalian cells. The DNA sequence was determined using a Dye Terminator Cycle Sequencing-Quick Start Kit (Beckman Coulter, Fullerton, CA, U.S.A.) and a CEQ 2000 DNA Analysis System (Beckman Coulter). The results were confirmed by sequencing at least twice in each direction.

Transient transfection and dual luciferase assays

HepG2 cells, FLC7 cells and V79 cells were plated at an appropriate density of in a 24-well dish one day before transfection. When the cells had reached 60 to 80 percent of confluence, they were transiently transfected with 200 ng of the reporter plasmids, 4 ng of phRL-TK vector (Promega) and 100 ng of empty pTARGET vector and/or cDNA expression vectors for using Trans IT (Mirus, Madison, WI) according to manufacturer's protocol. At 30 hr after transfection, the cells were washed with phosphate-buffered saline (PBS) and were harvested. The luminescence from transfected cell lysates was determined using a Dual-Luciferase Reporter Assay System (Promega) and a TD-20/20 luminometer (Promega) as discribed previously [131]. Results were expressed as relative ratio (firefly luciferase activity /*renilla* luciferase activity). Experiments were performed in triplicate, and each value presented is the mean (± S.D) from at least three independent experiments. For the assays to determine the effects of chenodeoxycholic acid (CDCA, Sigma, St. Lois, MO) on the promoter activity of the *mCES2* gene, CDCA (50, 75 or 100 μM) or its vehicle (dimethylsulfoxide, DMSO) was added to the serum-free medium at 3h after transfection. The luciferase activity was determined as described above.

Nuclear extraction and electrophoretic mobility shift assays (EMSAs)

Nuclear extracts were prepared from HepG2 cells and TLR2 cells as described in the section II-I-II. The protein concentration was determined by using a Bio-Rad *Dc* Protein Assay Kit (Bio-Rad Laboratories, Hercules, CA., U.S.A.). The nuclear extracts were stored at -80°C until used.

Detailed procedures for EMSAs were described in the secton II-I-II. The oligonucleotide sequence containing wild type or mutated DR1 element of the *mCES2* promoter were designed as follows: 5'-TTTAAATAGCTGCCTGTGCAAGGTTCACTCCTTAT-3' (mCES2DR1WT), and 5'-TTTAAATAGCTGCCTGTTTTTGGTTCACTCCTTAT -3' (mCES2DR1MT). Consensus and mutated consensus oligonucleotides for HNF-4a were designed on the basis of the previous report [115], which were 5'-TCGAGCGCTGGGCAAAGGTCACCTGC-3' (APF1WT) 5'-TCGAGCGCTAGGCACCGGTCACCTGC-3' (APF1MT). The only sense strand sequences were displayed above, and the letters underlined indicated the mutations introduced. The names of probe/competitor were indicated in the parentheses. For inhibition assays using antibodies, 2 μg of antibodies against HNF-4α (sc-6556x, Santa Cruz Biotech, CA) or heat shock transcription factor (HSTF) 1 (sc-8061x, Santa Cruz Biotech) was added to the binding reaction mixture at room temperature for 30 min prior to addition of the probe.

CDCA treatment to TLR2 cells and quantitative real-time PCR

TLR2 were seeded on the collagen-coated frask one day before treatment in the reduced serum condition (1.2%) to minimize the potential shock on the gene expression in TLR2 cells caused by serum depletion. Time point 0 (T=0) was set at the time just before addition of CDCA to the cells, and at this time the cultured medium of the cell to be treated were replaced to the serum free medium and subsequently

CDCA (45 μM) or DMSO were added. The cells and condition medium were recovered at 6, 12, 24 and 36 hr after treatment (T=6, 12, 24, and 36). Toxicity of CDCA was evaluated by the determination of the level of released lactate dehydrogenase (LDH) activity (In vitro toxicology assay kit lactate dehydrogenase based, Sigma) and by cell virability (0.4% trypane blue stain, Invitrogen). Total RNAs of the collected cells were extracted and cDNA was synthesized as described above. The expression profiles of mCES2, SHP and HNF-4α were analyzed by using Taqman Gene Expression Assays with ABI PRISM 7000 Sequence Detection System (Applied Biosystems, Foster City, CA). The reaction mixture consisted of Taqman Universal PCR Master Mix, Assays-on-Demand Gene Expression Assay Mix (Taqman probes and primers for the specific gene) and cDNA sample. PCR reaction was performed by the condition: 50°C for 2 min and 94°C for 10 min, followed by 94°C for 15 sec and 60°C for 60 sec, 40 cycles. The level of expression of 18S rRNA was used as an internal standard and was used for normalization of the level of expression of the objective gene. The value was the mean of three independent assays, each of which were performed in duplicate. For forced expression of HNF-4α in TLR2 cells, HNF-4α2 expression vector was transfected into TLR2 cells 12 h after treatment of CDCA by using CombiMag (Funakoshi, Tokyo, Japan) combined with Trans-IT. The cells were recovered at 24 h and 36 h for extraction of total RNA. Quantification of mRNA expression was performed as described above.

Preparation of TLR2 cell homogenates

The cultured cells in normal condition and those treated with CDCA or vehicle were collected and were disrupted by ultrasonicator. Then the homogenate was prepared using a homogenizer. The sample was stored at -80°C until used.

Determination of enzyme activity and Esterase activity staining after non-denaturing PAGE

Esterase activity staining after non-denaturing PAGE was performed as described in the section I-I-II.

Statistical analysis

Student's *t*-test was performed to determine significance of difference between the groups in luciferase assays and real-time PCR analysis. *P* values less than 0.05 were taken to be significant.

All results are representative of two or three independent experiments.

Chemicals used in this study were of reagent grade and obtained from commercial sources.

II-II-III Results

Enhancement of the promoter activity of the mCES2 gene by expression of HNF-4α

The experiment was begun with looking for a DR1 element by using searching programs for transcription factor binding sites (http://www.gene-regulation.com/). As shown in Fig. 1A, the putative DR1 element was found close to transcription start site, and the nucleotide sequence was very similar to those of DR1 elements in the human *transthyretin* gene and the human *apolipoprotein C III* gene to which it has been reported that HNF-4α could bind [115]. Next, we performed luciferase assays by using three different cell lines. Both HepG2 cells and FLC7 cells were derived from hepatocarcinoma, but HepG2 cells expressed endogenous HNF-4α at the higher levels than that of FLC7 (Fig. 1B). Expression of endogenous HNF-4α in V79 cells was very low, if any, since they were derived from lung carcinoma. In Fig. 1C, the results of luciferase assay showed that the level of the reporter activity was the highest in HepG2 cells and almost the same in FLC7 cells and V79 cells without exogenous expression of HNF-4α. With the forced expression of HNF-4α2, the level of the *mCES2* gene promoter activity was significantly increased in all three cell lines. We also tested effects of the forced expression of HNF-4α8, a splicing variant of HNF-4α2, on the *mCES2*

promoter activity. Although the extent of a stimulation of the promoter activity was a half of HNF-4α2, HNF-4α8 could also significantly induce the activity of the *mCES2* gene promoter (data not shown). To further examine roles of the DR1 element on HNF-4α2-driven transactivation of the *mCES2* gene promoter, deletion and mutation analyses were performed (Fig. 1D and 1E). The plasmid, p-29, lacking three cis elements that we reported previously [131] still possessed much higher level of the reporter activity than that of pGL3-basic,

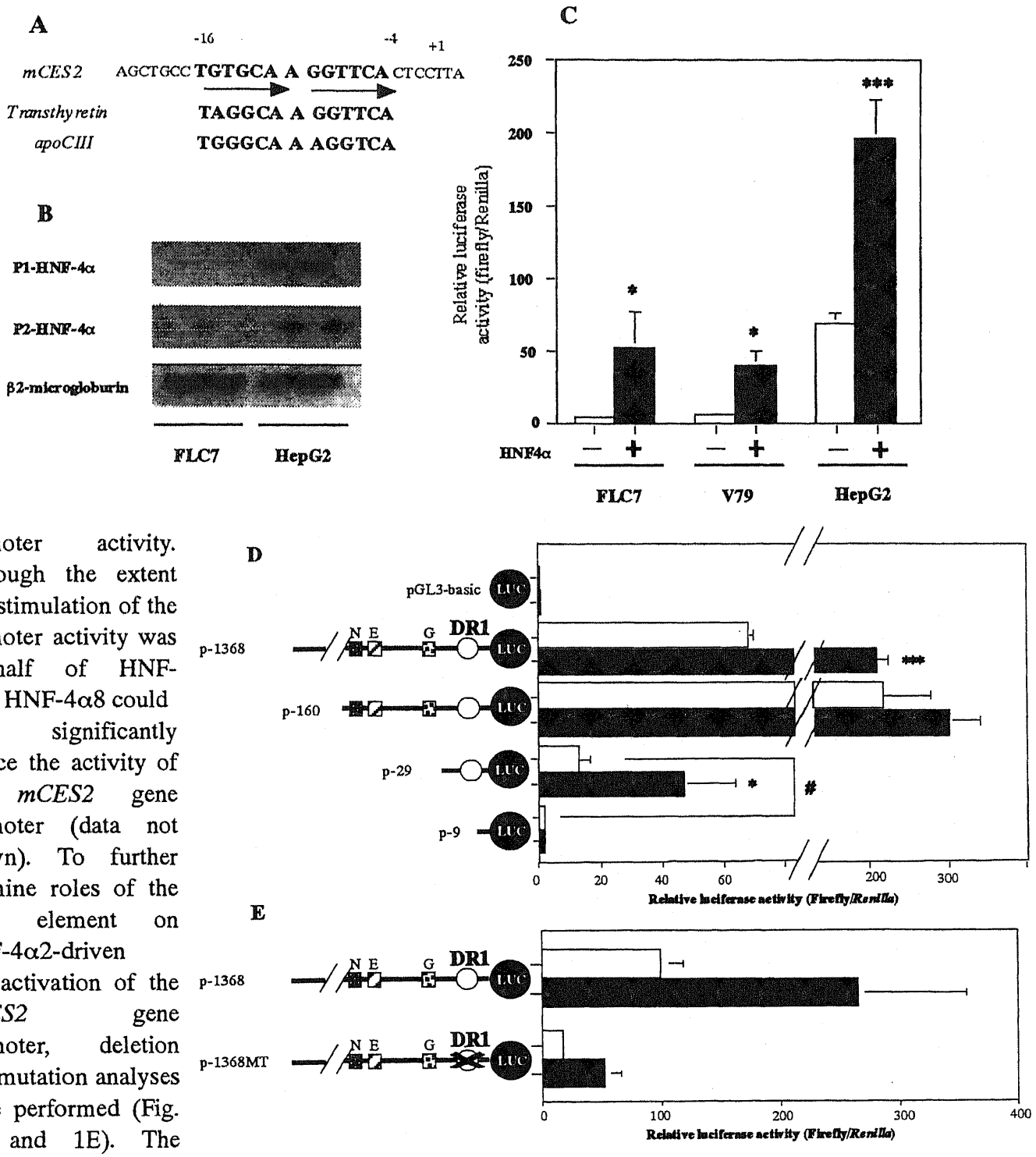

Fig. 1. Transactivation of the *mCES2* gene promoter by HNF-4α. A, Comparison of the nucleotide sequence of the mCES2 DR1 element with the known HNF-4α binding DR1 elements of the human *transthyretin* and the human *apolipoprotein CIII* genes. Arrows indicate the direction. B, Detection of HNF-4α expression in FLC7 cells and HepG2 cells by RT-PCR. P1-HNF-4α and P2- HNF-4α indicate the expression of isofoms regulated by P1 promoter and those regulated by P2 promoter, respectively. Expression of human β2-microgloburin was used as an internal standard. C, Effects of HNF-4α2 expression on the level of the promoter activity. The mCES2 reporter plasmid (p-1385) (200 ng), a phRL-TK plasmid (4 ng), and either an empty plasmid or an HNF-4α2 expression plasmid (100 ng) were transiently transfected with FLC7 cells, V79 cells and HepG2 cells. Symbols, (-) and (+), indicate the absence and the presence of the HNF-4α expression plasmid, respectively. Each value is the mean ± S.D. of relative activities (Firefly/*Renilla*) for at least three separate experiments, each performed in triplicate. D, Deletion analysis of the mCES2 gene promoter. Luciferase assays were performed in HepG2 cells as described above. Names of plasmid are shown on the left side. DR1, G, E and N indicate the direct repeat 1, a GC box, an E box and an NF-κB element, respectively. E, mutation assays for the DR1 element of the *mCES2* gene. Luciferase assays were performed in HepG2 cells as described above. A cross indicates the mutation introduced into the DR1 element. * and *** indicate statistically significant differences compared with the empty plasmid ($P<0.05$ and $P<0.005$, respectively). # indicates a statistically significant difference between two groups ($P<0.05$).

although the activity level was significantly low when compared with that of p-163. And p-29 showed responsiveness to the forced expression of HNF-4α2. Further deletion of the DR1 element caused great loss of the promoter activity and of the responsiveness to HNF-4α2 expression. Consistently, mutation introduced into the DR1 element resulted in remarkable reduction in the level of the promoter activity and responsiveness to HNF-4α2 expression. Together, it was possible that HNF-4α bound to the DR1 element of the *mCES2* gene.

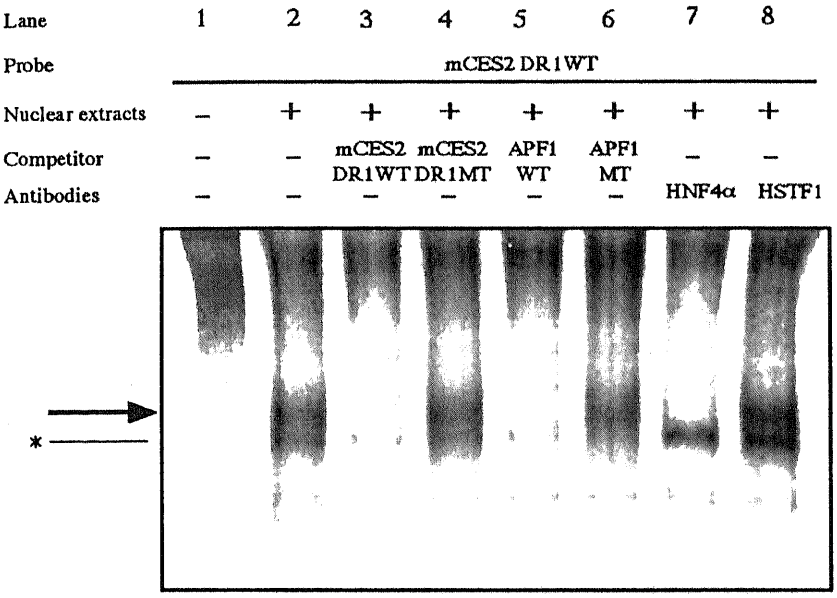

Fig. 2. Binding of HNF-4α to the DR1 element of the *mCES2* gene promoter. GMSAs were performed using the probe, mCES2DR1WT, in all lanes. Oligonucleotide competitors were added with 50-fold excess amounts of the probe as follows: mCES2DR1WT in lane 3, mCES2DR1MT in lane 4, APF1WT in lane 5 and APF1MT in lane 6. Anti-HNF-4α antibodies (2 μg) and anti-HSTF1 antibodies (2 μg) were added to the reaction mixture in lane 7 and in lane 8, respectively. The arrow indicates the complex containing HNF-4α. Symbols, (-) and (+), indicate the absence and the presence of HepG2 nuclear extracts, competitors or antibodies, respectively. Asterisk indicates an unknown complex. This is the representative data for three independent assays.

Binding of HNF-4α to the DR1 element of the mCES2 gene

To demonstrate that HNF-4α could bind to the DR1 element of the *mCES2* gene, gel mobility shift assays (GMSAs) were performed by using HepG2 nuclear extracts (Fig. 2). The oligonucleotide probe containing the DR1 element (mCES2 DR1WT) was incubated with the nuclear extracts, resulting in the formation of two complexes (lane 2). The upper one was clearly disappeared in the presence of 50-fold excess amount of either the self-competitor or the HNF-4α recognizing oligonucleotide (APF1WT) (lanes 3 and 5), but not either the mutated self-competitor (mCES2 DR1MT) nor the mutated HNF-4α binding oligonucleotide (APF1MT) (lanes 4 and 6). In the lanes 7 and 8, anti-HNF4α antibodies completely disrupted the formation of the upper complex, but anti-HSTF1 antibodies failed. Collectively, the nuclear factor in the upper complex was very likely to be HNF-4α. On the other hand, the lower complex remained to be unknown, since this complex was disappeared in the presence of either APF1WT or APF1MT and was stable in the presence of antibodies tested in this assays (lanes 5, 6, 7 and 8).

Repression of the HNF-4α-mediated transactivation of the mCES2 promoter by overexpression of SHP and bile acid

Extending the study, we examined the effects of expression of SHP and CDCA on the HNF-4α-mediated transactivation of the *mCES2* gene promoter by luciferase assays. As shown in Fig. 3A, the promoter activity of p-1368 was significantly repressed by the forced expression of SHP and, similarly, the transactivation of the promoter driven by HNF-4α2 were repressed by the co-transfection with SHP in a dose dependent manner. This SHP-mediated repression was not observed when p-1368MT, the reporter construct

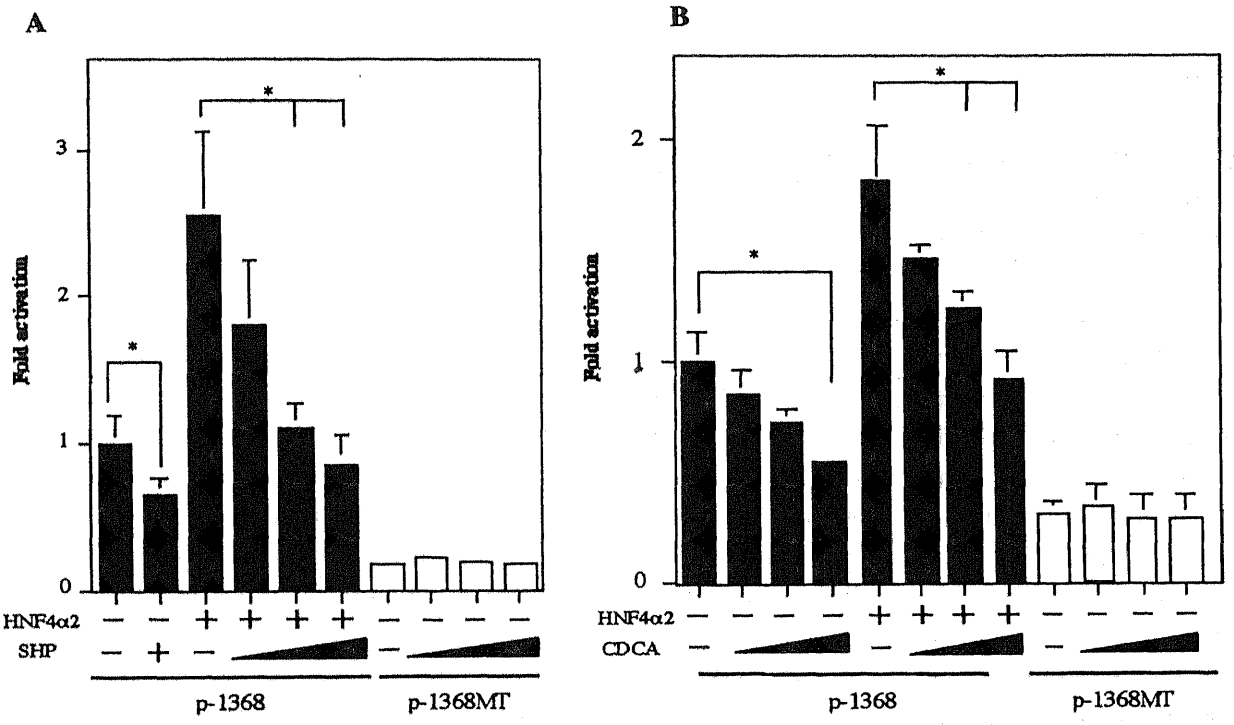

Fig. 3. Effects of the overexpression of SHP and CDCA on the promoter activity of the *mCES2* gene. A, HepG2 cells were co-transfected with 200 ng of the reporter plasmid (p-1385 or p-1385MT), 4 ng of the phRL-TK and 100 ng of the HNF4a2 expression plasmid and/ or different amount of the SHP expression plasmid (20, 40, 80 ng and 80 ng indicated by triangles and (+), respectively). Total amount of plasmid was adjusted to 304 ng by using the empty expression plasmid. Each value is the mean ±S.D. of the fold activation for three independent assays towards the relative activity (firefly/*renilla*) obtained from p-1385 alone. B, HepG2 cells were co-transfected with the reporter plasmid (p-1385), 4 ng of the phRL-TK and 100 ng of either the empty plasmid or the HNF4a2 expression plasmid. After 3h incubation, either vehicle (DMSO) or CDCA (50 μM, 75 μM, and 100 μM, indicated by triangles) was added to the medium. Each value is the mean ±S.D. of the fold activation for three independent assays towards the relative activity (firefly/*renilla*) obtained from p-1385 alone. * indicates statistically significant differences between two groups ($P<0.05$).

harboring the mutation in the DR1 element, was used in the same luciferase assay system. In Fig. 3B, one of the main primary bile acid, CDCA, was examined whether it could repress the activity of the *mCES2* gene promoter. The results showed that CDCA could strongly decrease in the level of the *mCES2* promoter activity as well as that driven by the forced expression of HNF-4α2 in a dose dependent manner. Again, the repressive effects of CDCA on the *mCES2* gene promoter activity were apparently dependent on the existence of the intact DR1 element.

Effects of CDCA on the level of expression of the mCES2 gene in TLR2 cells

To test the possibility that CDCA could affect the expression of the *mCES2* gene, the cell line in which endogenous mCES2 was expressed was required. As shown in Fig. 4A, the results of RT-PCR analysis and esterase activity staining after non-denaturing PAGE showed that mouse immortalized cell line, TLR2 cells, expressed mCES2 mRNA and protein, accordingly TLR2 cells were treated with CDCA or its vehicle (DMSO). In the left panel in Fig. 4B, the exposure of TLR2 cells to DMSO in their medium could somewhat but not significantly affect the levels of mRNA of any genes tested throughout the experiments. In contrast, the exposure of TLR2 cells to CDCA led to a transient induction of SHP mRNA expression with the peak time at 6 h after the addition. Then, the level of expression SHP mRNA got gradually decreased to the minimal (Fig. 4B, closed squares in the right panel). The level of mCES2 mRNA expression was not markedly changed until 12 h after the addition, but after that, it was substantially decreased to the approximately one tenth of the initial level (open squares). Interestingly, the level of HNF-4α

mRNA expression continued to decrease to the minimal at the early stage of exposure (closed circles).

The intrinsic cytotoxicity of CDCA was monitored by the determinations of the cell viability and the level of the leakage of LDH into the cultured medium. The cell viability was the same level between two groups (more than 95%). The level of LDH activity in the medium were slightly higher in the group treated with CDCA than that of the one treated with DMSO, but these levels were less than 7% of the total LDH level existed in TLR2 cells. Thus, it is thought that toxicity was not significant.

Rescue of mCES2 mRNA expression by exogenous expression of HNF-4α

HNF-4α expression vector was transfected with TLR2 cells 12 h after the addition of CDCA, resulting in the increase in the levels of HNF-4α mRNA expression in the cells at 24 h and 36 h when compared with those in the cell transfected with empty vector (to 1.8-fold and 1.5-fold, respectively) (Fig. 4C in the left panel). Concomitantly, the levels of mCES2 mRNA expression in the cell transfected HNF-4α expression vector were increased

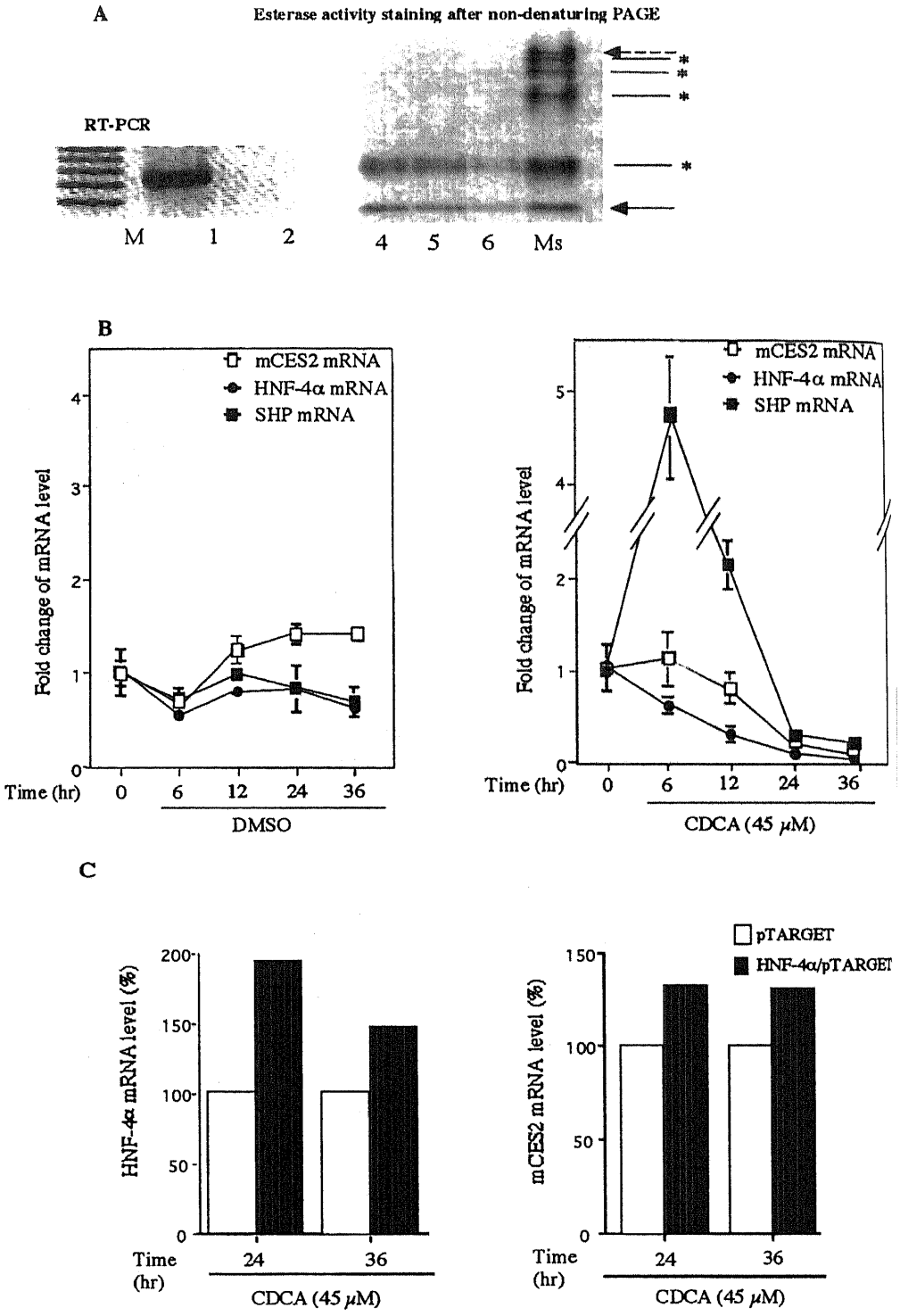

Fig. 4. Effects of CDCA on the expression of mCES2 mRNA, SHP mRNA and HNF-4α mRNA. A, Detection of mCES2 expression in TLR2 cells. M, DNA size marker; 1, TLR2 cDNA was used as a template; 2, negative control; 3 - 5, TLR2 homogenate (15, 10, and 5 μg, respectively) was loaded; Ms, mouse liver microsomes prepared previously [5]. Arrows with solid line and dashed line indicate mCES2 protein and mCES1 protein, respectively. Asterisks indicate unknown CES isozymes. B, The alteration of mCES2, SHP and HNF-4α mRNA expression by treatment of DMSO or CDCA. Time = 0 was set at the time just before the addition of DMSO or CDCA (45 μM). The mRNA amount was determined by Taqman Real-time PCR. The time points when the cells were collected were indicated below the graph. The amount of each gene mRNA was normalized by that of 18s rRNA. The values of each gene are the mean ± S.D. of fold change for three independent assays towards the value obtained at Time = 0. This is the representative result for three independent experiments. Open square, mCES mRNA; solid square, SHP mRNA; solid circle, HNF-4α mRNA_C, rescue of mCES2 mRNA expression by exogenous expression of HNF-4α in CDCA treated cells. Either the empty plasmid (pTARGET) (2.5 μg) or the HNF-4α expression plasmid (HNF-4α/pTARGET) (2.5 μg) was transfected with TLR2 cells at 12 h after the addition of CDCA to the medium. Total RNA was extracted at 24 h or 36 h after the addition. The determination of the amount of mCES2 mRNA and HNF-4α mRNA was described above. The values of HNF-4α mRNA level and mCES mRNA level in the cells transfected with HNF-4α/pTARGET were the mean of fold change towards those obtained in the cells transfected with pTARGET, respectively

to 1.4-fold and 1.3-fold at 24 h and 36 h after the addition of CDCA, respectively (Fig. 4C in the right panel). These results showed that the level of mCES2 mRNA expression were apparently correlated to that of HNF-4α mRNA expression

II-II-IV Discussion

In the beginning part of our work, we have demonstrated our initial hypothesis that HNF-4α can directly transactivate the *mCES2* gene promoter. In the second part, our results have also showed that a nuclear factor cascade triggered by bile acid signal could also affect mCES2 expression. To our best knowledge, this is the first time to show the involvement of nuclear receptors in the transcription of the *CES* genes.

Several HNF-4α isoforms are known, HNF-4α1 and HNF-4α2 being the predominant forms in the adult liver while HNF-4α7 and HNF-4α8 being those in the fetal liver [117, 132]. And HNF-4α2 expression is more abundant and showed stronger transactivation potential than those of HNF-4α1 [132, 133]. Thus, we used HNF-4α2 cDNA clone in a series of experiments. In hepatocarcinoma cell lines, the level of HNF-4α expression varied from cell types. Taking advantage of this fact, we used two hepatocarcinoma cell lines (HepG2 cells and FLC7 cells) in addition to HNF-4α negative cell lines (V79 cells) to examine effects of endogenous HNF-4α expression on the promoter activity of the *mCES2* gene. The results showing that the level of endogenous and exogenous HNF-4α expression paralleled the *mCES2* promoter activity indicated direct involvement of HNF-4α in the *mCES2* promoter activation.

The results of the following experiments indicated that HNF-4α bound to the DR1 elements in the *mCES2* gene promoter. The DR1 element was located in adjacent to the transcription start site. This positioning of the DR1 element has also been reported in the mouse *very long chain acyl-CoA synthase-related* gene [134]. It was reported that HNF-4α could interact with TFIIB and recruit it to the promoter complex, leading to form the preinitiation complex acting downstream of TFIIB [135]; thus, HNF-4α may play an important role in determination of transcription start site of these genes in the liver. Collectively, the involvement of HNF-4α in the transactivation of the *mCES2* gene promoter would be the mechanism by which mCES2 is expressed in the liver at higher levels than in other tissues, since HNF-4α has been shown to function as a transcriptional activator for tissue-specific gene expressions [136, 137]. Although additional experiment are definitely needed, this context may be extended to interpretation of the high level of mCES2 expression in the kidney and small intestine since HNF-4α is also expressed in these tissue at the high levels.

Bile acids homeostasis is strictly regulated by various nuclear factors. Among them, SHP, which is induced by farnesoid X receptor (FXR), has been shown to play important roles in the negative feedback regulation of bile acid biosynthsis as well as in the repression of other metabolism by inhibiting transactivation of various nuclear factors [127, 138-141]. It has been reported that the transcriptional potential of HNF-4α can be directly repressed by SHP, showing that one of the targets for SHP was HNF-4α [125]. Given these facts, we hypothesized that bile acid could repress expression of the *mCES2* gene by inhibiting HNF-4α-mediated transactivation.

To examine effects of bile acid on expression of the *mCES2* gene, we used CDCA in the experiments since CDCA is one of the primary bile acid, and CDCA and its conjugated derivatives have been identified as good ligands for FXR [142, 143]. The mCES2 promoter activity enhanced by HNF-4α was greatly inhibited by SHP and CDCA in the DR1 element dependent manner, which indicated that no other HNF-4α binding site as well as the site for other factors

that could be target for SHP and CDCA was existed in this *mCES2* promoter region. These results are interesting because it has been shown that CDCA triggers several signaling pathway in addition to the FXR-SHP cascade as discussing below. Although the possibility that there are some bile acid responsive elements in the distant regulatory region of the *mCES2* gene should be concerned, the HNF-4α binding site in the *mCES2* promoter region appears to be important downstream target for bile acid signals. Therefore, we subsequently examined whether CDCA repressed expression of the *mCES2* gene in cells.

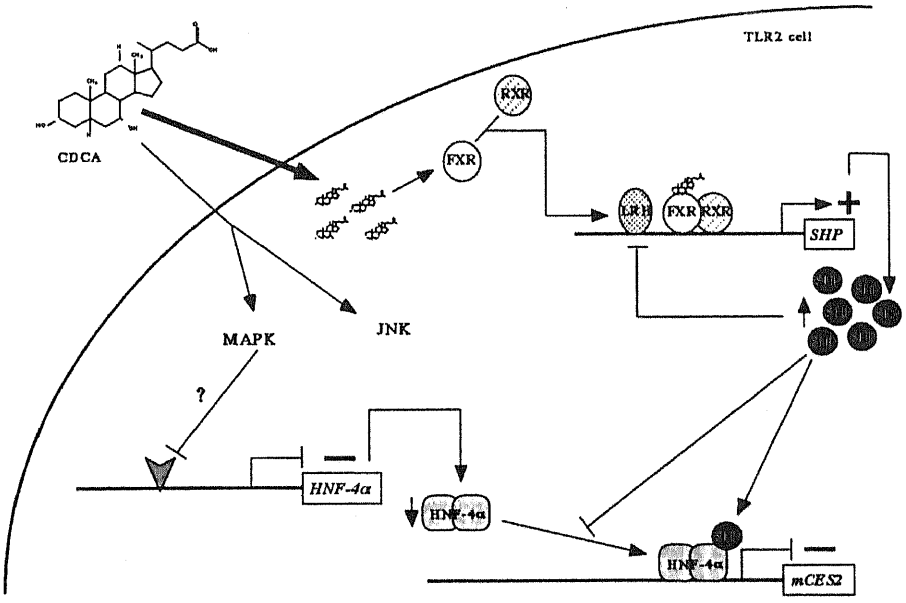

Fig. 5. Summery of the mechanisms by which CDCA represses the mCES2 gene expression. Symbols, (+) and (-), indicate the activation and the inhibition of the gene transcription, respectively. Open arrows indicate the increase or decrease in the level of protein expression. Symbol (?) indicates an unidentified pathway.

Mouse immortalized hepatocyte, TLR2 cells, was first identified as the cell line expressing mCES2. The concentration of CDCA in the medium (45 μM) was well within the physiologic intracellular range reported *in vivo* [144, 145]. The experiments using TLR2 cells provided the results indicating that there are two pathways by which mCES2 transcription was inhibited; one was classical FXR-SHP pathway and another was the bile acid-mediated repression of HNF-4α expression (summarized in Fig. 5). The involvement of FXR-SHP pathway was in good accordance with the results showing the repression effects of SHP and CDCA on the *mCES2* promoter activity. Unexpectedly and interestingly, we found that the amount of HNF-4α mRNA was decreased in CDCA treated cells and the down-regulation was observed from the early stages of the exposure. Considering the results that exogenous expression of HNF-4α could partially rescue the repressive expression of mCES2 mRNA, this reduction of the amount of HNF-4α would also contribute to the bile acid-mediated decrease in the level of the mCES2 mRNA expression. There has been only one report that the level of HNF-4α expression was decreased by treatment of bile acid [127]. We did not have any experimental results supporting this repression, but we speculated that mitogen-activated protein kinase (MAPK) pathway was involved in the repression of HNF-4α expression by bile acid. The involvement of SHP in this repression seems unlikely because the repression was observed in the early stage when SHP was not fully induced. Thus, this rapid response of HNF-4α mRNA expression may be accounted for by the involvement of kinase signaling pathway. It has been reported that treatment of MAPK inhibitor results in the increase in the level of HNF-4α expression [146] and that bile acid can activate MAPK [147]. Although further studies are needed to elucidate how HNF-4α expression is repressed by bile acid, the results of the present pathway could provide another pathway by which bile acid can repress various hepatic genes.

In conclusion, our results have demonstrated that HNF-4α can strongly transactivate the *mCES2* gene promoter, and the involvement of HNF-4α may account for the high expression

level of mCES in the liver. In addition, we have found that bile acid can repress the *mCES2* gene transcription by repressing HNF-4α-mediated transactivation. Physiological significance in this repression is currently unknown. However, mCES2 can hydrolyze various endogenous fatty acid esters and are predominantly expressed in the liver, kidney, and small intestine, tissues that are exposed to significant bile acid fluxes and in which FXR is also most abundantly expressed [148, 149]. Therefore, the repression is likely to reflect physiological functions of mCES2 in lipid metabolism, accordingly mCES2 might play important roles in bile acid homeostasis or in the secondary responses to bile acid signals, such as the inhibitory effects of bile acid on very-low-density lipoprotein section. Further detailed study amid at the elucidation of the physiological roles of mCES2 would provide important insights into lipid metabolism.

Conclusion

1. DEHP-induced mouse liver temocapril hydrolase belongs to carboxylesterase 1 family, termed mCES1.

2. mCES1 can hydrolyze various prodrug, suggesting that mCES1 plays important roles in drug metabolism.

3. Dexamethasone-induced rat liver methylprednisolone hemisuccinate hydrolase belongs to carboxylesterase 2 family, termed rCES2, and rCES2 is also thought to play important roles in drug metabolism. Interestingly, rCES2 can exist in plasma as well as liver microsomes.

4. DEHP-induced mouse liver acylcarnitine hydrolase belongs to carboxylesterase 2 family, termed mCES2.

5. mCES2 can hydrolyze various endogenous fatty acid esters and prodrug, suggesting that mCES2 plays important roles in drug and lipid metabolism.

6. mCES2 are expressed in various tissues with the higher levels of expression present in the liver, kidney and small intestine.

7. Sp1, Sp3 and USF1 can synergistically transactivate the *mCES2* gene promoter, which may be a part of the mechanisms controlling the basal transcription of the *mCES2* gene.

8. A liver-enriched transcription factor, HNF-4α, is thought to contribute to the high level of expression of mCES2 in the liver.

9. Bile acid represses transcription of the *mCES2* gene through the inhibition of the HNF-4α–mediated transactivation and the decrease in the level of HNF-4α expression.

References

[1] Satoh T and Hosokawa M. The mammalian carboxylesterases: from molecules to functions. Annu Rev Pharmacol Toxicol 1998;38:257-88.

[2] Satoh T, Taylor P, Bosron WF, Sanghani SP, Hosokawa M and La Du BN. Current progress on esterases: from molecular structure to function. Drug Metab Dispos 2002;30:488-93.

[3] Zhang J, Burnell JC, Dumaual N and Bosron WF. Binding and hydrolysis of meperidine by human liver carboxylesterase hCE-1. J Pharmacol Exp Ther 1999;290:314-8.

[4] Pindel EV, Kedishvili NY, Abraham TL, Brzezinski MR, Zhang J, Dean RA and Bosron WF. Purification and cloning of a broad substrate specificity human liver carboxylesterase that catalyzes the hydrolysis of cocaine and heroin. J Biol Chem 1997;272:14769-75.

[5] Furihata T, Hosokawa M, Koyano N, Nakamura T, Satoh T, Chiba K, Tabata T, Katoh M, Tokudome S, Nakajima M and Yokoi T. Identification of di-(2-ethylhexyl) phthalate-induced carboxylesterase 1 in C57BL/6 mouse liver microsomes: purification, cDNA cloning, and baculovirus-mediated expression. Drug Metab Dispos 2004;32:1170-7.

[6] Takai S, Matsuda A, Usami Y, Adachi T, Sugiyama T, Katagiri Y, Tatematsu M and Hirano K. Hydrolytic profile for ester- or amide-linkage by carboxylesterases pI 5.3 and 4.5 from human liver. Biol Pharm Bull 1997;20:869-73.

[7] Satoh T, Hosokawa M, Atsumi R, Suzuki W, Hakusui H and Nagai E. Metabolic activation of CPT-11, 7-ethyl-10-[4-(1-piperidino)-1- piperidino]carbonyloxycamptothecin, a novel antitumor agent, by carboxylesterase. Biol Pharm Bull 1994;17:662-4.

[8] Tabata T, Katoh M, Tokudome S, Nakajima M and Yokoi T. Identification of the cytosolic carboxylesterase catalyzing the 5'-deoxy-5-fluorocytidine formation from capecitabine in human liver. Drug Metab Dispos 2004;32:1103-10. Epub 2004 Jul 21.

[9] Imai T, Yoshigae Y, Hosokawa M, Chiba K and Otagiri M. Evidence for the involvement of a pulmonary first-pass effect via carboxylesterase in the disposition of a propranolol ester derivative after intravenous administration. J Pharmacol Exp Ther 2003;307:1234-42. Epub 2003 Oct 8.

[10] Ohtsuka K, Inoue S, Kameyama M, Kanetoshi A, Fujimoto T, Takaoka K, Araya Y and Shida A. Intracellular conversion of irinotecan to its active form, SN-38, by native carboxylesterase in human non-small cell lung cancer. Lung Cancer 2003;41:187-98.

[11] Sanghani SP, Quinney SK, Fredenburg TB, Sun Z, Davis WI, Murry DJ, Cummings OW, Seitz DE and Bosron WF. Carboxylesterases expressed in human colon tumor tissue and their role in CPT-11 hydrolysis. Clin Cancer Res 2003;9:4983-91.

[12] Kroetz DL, McBride OW and Gonzalez FJ. Glycosylation-dependent activity of baculovirus-expressed human liver carboxylesterases: cDNA cloning and characterization of two highly similar enzyme forms. Biochemistry 1993;32:11606-17.

[13] Inoue M, Morikawa M, Tsuboi M and Sugiura M. Species difference and characterization of intestinal esterase on the hydrolizing activity of ester-type drugs. Jpn J Pharmacol 1979;29:9-16.

[14] Hosokawa M, Maki T and Satoh T. Characterization of molecular species of liver microsomal carboxylesterases of several animal species and humans. Arch Biochem Biophys 1990;277:219-27.

[15] Prueksaritanont T, Gorham LM, Hochman JH, Tran LO and Vyas KP. Comparative studies of drug-metabolizing enzymes in dog, monkey, and human small intestines, and in Caco-2 cells. Drug Metab Dispos 1996;24:634-42.

[16] Zhu W, Song L, Zhang H, Matoney L, LeCluyse E and Yan B. Dexamethasone differentially regulates expression of carboxylesterase genes in humans and rats. Drug Metab Dispos 2000;28:186-91.

[17] Hosokawa M, Hirata K, Nakata F, Suga T and Satoh T. Species differences in the induction of hepatic microsomal carboxylesterases caused by dietary exposure to di(2-ethylhexyl)phthalate, a peroxisome proliferator. Drug Metab Dispos 1994;22:889-94.

[18] Robbi M, Van Schaftingen E and Beaufay H. Cloning and sequencing of rat liver carboxylesterase ES-4 (microsomal palmitoyl-CoA hydrolase). Biochem J 1996;313:821-6.

[19] Hosokawa M, Suzuki K, Takahashi D, Mori M, Satoh T and Chiba K. Purification, molecular cloning, and functional expression of dog liver microsomal acyl-CoA hydrolase: a member of the carboxylesterase multigene family. Arch Biochem Biophys 2001;389:245-53.

[20] Furihata T, Hosokawa M, Nakata F, Satoh T and Chiba K. Purification, molecular cloning, and functional expression of inducible liver acylcarnitine hydrolase in C57BL/6 mouse, belonging to the carboxylesterase multigene family. Arch Biochem Biophys 2003;416:101-9.

[21] Mentlein R, Reuter G and Heymann E. Specificity of two different purified acylcarnitine hydrolases from rat liver, their identity with other carboxylesterases, and their possible function. Arch Biochem Biophys 1985;240:801-10.

[22] Ito M, Tchoua U, Okamoto M and Tojo H. Purification and properties of a phospholipase A2/lipase preferring phosphatidic acid, bis(monoacylglycerol) phosphate, and monoacylglycerol from rat testis. J Biol Chem 2002;277:43674-81.

[23] Soni KG, Lehner R, Metalnikov P, O'Donnell P, Semache M, Gao W, Ashman K, Pshezhetsky AV and Mitchell GA. Carboxylesterase 3 (EC 3.1.1.1) is a major adipocyte lipase. J Biol Chem 2004;279:40683-9. Epub 2004 Jun 25.

[24] Dolinsky VW, Gilham D, Alam M, Vance DE and Lehner R. Triacylglycerol hydrolase: role in intracellular lipid metabolism. Cell Mol Life Sci 2004;61:1633-51.

[25] Gilham D and Lehner R. The physiological role of triacylglycerol hydrolase in lipid metabolism. Rev Endocr Metab Disord 2004;5:303-9.

[26] Ghosh S, St Clair RW and Rudel LL. Mobilization of cytoplasmic CE droplets by overexpression of human macrophage cholesteryl ester hydrolase. J Lipid Res 2003;44:1833-40. Epub 2003 Jul 01.

[27] Baciewicz AM, Self TH and Bekemeyer WB. Update on rifampin drug interactions. Arch Intern Med 1987;147:565-8.

[28] Baker AF and Dorr RT. Drug interactions with the taxanes: clinical implications. Cancer Treat Rev 2001;27:221-33.

[29] Hosokawa M, Maki T and Satoh T. Multiplicity and regulation of hepatic microsomal carboxylesterases in rats. Mol Pharmacol 1987;31:579-84.

[30] Hosokawa M, Maki T and Satoh T. Differences in the induction of carboxylesterase isozymes in rat liver microsomes by xenobiotics. Biochem Pharmacol 1988;37:2708-11.

[31] Hosokawa M and Satoh T. Differences in the induction of carboxylesterase isozymes in rat liver microsomes by perfluorinated fatty acids. Xenobiotica 1993;23:1125-33.

[32] Mentlein R, Lembke B, Vik H and Berge RK. Different induction of microsomal carboxylesterases, palmitoyl-CoA hydrolase and acyl-L-carnitine hydrolase in rat liver after treatment with clofibrate. Biochem Pharmacol 1986;35:2727-30.

[33] Ovnic M, Swank RT, Fletcher C, Zhen L, Novak EK, Baumann H, Heintz N and Ganschow RE. Characterization and functional expression of a cDNA encoding egasyn (esterase-22): the endoplasmic reticulum-targeting protein of beta-glucuronidase. Genomics 1991;11:956-67.

[34] Ovnic M, Tepperman K, Medda S, Elliott RW, Stephenson DA, Grant SG and Ganschow RE. Characterization of a murine cDNA encoding a member of the carboxylesterase multigene family. Genomics 1991;9:344-54.

[35] Aida K, Moore R and Negishi M. Cloning and nucleotide sequence of a novel, male-predominant carboxylesterase in mouse liver. Biochim Biophys Acta 1993;1174:72-4.

[36] Dolinsky VW, Sipione S, Lehner R and Vance DE. The cloning and expression of a murine triacylglycerol hydrolase cDNA and the structure of its corresponding gene. Biochim Biophys Acta 2001;1532:162-72.

[37] Xie M, Yang D, Wu M, Xue B and Yan B. Mouse Liver and Kidney Carboxylesterase (M-LK) Rapidly Hydrolyzes Antitumor Prodrug Irinotecan and the N-Terminal Three Quarter Sequence Determines Substrate Selectivity. Drug Metab Dispos 2003;31:21-7.

[38] Krisch K. Reaction of a microsomal esterase from hog-liver with diethyl rho-nitrophenyl phosphate. Biochim Biophys Acta 1966;122:265-80.

[39] Mori M, Hosokawa M, Ogasawara Y, Tsukada E and Chiba K. cDNA cloning, characterization and stable expression of novel human brain carboxylesterase. FEBS Lett 1999;458:17-22.

[40] Takanashi K, Tainaka H, Kobayashi K, Yasumori T, Hosakawa M and Chiba K. CYP2C9 Ile359 and Leu359 variants: enzyme kinetic study with seven substrates. Pharmacogenetics 2000;10:95-104.

[41] Mentlein R, Heiland S and Heymann E. Simultaneous purification and comparative characterization of six serine hydrolases from rat liver microsomes. Arch Biochem Biophys 1980;200:547-59.

[42] Robbi M and Beaufay H. The COOH terminus of several liver carboxylesterases targets these enzymes to the lumen of the endoplasmic reticulum. J Biol Chem 1991;266:20498-503.

[43] Brandt E, E. Heymann, R. Mentlein. Selective inhibition of rat liver carboxylesterases by various organophosphorus diesters *in vivo* and *in vitro*. Biochem. Pharmacol. 1980;**29**:1927-1931.

[44] Robbi M, Beaufay H and Octave JN. Nucleotide sequence of cDNA coding for rat liver pI 6.1 esterase (ES-10), a carboxylesterase located in the lumen of the endoplasmic reticulum. Biochem J 1990;269:451-8.

[45] Schindler R, Mentlein R and Feldheim W. Purification and characterization of retinyl ester hydrolase as a member of the non-specific carboxylesterase supergene family. Eur J Biochem 1998;251:863-73.

[46] Xie M, Yang D, Liu L, Xue B and Yan B. Human and rodent carboxylesterases: immunorelatedness, overlapping substrate specificity, differential sensitivity to serine enzyme inhibitors, and tumor-related expression. Drug Metab Dispos 2002;30:541-7.

[47] Huber WW, Grasl-Kraupp B and Schulte-Hermann R. Hepatocarcinogenic potential of di(2-ethylhexyl)phthalate in rodents and its implications on human risk. Crit Rev Toxicol

1996;26:365-481.

[48] Ward JM, Peters JM, Perella CM and Gonzalez FJ. Receptor and nonreceptor-mediated organ-specific toxicity of di(2-ethylhexyl)phthalate (DEHP) in peroxisome proliferator-activated receptor alpha-null mice. Toxicol Pathol 1998;26:240-6.

[49] Douglas DN, Dolinsky VW, Lehner R and Vance DE. A role for Sp1 in the transcriptional regulation of hepatic triacylglycerol hydrolase in the mouse. J Biol Chem 2001;276:25621-30.

[50] Dolinsky VW, Gilham D, Hatch GM, Agellon LB, Lehner R and Vance DE. Regulation of triacylglycerol hydrolase expression by dietary fatty acids and peroxisomal proliferator-activated receptors. Biochim Biophys Acta 2003;1635:20-8.

[51] Poole M, Bridgers K, Alexson SE and Corton JC. Altered expression of the carboxylesterases ES-4 and ES-10 by peroxisome proliferator chemicals. Toxicology 2001;165:109-19.

[52] Desvergne B and Wahli W. Peroxisome proliferator-activated receptors: nuclear control of metabolism. Endocr Rev 1999;20:649-88.

[53] Howarth JA, Price SC, Dobrota M, Kentish PA and Hinton RH. Effects on male rats of di-(2-ethylhexyl) phthalate and di-n-hexylphthalate administered alone or in combination. Toxicol Lett 2001;121:35-43.

[54] Mentlein R, Suttorp M and Heymann E. Specificity of purified monoacylglycerol lipase, palmitoyl-CoA hydrolase, palmitoyl-carnitine hydrolase, and nonspecific carboxylesterase from rat liver microsomes. Arch Biochem Biophys 1984;228:230-46.

[55] Shevchenko A, Wilm M, Vorm O and Mann M. Mass spectrometric sequencing of proteins silver-stained polyacrylamide gels. Anal Chem 1996;68:850-8.

[56] Hattori K, Igarashi M, Itoh M, Tomisawa H and Tateishi M. Specific induction by glucocorticoids of steroid esterase in rat hepatic microsomes and its release into serum. Biochem Pharmacol 1992;43:1921-7.

[57] Cygler M, Schrag JD, Sussman JL, Harel M, Silman I, Gentry MK and Doctor BP. Relationship between sequence conservation and three-dimensional structure in a large family of esterases, lipases, and related proteins. Protein Sci 1993;2:366-82.

[58] Smialowski-Fleter S, Moulin A, Villard C and Puigserver A. Structure-function relationships in the carboxylic-ester-hydrolase superfamily. Disulfide bridge arrangement in porcine intestinal glycerol-ester hydrolase. Eur J Biochem 2000;267:2227-34.

[59] Sanghani SP, Davis WI, Dumaual NG, Mahrenholz A and Bosron WF. Identification of microsomal rat liver carboxylesterases and their activity with retinyl palmitate. Eur J Biochem 2002;269:4387-98.

[60] Sone T, Isobe M, Takabatake E and Wang CY. Cloning and sequence analysis of a hamster liver cDNA encoding a novel putative carboxylesterase. Biochim Biophys Acta 1994;1207:138-42.

[61] Ozols J. Isolation, properties, and the complete amino acid sequence of a second form of 60-kDa glycoprotein esterase. Orientation of the 60-kDa proteins in the microsomal membrane. J Biol Chem 1989;264:12533-45.

[62] Robbi M and Beaufay H. Topogenesis of carboxylesterases: a rat liver isoenzyme ending in -HTEHT-COOH is a secreted protein. Biochem Biophys Res Commun 1992;183:836-41.

[63] Paul HS, Gleditsch CE and Adibi SA. Mechanism of increased hepatic concentration of carnitine by clofibrate. Am J Physiol 1986;251:E311-5.

[64] Abo-Hashema KA, Cake MH, Power GW and Clarke D. Evidence for triacylglycerol synthesis

in the lumen of microsomes via a lipolysis-esterification pathway involving carnitine acyltransferases. J Biol Chem 1999;274:35577-82.

[65] Schuetz EG and Guzelian PS. Induction of cytochrome P-450 by glucocorticoids in rat liver. II. Evidence that glucocorticoids regulate induction of cytochrome P-450 by a nonclassical receptor mechanism. J Biol Chem 1984;259:2007-12.

[66] Watkins PB, Wrighton SA, Maurel P, Schuetz EG, Mendez-Picon G, Parker GA and Guzelian PS. Identification of an inducible form of cytochrome P-450 in human liver. Proc Natl Acad Sci U S A 1985;82:6310-4.

[67] Watanabe M, Tateishi T, Asoh M, Nakura H, Tanaka M, Kumai T and Kobayashi S. Effects of glucocorticoids on pharmacokinetics and pharmacodynamics of midazolam in rats. Life Sci 1998;63:1685-92.

[68] Brain EG, Yu LJ, Gustafsson K, Drewes P and Waxman DJ. Modulation of P450-dependent ifosfamide pharmacokinetics: a better understanding of drug activation in vivo. Br J Cancer 1998;77:1768-76.

[69] Hattori K, Kamio M, Nakajima E, Oshima T, Satoh T and Kitagawa H. Characterization of steroid hormone ester hydrolyzing enzymes in liver microsomes. Biochem Pharmacol 1981;30:2051-6.

[70] Hosokawa M, Hattori K and Satoh T. Differential responses of rat hepatic microsomal carboxylesterase isozymes to glucocorticoids and pregnenolone 16 alpha-carbonitrile. Biochem Pharmacol 1993;45:2317-22.

[71] Morgan EW, Yan B, Greenway D and Parkinson A. Regulation of two rat liver microsomal carboxylesterase isozymes: species differences, tissue distribution, and the effects of age, sex, and xenobiotic treatment of rats. Arch Biochem Biophys 1994;315:513-26.

[72] Derbel M, Hosokawa M and Satoh T. Differences in the induction of carboxylesterase RL4 in rat liver microsomes by various perfluorinated fatty acids, metabolically inert derivatives of fatty acids. Biol Pharm Bull 1996;19:765-7.

[73] Konishi H, Sumi M, Shibata N, Takada K, Minouchi T and Yamaji A. Influence of intravenous methylprednisolone pulse treatment on the disposition of ciclosporin and hepatic CYP3A activity in rats. J Pharm Pharmacol 2004;56:477-83.

[74] Munro S and Pelham HR. A C-terminal signal prevents secretion of luminal ER proteins. Cell 1987;48:899-907.

[75] Tartakoff AM. Perturbation of vesicular traffic with the carboxylic ionophore monensin. Cell 1983;32:1026-8.

[76] Murasawa S, Matsubara H, Kizima K, Maruyama K, Mori Y and Inada M. Glucocorticoids regulate V1a vasopressin receptor expression by increasing mRNA stability in vascular smooth muscle cells. Hypertension 1995;26:665-9.

[77] Rosewicz S, Riecken EO and Kaiser A. Transient stabilization of cholecystokinin A receptor mRNA by glucocorticoids in pancreatic AR42J cells. Am J Physiol 1994;267:G772-7.

[78] Gibbons GF, Islam K and Pease RJ. Mobilisation of triacylglycerol stores. Biochim Biophys Acta 2000;1483:37-57.

[79] Broadway NM and Saggerson ED. Inhibition of liver microsomal carnitine acyltransferases by sulphonylurea drugs. FEBS Lett 1995;371:137-9.

[80] Washington L, Cook GA and Mansbach CM, 2nd. Inhibition of carnitine palmitoyltransferase in

the rat small intestine reduces export of triacylglycerol into the lymph. J Lipid Res 2003;44:1395-403. Epub 2003 Apr 16.

[81] Natarajan R, Ghosh S and Grogan WM. Molecular cloning of the promoter for rat hepatic neutral cholesterol ester hydrolase: evidence for transcriptional regulation by sterols. Biochem Biophys Res Commun 1998;243:349-55.

[82] Langmann T, Aslanidis C, Schuierer M and Schmitz G. Differentiation-dependent expression of a human carboxylesterase in monocytic cells and transcription factor binding to the promoter. Biochem Biophys Res Commun 1997;230:215-9.

[83] Wu MH, Chen P, Remo BF, Cook EH, Jr., Das S and Dolan ME. Characterization of multiple promoters in the human carboxylesterase 2 gene. Pharmacogenetics 2003;13:425-35.

[84] Courey AJ and Tjian R. Analysis of Sp1 in vivo reveals multiple transcriptional domains, including a novel glutamine-rich activation motif. Cell 1988;55:887-98.

[85] Kadonaga JT, Carner KR, Masiarz FR and Tjian R. Isolation of cDNA encoding transcription factor Sp1 and functional analysis of the DNA binding domain. Cell 1987;51:1079-90.

[86] Hirano F, Tanaka H, Hirano Y, Hiramoto M, Handa H, Makino I and Scheidereit C. Functional interference of Sp1 and NF-kappaB through the same DNA binding site. Mol Cell Biol 1998;18:1266-74.

[87] Brasier AR, Ron D, Tate JE and Habener JF. A family of constitutive C/EBP-like DNA binding proteins attenuate the IL-1 alpha induced, NF kappa B mediated trans-activation of the angiotensinogen gene acute-phase response element. Embo J 1990;9:3933-44.

[88] Baldwin AS, Jr. and Sharp PA. Two transcription factors, NF-kappa B and H2TF1, interact with a single regulatory sequence in the class I major histocompatibility complex promoter. Proc Natl Acad Sci U S A 1988;85:723-7.

[89] Saito T, Takahashi Y, Hashimoto H and Kamataki T. Novel transcriptional regulation of the human CYP3A7 gene by Sp1 and Sp3 through nuclear factor kappa B-like element. J Biol Chem 2001;276:38010-22.

[90] Moore AW, Barbel S, Jan LY and Jan YN. A genomewide survey of basic helix-loop-helix factors in Drosophila. Proc Natl Acad Sci U S A 2000;97:10436-41.

[91] Langmann T, Becker A, Aslanidis C, Notka F, Ullrich H, Schwer H and Schmitz G. Structural organization and characterization of the promoter region of a human carboxylesterase gene. Biochim Biophys Acta 1997;1350:65-74.

[92] Li N and Seetharam B. A 69-base pair fragment derived from human transcobalamin II promoter is sufficient for high bidirectional activity in the absence of a TATA box and an initiator element in transfected cells. Role of an E box in transcriptional activity. J Biol Chem 1998;273:28170-7.

[93] Suske G. The Sp-family of transcription factors. Gene 1999;238:291-300.

[94] Sirito M, Lin Q, Maity T and Sawadogo M. Ubiquitous expression of the 43- and 44-kDa forms of transcription factor USF in mammalian cells. Nucleic Acids Res 1994;22:427-33.

[95] Viollet B, Lefrancois-Martinez AM, Henrion A, Kahn A, Raymondjean M and Martinez A. Immunochemical characterization and transacting properties of upstream stimulatory factor isoforms. J Biol Chem 1996;271:1405-15.

[96] Kingsley C and Winoto A. Cloning of GT box-binding proteins: a novel Sp1 multigene family regulating T-cell receptor gene expression. Mol Cell Biol 1992;12:4251-61.

[97] Hagen G, Muller S, Beato M and Suske G. Cloning by recognition site screening of two novel GT box binding proteins: a family of Sp1 related genes. Nucleic Acids Res 1992;20:5519-25.

[98] Hagen G, Muller S, Beato M and Suske G. Sp1-mediated transcriptional activation is repressed by Sp3. Embo J 1994;13:3843-51.

[99] Supp DM, Witte DP, Branford WW, Smith EP and Potter SS. Sp4, a member of the Sp1-family of zinc finger transcription factors, is required for normal murine growth, viability, and male fertility. Dev Biol 1996;176:284-99.

[100] Iynedjian PB. Identification of upstream stimulatory factor as transcriptional activator of the liver promoter of the glucokinase gene. Biochem J 1998;333:705-12.

[101] Casado M, Vallet VS, Kahn A and Vaulont S. Essential role in vivo of upstream stimulatory factors for a normal dietary response of the fatty acid synthase gene in the liver. J Biol Chem 1999;274:2009-13.

[102] Roder K, Wolf SS, Sickinger S and Schweizer M. FIRE3 in the promoter of the rat fatty acid synthase (FAS) gene binds the ubiquitous transcription factors CBF and USF but does not mediate an insulin response in a rat hepatoma cell line. Eur J Biochem 1999;260:743-51.

[103] Emili A, Greenblatt J and Ingles CJ. Species-specific interaction of the glutamine-rich activation domains of Sp1 with the TATA box-binding protein. Mol Cell Biol 1994;14:1582-93.

[104] Karlseder J, Rotheneder H and Wintersberger E. Interaction of Sp1 with the growth- and cell cycle-regulated transcription factor E2F. Mol Cell Biol 1996;16:1659-67.

[105] Rodriguez CI, Girones N and Fresno M. Cha, a basic helix-loop-helix transcription factor involved in the regulation of upstream stimulatory factor activity. J Biol Chem 2003;278:43135-45. Epub 2003 Aug 15.

[106] Sieweke MH, Tekotte H, Jarosch U and Graf T. Cooperative interaction of ets-1 with USF-1 required for HIV-1 enhancer activity in T cells. Embo J 1998;17:1728-39.

[107] Ge Y, Jensen TL, Matherly LH and Taub JW. Physical and functional interactions between USF and Sp1 proteins regulate human deoxycytidine kinase promoter activity. J Biol Chem 2003;278:49901-10. Epub 2003 Sep 26.

[108] Zhang X, Li Y, Dai C, Yang J, Mundel P and Liu Y. Sp1 and Sp3 transcription factors synergistically regulate HGF receptor gene expression in kidney. Am J Physiol Renal Physiol 2003;284:F82-94.

[109] Wolf SS, Roder K and Schweizer M. Role of Sp1 and Sp3 in the transcriptional regulation of the fatty acid synthase gene. Arch Biochem Biophys 2001;385:259-66.

[110] Yu B, Datta PK and Bagchi S. Stability of the Sp3-DNA complex is promoter-specific: Sp3 efficiently competes with Sp1 for binding to promoters containing multiple Sp-sites. Nucleic Acids Res 2003;31:5368-76.

[111] Samson SL and Wong NC. Role of Sp1 in insulin regulation of gene expression. J Mol Endocrinol 2002;29:265-79.

[112] Keembiyehetty CN, Candelaria RP, Majumdar G, Raghow R, Martinez-Hernandez A and Solomon SS. Paradoxical regulation of Sp1 transcription factor by glucagon. Endocrinology 2002;143:1512-20.

[113] Roder K, Wolf SS, Beck KF and Schweizer M. Cooperative binding of NF-Y and Sp1 at the DNase I-hypersensitive site, fatty acid synthase insulin-responsive element 1, located at -500 in the rat fatty acid synthase promoter. J Biol Chem 1997;272:21616-24.

[114] Latasa MJ, Griffin MJ, Moon YS, Kang C and Sul HS. Occupancy and function of the -150 sterol regulatory element and -65 E-box in nutritional regulation of the fatty acid synthase gene in living animals. Mol Cell Biol 2003;23:5896-907.

[115] Sladek FM, Zhong WM, Lai E and Darnell JE, Jr. Liver-enriched transcription factor HNF-4 is a novel member of the steroid hormone receptor superfamily. Genes Dev 1990;4:2353-65.

[116] Hertz R, Magenheim J, Berman I and Bar-Tana J. Fatty acyl-CoA thioesters are ligands of hepatic nuclear factor-4alpha. Nature 1998;392:512-6.

[117] Nakhei H, Lingott A, Lemm I and Ryffel GU. An alternative splice variant of the tissue specific transcription factor HNF4alpha predominates in undifferentiated murine cell types. Nucleic Acids Res 1998;26:497-504.

[118] Thomas H, Jaschkowitz K, Bulman M, Frayling TM, Mitchell SM, Roosen S, Lingott-Frieg A, Tack CJ, Ellard S, Ryffel GU and Hattersley AT. A distant upstream promoter of the HNF-4alpha gene connects the transcription factors involved in maturity-onset diabetes of the young. Hum Mol Genet 2001;10:2089-97.

[119] Watt AJ, Garrison WD and Duncan SA. HNF4: a central regulator of hepatocyte differentiation and function. Hepatology 2003;37:1249-53.

[120] Odom DT, Zizlsperger N, Gordon DB, Bell GW, Rinaldi NJ, Murray HL, Volkert TL, Schreiber J, Rolfe PA, Gifford DK, Fraenkel E, Bell GI and Young RA. Control of pancreas and liver gene expression by HNF transcription factors. Science 2004;303:1378-81.

[121] Spath GF and Weiss MC. Hepatocyte nuclear factor 4 provokes expression of epithelial marker genes, acting as a morphogen in dedifferentiated hepatoma cells. J Cell Biol 1998;140:935-46.

[122] Spath GF and Weiss MC. Hepatocyte nuclear factor 4 expression overcomes repression of the hepatic phenotype in dedifferentiated hepatoma cells. Mol Cell Biol 1997;17:1913-22.

[123] Hayhurst GP, Lee YH, Lambert G, Ward JM and Gonzalez FJ. Hepatocyte nuclear factor 4alpha (nuclear receptor 2A1) is essential for maintenance of hepatic gene expression and lipid homeostasis. Mol Cell Biol 2001;21:1393-403.

[124] Chen WS, Manova K, Weinstein DC, Duncan SA, Plump AS, Prezioso VR, Bachvarova RF and Darnell JE, Jr. Disruption of the HNF-4 gene, expressed in visceral endoderm, leads to cell death in embryonic ectoderm and impaired gastrulation of mouse embryos. Genes Dev 1994;8:2466-77.

[125] Lee YK, Dell H, Dowhan DH, Hadzopoulou-Cladaras M and Moore DD. The orphan nuclear receptor SHP inhibits hepatocyte nuclear factor 4 and retinoid X receptor transactivation: two mechanisms for repression. Mol Cell Biol 2000;20:187-95.

[126] Yamagata K, Daitoku H, Shimamoto Y, Matsuzaki H, Hirota K, Ishida J and Fukamizu A. Bile acids regulate gluconeogenic gene expression via small heterodimer partner-mediated repression of hepatocyte nuclear factor 4 and Foxo1. J Biol Chem 2004;279:23158-65. Epub 2004 Mar 26.

[127] Hirokane H, Nakahara M, Tachibana S, Shimizu M, Sato R, A, De Fabiani E, Mitro N, Anzulovich AC, Pinelli A, Galli G and Crestani M. Bile acid reduces the secretion of very low density lipoprotein by repressing microsomal triglyceride transfer protein gene expression mediated by hepatocyte nuclear factor-4. J Biol Chem 2004;279:45685-92.

[128] Kawada M, Nagamori S, Aizaki H, Fukaya K, Niiya M, Matsuura T, Sujino H, Hasumura S, Yashida H, Mizutani S and Ikenaga H. Massive culture of human liver cancer cells in a newly

developed radial flow bioreactor system: ultrafine structure of functionally enhanced hepatocarcinoma cell lines. In Vitro Cell Dev Biol Anim 1998;34:109-15.

[129] Yanai N and Obinata M. Apoptosis is induced at nonpermissive temperature by a transient increase in p53 in cell lines immortalized with temperature-sensitive SV40 large T-antigen gene. Exp Cell Res 1994;211:296-300.

[130] Eeckhoute J, Moerman E, Bouckenooghe T, Lukoviak B, Pattou F, Formstecher P, Kerr-Conte J, Vandewalle B and Laine B. Hepatocyte nuclear factor 4 alpha isoforms originated from the P1 promoter are expressed in human pancreatic beta-cells and exhibit stronger transcriptional potentials than P2 promoter-driven isoforms. Endocrinology 2003;144:1686-94.

[131] Furihata T, Hosokawa M, Satoh T and Chiba K. Synergistic role of specificity proteins and upstream stimulatory factor 1 in transactivation of the mouse carboxylesterase 2/microsomal acylcarnitine hydrolase gene promoter. Biochem J 2004;384:101-10.

[132] Torres-Padilla ME, Fougere-Deschatrette C and Weiss MC. Expression of HNF4alpha isoforms in mouse liver development is regulated by sequential promoter usage and constitutive 3' end splicing. Mech Dev 2001;109:183-93.

[133] Sladek FM, Ruse MD, Jr., Nepomuceno L, Huang SM and Stallcup MR. Modulation of transcriptional activation and coactivator interaction by a splicing variation in the F domain of nuclear receptor hepatocyte nuclear factor 4alpha1. Mol Cell Biol 1999;19:6509-22.

[134] Inoue Y, Yu AM, Inoue J and Gonzalez FJ. Hepatocyte nuclear factor 4alpha is a central regulator of bile acid conjugation. J Biol Chem 2004;279:2480-9. Epub 2003 Oct 28.

[135] Malik S and Karathanasis SK. TFIIB-directed transcriptional activation by the orphan nuclear receptor hepatocyte nuclear factor 4. Mol Cell Biol 1996;16:1824-31.

[136] Chan J, Nakabayashi H and Wong NC. HNF-4 increases activity of the rat Apo A1 gene. Nucleic Acids Res 1993;21:1205-11.

[137] Galson DL, Tsuchiya T, Tendler DS, Huang LE, Ren Y, Ogura T and Bunn HF. The orphan receptor hepatic nuclear factor 4 functions as a transcriptional activator for tissue-specific and hypoxia-specific erythropoietin gene expression and is antagonized by EAR3/COUP-TF1. Mol Cell Biol 1995;15:2135-44.

[138] Seol W, Hanstein B, Brown M and Moore DD. Inhibition of estrogen receptor action by the orphan receptor SHP (short heterodimer partner). Mol Endocrinol 1998;12:1551-7.

[139] Goodwin B, Jones SA, Price RR, Watson MA, McKee DD, Moore LB, Galardi C, Wilson JG, Lewis MC, Roth ME, Maloney PR, Willson TM and Kliewer SA. A regulatory cascade of the nuclear receptors FXR, SHP-1, and LRH-1 represses bile acid biosynthesis. Mol Cell 2000;6:517-26.

[140] Lu TT, Makishima M, Repa JJ, Schoonjans K, Kerr TA, Auwerx J and Mangelsdorf DJ. Molecular basis for feedback regulation of bile acid synthesis by nuclear receptors. Mol Cell 2000;6:507-15.

[141] Shimamoto Y, Ishida J, Yamagata K, Saito T, Kato H, Matsuoka T, Hirota K, Daitoku H, Nangaku M, Fujii H, Takeda J and Fukamizu A. Inhibitory effect of the small heterodimer partner on hepatocyte nuclear factor-4 mediates bile acid-induced repression of the human angiotensinogen gene. J Biol Chem 2004;279:7770-6. Epub 2003 Dec 12.

[142] Makishima M, Okamoto AY, Repa JJ, Tu H, Learned RM, Luk A, Hull MV, Lustig KD, Mangelsdorf DJ and Shan B. Identification of a nuclear receptor for bile acids. Science

1999;284:1362-5.

[143] Parks DJ, Blanchard SG, Bledsoe RK, Chandra G, Consler TG, Kliewer SA, Stimmel JB, Willson TM, Zavacki AM, Moore DD and Lehmann JM. Bile acids: natural ligands for an orphan nuclear receptor. Science 1999;284:1365-8.

[144] Setchell KD, Rodrigues CM, Clerici C, Solinas A, Morelli A, Gartung C and Boyer J. Bile acid concentrations in human and rat liver tissue and in hepatocyte nuclei. Gastroenterology 1997;112:226-35.

[145] Akashi Y, Miyazaki H and Nakayama F. Correlation of bile acid composition between liver tissue and bile. Clin Chim Acta 1983;133:125-32.

[146] Reddy S, Yang W, Taylor DG, Shen X, Oxender D, Kust G and Leff T. Mitogen-activated protein kinase regulates transcription of the ApoCIII gene. Involvement of the orphan nuclear receptor HNF4. J Biol Chem 1999;274:33050-6.

[147] Nakahara M, Fujii H, Maloney PR, Shimizu M and Sato R. Bile acids enhance low density lipoprotein receptor gene expression via a MAPK cascade-mediated stabilization of mRNA. J Biol Chem 2002;277:37229-34. Epub 2002 Jul 30.

[148] Forman BM, Goode E, Chen J, Oro AE, Bradley DJ, Perlmann T, Noonan DJ, Burka LT, McMorris T, Lamph WW and et al. Identification of a nuclear receptor that is activated by farnesol metabolites. Cell 1995;81:687-93.

[149] Seol W, Choi HS and Moore DD. Isolation of proteins that interact specifically with the retinoid X receptor: two novel orphan receptors. Mol Endocrinol 1995;9:72-85.

Lists of papers on publication

This work was published on the following manuscripts;

1. Tomomi Furihata, Masakiyo Hosokawa, Fumiko Nakata, Tetsuo Satoh, and Kan Chiba. (2003) "Purification, molecular cloning, and functional expression of inducible liver acylcarnitine hydrolase in C57BL/6 mouse, belonging to the carboxylesterase multigene family." *Arch. Biochem. Biophys.* **416** 101-109.

2. Tomomi Furihata, Masakiyo Hosokawa, Nao Koyano, Takahiro Nakamura, Tetsuo Satoh, and Kan Chiba. (2004) "Identification of di-(2-ethylhexyl)phthalate-induced carboxylesterase 1 in mouse liver microsomes: Purification, cDNA cloning, and baculovirus-mediated expression." *Drug Metab. Dispos.* **32** 1170-1177.

3. Tomomi Furihata, Masakiyo Hosokawa, Tetsuo Satoh, and Kan Chiba. (2004) "Synergistic role of specificity proteins and upstream stimulatory factor 1 in transactivation of the *mouse carboxylesterase 2/microsomal acylcarnitine hydrolase* gene promoter." *Biochem. J.* **384** 101-110.

4. Tomomi Furihata, Masakiyo Hosokawa, Ayako Fujii, Maher Derber, Tetsuo Satoh, and Kan Chiba. "Dexamethasone-induced methylprednisolone hemisuccinate hydrolase: its identification as a member of the rat carboxylesterase 2 family and its unique disposition to exist in plasma." *Biochem. Pharmacol.* accepted.

Acknowledgement

I deeply appreciate Professor Kan Chiba who gave me an opportunity to study the roles of carboxylesterase in drug and lipid metabolism and greatly helped me to take a doctor degree for two years. I also appreciate him for helpful advices and critical review of all of the manuscripts.

I greatly appreciate Dr. Masakiyo Hosokawa who also gave me an opportunity to study the roles of carobxylesterase in drug and lipid metabolism and helped me to take a doctor degree for two years. I also appreciate him for numerous helpful advices, technical supports, and discussion for this work and for critical review of all of the manuscripts.

I greatly appreciate Dr. Kaoru Kobayashi who also helped me to take a doctor degree for two years and gave me many valuable advices and technical supports for this work.

I am very thankful to Ayako Fujii, MS., Nao Koyano, BS., for their great contributions of this work.

I am very thankful to Mio Masuda, MS., for her technical supports and advices for this work.

I would like to say thanks to all of my friends, laboratory members and alumni for their practical and mental supports.

Finally, I would like to deeply appreciate my family for their great and thoughtful cooperation to my graduation.

Reviewers

This work, for the Degree of Doctor of Pharmaceutical Sciences, was examined by following reviewers authorized by Graduate School of Pharmaceutical Sciences, Chiba University.

Dr. Kazuei Igarashi, Professor of Chiba University
(Faculty of Pharmaceutical Sciences), Chief reviewer.

Dr. Kazuki Saito, Professor of Chiba University
(Faculty of Pharmaceutical Sciences), reviewer.

Dr. Naoto Yamaguchi, Professor of Chiba University
(Faculty of Pharmaceutical Sciences), reviewer.